DEVELOPMENT OF MODELING CAPABILITIES FOR CONTAMINANT FLOWS IN UNDERGROUND WATER: FINAL REPORT

February, 1986

WWRC-86-07

Submitted by

Myron B. Allen
Department of Mathematics
University of Wyoming
Laramie, Wyoming

to

WYOMING WATER RESEARCH CENTER
UNIVERSITY OF WYOMING
LARAMIE, WYOMING

ABSTRACT

This investigation focuses on the development of a methodology for modeling contaminant movements in the unsaturated zones of soil columns. Such problems are of great technical as well as social interest. They are mathematically difficult and poorly understood from the physical point of view, yet they arise in most incidents of aquifer contamination by sources near the earth's surface. Of particular concern are multiphase flows, which occur when contaminants having limited solubility in water enter the soil column. This document reports progress on several fronts in modeling subsurface contamination. First, we advance a one-dimensional finite-element collocation scheme for solving the nonlinear equation governing unsaturated water flows. The new scheme overcomes mass balance errors characteristic of this class of problems. Second, we discuss the extension of the collocation method to two space dimensions. Third, we propose a continuum-mechanical formulation of the equations governing multiphase unsaturated flows. These equations are extend the classical equation for unsaturated water flow. Finally, we briefly report ongoing research into the numerical solution of the equations for multiphase unsaturated flows. An appendix includes published articles detailing the mathematics of the results summarized in the main report.

TABLE OF CONTENTS

INTRODUCTION

Groundwater is a precious resource. Through most of Western history economics have partially masked this fact. Groundwater has usually been available in sufficient quantity and quality to satisfy most needs fairly cheaply. Consequently, the price per unit volume of groundwater remains very low compared to that of oil, a resource that is similar in many respects. Nevertheless, demand for groundwater is rising dramatically in parts of the country where surface water supplies either are declining in quality or, as in the water-scarce Western United States, are simply inadequate in volume. Declining aquifer levels coupled with increased pumping offer convincing evidence that groundwater is a bounded and easily threatened natural asset.

Along with the rise in demand has come a different threat to groundwater: contamination. Disposal of industrial wastes at or near the earth's surface often leads to pollution of nearby underground water supplies. For many years this problem drew less attention than the problems of air and surface-water pollution caused by other waste disposal practices. The reasons for this are simple. Groundwater is relatively inaccessible to observation, so contamination seems invisible until it appears at a production well. However, groundwater typically moves through the subsurface so slowly that a contaminant source may not affect water produced at wells for many years. Inaccessibility and large time scales make groundwater contamination a particularly insidious form of pollution. A contaminated aquifer is difficult, if not impossible, to clean, and by the time the contamination is discovered it is often hopelessly widespread and hard to trace.

Inaccessibility and large time scales also mean that quantitative understanding of an aquifer's contaminant transport properties can be difficult to establish. Groundwater obeys fairly complicated dynamical laws, and even with good mea-

surements of an aquifer's rock and fluid properties hydrologists may have difficulty predicting or tracing contaminant movements. Here is where mathematical simulation plays a role. Given an adequate description of a groundwater system, a hydrologist can use a mathematical model as a conceptual surrogate for the natural system. A properly constructed simulator—one that is faithful to both the fundamental mechanics of groundwater flow and the geologic peculiarities of the aquifer under study—can approximately reconstruct the history of a contaminant flow, can estimate how the contaminant will move in the future, and can furnish a method for comparing proposed remedial measures. For these reasons, mathematical techniques for modeling underground contaminant flows have attracted intensive research in the past two decades.

There is a class of contaminant flows, however, for which available mathematical techniques remain inadequate. These flows involve movement of contaminants in the unsaturated zone of the soil column. This zone typically connects surface disposal sites with the water table and is therefore an important pathway for aquifer contamination. Flows of water-soluble contaminants in the unsaturated zone have received a fair amount of attention in the simulation community, although there are still many open issues there. However, in a surprising number of cases contaminants percolate downward from near-surface dumpsites in the form of nonaqueous, relatively insoluble liquid phases. Such flows have received relatively scant scientific attention.

Nevertheless, the contamination of underground water resources by nonaqueous organic liquids has become a matter of urgent concern in the United States in the past few years. While such exotic and extreme cases as Love Canal in Niagara Falls, New York, have received much of the public's attention, less dramatic instances of groundwater contamination by organics abound. Leaking tanks

at gasoline filling stations, settling ponds at chemical plants, and leaching from contaminated landfills are all common sources of nonaqueous contaminants. Despite its low level of heavy industry, Wyoming has not escaped this problem. The Baxter Tie Treating Plant, owned by the Union Pacific Railroad in Laramie, is so severely contaminated by organic wastes that the site has been targeted by the U.S. Environmental Protection Agency as qualifying for "superfund" monies.

In many sites, the nonaqueous-phase liquid (NAPL) contaminants enter the groundwater from sources near the earth's surface. In these cases, the NAPL must ordinarily seep through a zone of soil that is only partially saturated with water before the contaminants reach the water table, or the upper limit of water-saturated soil. The simultaneous movement of water, NAPL, and air in the interstices of this partially saturated, or vadose, soil obeys a complicated set of physics governing multiphase flows in porous media. Understanding the fundamental continuum mechanics of these flows is crucial to the assessment of remediation schemes for near-surface NAPL contamination. Equally crucial is the need to develop predictive techniques that can use this physical understanding to furnish engineering tools for the design of remedial measures.

This report documents the accomplishments of a project aimed at developing predictive techniques for NAPL contamination in variably saturated soils. The project, funded by the Wyoming Water Research Center, has been a two-year effort to develop mathematical techniques suitable for solving the equations governing flows in unsaturated porous media. Because of the complexity and inherent nonlinearity of these governing equations, the solution techniques take the form of numerical approximations. The particular techniques employed here rely on the method of finite-element collocation to approximate spatial variations in the flow variables, accommodating temporal variations by the method of finite differ-

ences. The result of this methodology is a class of numerical techniques that is mathematically appropriate for the types of flow equations that arise in actual applications.

It is important to recognize that this project does not furnish a working simulator adequate for immediate engineering applications on specific sites. Indeed, it is doubtful that such applications could occur right now, given the nascent state of the art in the physical characterization of sites and hence the paucity of reliable data to be used as model inputs. The project does furnish sound, new *methodologies* for use in simulators of NAPL-water flows in unsaturated soils—methodologies that should prove useful as contamination assessment technologies continue to emerge.

In summary, the project has yielded the following results. A continuum-mechanical investigation of multiphase flows in porous media, using notions from mixture theory, has indicated the governing equations. These equations extend Richards' (1931) classic study of air-water flow. The results (Allen, to appear; see Appendix) are apparently the first discussion of the mechanics of multiphase unsaturated flows in the literature. An investigation of finite-element collocation methods for the single-liquid version of Richards' equation in one space dimension has led to the development of a mass-conserving finite-element formulation of this nonlinear problem. As reviewed in Allen and Murphy (1985b; see Appendix), mass conservation has long been a difficulty with unsaturated flow models. An extension of the one-dimensional method has yielded a solution technique for two-dimensional unsaturated flows in a vertical plane. This method, reported in Murphy and Allen (to appear; see Appendix), formed the basis for an M.S. thesis in Mathematics, written by Carolyn L. Murphy and submitted to the Water Research Center in the fall of 1985 (Murphy, 1985). Finally, the extension of the

finite-element collocation method to flows with two liquid phases is in progress. The fundamental formulation is established, but at this writing the computer code needs further debugging. This task has been slowed by lack of graduate student support.

Copies of all published articles resulting from this report, with the exception of C. L. Murphy's M.S. thesis, a progress report given at the Wyoming Water '85 conference (Allen and Murphy, 1985a), and an invited article in preparation for the inaugural issue of *Hydraulic Engineering Software*, appear in the Appendix to this report. These articles include the following:

Allen, M.B. (1984), "Why upwinding is reasonable," in J.P. Laible et al., eds., *Proceedings of the Fifth International Conference on Finite Elements in Water Resources*, Burlington, Vermont, June 14–18, Berlin: Springer-Verlag.

Allen, M.B. (1985), "Numerical modeling of multiphase flows in porous media," presented at the NATO Advanced Study Institute on Fundamentals of Fluid Flow and Transport in Porous Media, Newark, Delaware, July 14–23, 1985; to appear in *Adv. Water Resources.*

Allen, M.B. (to appear), "Mechanics of multiphase fluid flows in variably saturated porous media," *Int. Jour. Engrg. Sci.*

Allen, M.B., Ewing, R.E., and Koebbe, J.V. (1985), "Mixed finite-element methods for computing groundwater velocities," *Numer. Meth. for P.D.E.*, 3, 195–207.

Allen, M.B., and Murphy, C.L. (1985b), "A finite-element collocation method for variably saturated flows in porous media," *Numer. Meth. for P.D.E.*, 3, 229–239.

Murphy, C.L., and Allen, M.B. (to appear), "A collocation model of two-dimensional unsaturated flow," in A. Sa da Costa et al., eds., *Proceedings of the Sixth International Conference on Finite Elements in Water Resources*, Lisbon, Portugal, June 1–6, 1986, Southampton, U.K.: CML Publications Ltd.

Because the technical articles provide sufficient detail to reproduce the results of the study, the remainder of this report focuses on the results without elaborating on the details of the mathematics.

OBJECTIVES

As described in the original proposal (Allen, 1983), the overall objective of this project was the development of modeling techniques for solving the equations governing multiphase contaminant flows in the unsaturated zone. The proposal outlined several intermediate objectives leading to this overall aim. These were as follows.

The first task in the project was to derive the basic physics and governing equations. The equations governing NAPL-water flows in variably saturated soils had not appeared in the technical literature at the time the project began. The second task was to formulate numerical methods for the discretization of the governing equations. The third task was to develop and test Fortran code implementing the methods devised in the second task. The second and third tasks are actually concomitant in nature, since the development of a numerical method for multidimensional and multiphase flows best proceeds via development and computer implementation of methods for a sequence of problems of increasing complexity. The fourth task was to document the results of the project. This report embodies the output of this last task.

METHODOLOGY

This section reviews the methodologies used in addressing the various tasks in the project. Detailed descriptions of the mathematics developed appears in the technical articles reproduced in the Appendix to this report. The articles are sufficiently complete that a mathematically inclined reader could reproduce the results of the project. The remainder of this section gives a description of unsaturated flows, outlines the numerical solution techniques developed in the course of the research for flows involving a single liquid, and reviews the extension of the

classical single-liquid theory to multiphase unsaturated flows. For conceptual ease it seems better to present the numerical methods in the context of single-liquid flows before discussing the mechanics of multiphase flows, even though this order reverses that of the original tasks.

Description of unsaturated flows

By definition, a groundwater flow is *unsaturated* if it occurs in a porous medium, such as soil, whose accessible pores are partly occupied by air. Such flows occur just beneath the earth's surface, where cycles of precipitation and dry weather lead to incomplete saturation and dessication of the soil. Unsaturated flows stand in contrast with saturated groundwater flows, in which the pore space of the rock or soil matrix is occupied completely by liquid.

From a physical standpoint, unsaturated groundwater flows are quite a bit more complicated than saturated flows. One source of complication arises essentially because the presence of air in the void spaces of the medium interferes with the flow of liquid. In general, water flows more easily in a porous medium when a larger fraction of its pore space is occupied by water. In other words, the *hydraulic conductivity* of the medium increases with its *moisture content.* Another source of complication arises from the surface physics that act at a scale of observation comparable to the size of a typical pore. The interaction between the surface tensions of air and water and the microscopic geometry of the porous medium imply a direct relationship between the moisture content of the soil and the average water pressure. Thus the moisture content depends on the water pressure. This phenomenon, known as *capillarity*, means that we can compute water pressure (or pressure head) and then compute the corresponding moisture content using the functional relationship between the two.

From the mathematical point of view, these two complications make the equations governing unsaturated flow significantly more difficult to solve than the equations governing saturated flows. To see why, consider the task of computing pressure head as an unknown function of space and time in the soil column. The equation governing pressure head contains as parameters the moisture content and the hydraulic conductivity. To solve for pressure head, we must therefore know values for the moisture content and hydraulic conductivity, but to compute these parameters we need values of the unknown pressure head. Problems in which the parameters in an equation depend on the unknowns are *nonlinear*, and often they can be solved only using approximate numerical methods. Except for certain physically unrealistic simple cases, this is the case with unsaturated flows. Huyakorn and Pinder (1984, Chapter 4) review some of the last decade's research in this area.

So far we have considered only unsaturated flows in which water and air are present. As mentioned, however, many contamination problems involve flows of water and air in a soil matrix together with the simultaneous flow of some non-aqueous liquid that is immiscible with water. When such "oily" contaminants are present the physics, and hence the mathematics, become even more complicated. Now, in addition to the old nonlinearities, the presence of nonaqueous liquid will affect the flow of water and vice versa. Also, there will be another capillarity relationship coupling the pressure head in the water to that in the immiscible contaminant. Again, numerical solution techniques are necessary, but in this case we have very little in the way of previous research to guide our approach.

Numerical methods developed

One task facing the applied mathematician wishing to model unsaturated

flows is to select a numerical method capable of producing veracious solutions to the governing equations. In the simplest of cases—one-dimensional flow of a single liquid—the governing equation is a partial differential equation derived by Richards (1931). In its primitive form, Richards' equation is

$$\underset{\text{(I)}}{\frac{\partial \theta(h)}{\partial t}} = \underset{\text{(II)}}{\frac{\partial}{\partial z}\left[k(h)\frac{\partial h}{\partial z}\right]} - \underset{\text{(III)}}{\frac{\partial k(h)}{\partial z}} \tag{1}$$

The first term (I) is the temporal rate of change of the moisture content θ [m^3 water/m^3 soil matrix] expressed as a function of pressure head h [m] according to the capillarity relationship. The second term (II) arises from Darcy's law for flow in a porous medium and accounts for fluxes of water attributable to gradients in pressure head with respect to height z above a datum. The parameter $k(h)$ [m/s] in this term is the hydraulic conductivity of the soil, again expressed as a function of pressure head. The third term (III) accounts for the influence of gravity on the fluid flow. Given information about the initial pressure head distribution in a soil column and conditions at the spatial boundary of the column, Equation (1) determines a function $h(z,t)$ giving the pressure head distribution, and hence the moisture content θ, throughout the soil column at all subsequent times. However, the dependencies $\theta(h)$ and $k(h)$ that render the equation nonlinear make the actual calculation of $h(z,t)$ a tricky job.

One apparent simplification to Equation (1) is both quick and quite common among modelers. By using the chain rule, one can write

$$\frac{\partial \theta(h)}{\partial t} = \frac{d\theta(h)}{dt}\frac{\partial h}{\partial t} = C(h)\frac{\partial h}{\partial t}$$

This device allows us to rewrite Equation (1) as a partial differential equation in which the pressure head h appears explicitly as an unknown in each term:

$$C(h)\frac{\partial h}{\partial t} = \frac{\partial}{\partial z}\left[k(h)\frac{\partial h}{\partial z}\right] - \frac{\partial k(h)}{\partial z} \tag{2}$$

The new parameter $C(h)$ is the *specific moisture capacity* [1/m], and, as the notation indicates, it too depends on the pressure head. Hydrologists sometimes call Equation 2 the "head-based formulation" of Richards' equation.

We solve Equation (2), subject to a commonly used set of initial and boundary data, using the numerical technique of finite-element collocation. This method is attractive for several reasons. First, it shares with the more conventional Galerkin finite-element methods a degree of accuracy that forces errors in the approximate solution to diminish very rapidly for given increases in the computational effort. This rapid improvement in solution quality stands in contrast to the relatively slow improvements available through standard finite-difference approximations. Second, finite-element collocation bypasses some of the computational complexity of Galerkin methods and thus promises even more efficient use of computational resources. Third, finite-element collocation in recent years has produced good numerical solutions to other problems involving multiphase flows in porous media (Allen and Pinder, 1983; Allen, 1984; Allen and Pinder, 1985), so it is a natural candidate for unsaturated flows.

Roughly speaking, the idea behind finite-element collocation is to replace the unknown function $h(x,t)$, whose spatial variation has an infinite number of degrees of freedom, with an approximating trial function $\hat{h}(x,t)$ whose spatial variation has a finite (and therefore computable) number of degrees of freedom. In particular, we choose the degrees of freedom of $\hat{h}$ to represent the values of pressure head and its vertical gradient $\partial\hat{h}/\partial z$ at each of a collection of representative spatial locations $z_0,\ldots,z_N$, called nodes, spread throughout the column. Then we can model the variation of $\hat{h}$ between nodes by smoothly interpolating between adjacent nodes. This interpolation relies on a set of interpolating functions known as Hermite cubic polynomials (see Prenter, 1975, Chapter 3). To get an approximate version

of Equation (2), for example, we substitute the trial function $\hat{h}$ for the true solution h and demand that the resulting equation hold at a number of *collocation points* $\bar{z}_1, \ldots, \bar{z}_M$ located throughout the soil column:

$$\hat{C}(\bar{z}_k,t)\frac{\partial \hat{h}}{\partial t}(\bar{z}_k,t) = \frac{\partial}{\partial z}\left[\hat{k}(\bar{z}_k,t)\,\frac{\partial \hat{h}}{\partial z}(\bar{z}_k,t)\right] - \frac{\partial \hat{k}}{\partial z}(\bar{z}_k,t)\ , \qquad k = 1,\ldots,M \tag{3}$$

Here $\hat{k}$ and $\hat{C}$ are interpolatory representations of the parameters k and C. Notice that the collocation points $\bar{z}_k$ are logically different from the nodes. We choose exactly as many collocation points as are necessary to furnish the correct number of equations of the form (3) to solve for the unknown nodal values and gradients of $\hat{h}$.

This solution scheme tends to exhibit certain characteristic types of error with respect to true solutions of Equation (2). In particular, it is difficult to discretize Equation (3) temporally without confronting the question of where to evaluate the coefficient $\hat{C}$ in time. Straightforward evaluation at a temporal node typically leads to mass balance errors, as Allen and Murphy (1985b; see Appendix) describe. Such errors are generally deleterious, since an incorrectly computed frontal advance of liquid into a soil will lead to incorrect estimates of contaminant transport.

It is only fair to mention that mass-balance errors are not uncommon in numerical solutions to Richards' equation. Milly (1984), for example, discusses an iterative procedure for improving mass balances in the time-stepping algorithms for Equation (2). His approach essentially prescribes a technique for choosing a representative time level at which to evaluate the nonlinear coefficient $C(h)$.

Our approach to reducing the mass balance error is in some ways more natural. We return to the primitive form of the governing equation, Equation (1).

In bypassing the apparent simplification offered by the chain rule, we circumvent the issue of where to evaluate $C(h)$ in time. Instead, we approximate term (I) in Equation (1) directly using an interpolatory finite-element representation. In this way the discrete analog of term (I) truly represents the rate of change of moisture content over a time step. Again, Allen and Murphy (1985b; see Appendix) give the details of the procedure, showing by means of a computable index that the new scheme conserves mass.

In two space dimensions, say a vertical (x, z)-plane, Richards' equation is

$$\nabla \cdot \left[k(\nabla h - \mathbf{e}_z)\right] = \frac{\partial \theta}{\partial t}$$

where $\mathbf{e}_z$ is the unit vector pointing upward. We solve this equation using a two-dimensional extension of the mass-conserving finite-element collocation procedure developed in one space dimension. For the finite-element representations of the spatially varying quantities in this equation we use two-dimensional tensor-product spaces associated with the interpolating representations used in one dimension. While this approach is conceptually straightforward, the coding becomes somewhat more complex in two dimensions. Murphy (1985) and Murphy and Allen (to appear; see Appendix) describe the two-dimensional formulation in detail.

Research into the mechanics of multiphase flows

While Richards' equation is well established as the equation governing unsaturated flows of water, there has been very little investigation into the fundamental mechanics of multi-liquid flows in unsaturated soils. Therefore part of our effort has been to propose a continuum-mechanical formulation of multiphase contaminant flows in porous media. This line of inquiry differs from our investigation into finite-element collocation. There we were concerned with the development

of effective solution procedures given an established governing equation. With multiphase unsaturated flows our contribution has been more basic: we have derived a set of governing equations consistent with sound physical principles and plausible assumptions about unsaturated porous media.

Several other investigators have looked at physics similar to those of interest here. Raats (1984), for example, discusses a general mechanical formalism for treating unsaturated flows of air and water in soils using the *theory of mixtures* developed by Eringen and Ingraham (1965). Schwille (1984) discusses practical aspects of multiphase flows in the unsaturated zone, but presents no continuum-mechanical formulation for the governing equations. Corapcioglu and Baehr (to appear) derive a governing equation without referring specifically to a velocity field equation such as Darcy's law.

Our work is similar in spirit to that of Raats in that we use principles from continuum mixture theory. However, the current project focusses on *multiphase* flows in unsaturated zone. By considering a mixture containing soil, air, water and nonaqueous liquid and neglecting interphase mass transfer and chemical reactions, one can derive an extension of Richards' equation to two liquid phases (Allen, to appear; see Appendix). In three space dimensions the new equations take the form

$$\begin{aligned} \left(C_W + \frac{\theta_W s_W}{\phi}\right) \frac{\partial h_W}{\partial t} &= \nabla \cdot (k_W \nabla h_W) + \nabla \cdot (k_W \mathbf{e}_z) \\ \left(C_N + \frac{\theta_N s_N}{\phi}\right) \frac{\partial h_N}{\partial t} &= \nabla \cdot (k_N \nabla h_N) + \nabla \cdot (k_N \mathbf{e}_z) \end{aligned} \tag{4}$$

Here h_W and h_N stand for the pressure heads in the water and nonaqueous liquid, respectively; C_W and C_N stand for the specific moisture capacity of the soil with respect to water and nonaqueous liquid; θ_W and θ_N stand for the aqueous and nonaqueous moisture contents; s_W and s_N stand for the specific storage coeffi-

cients for the soil in the presence of water and nonaqueous liquid, and k_W and k_N stand for the effective hydraulic conductivities of the soil to water and nonaqueous liquid. The vector $\mathbf{e}_z$ is the unit vector pointing vertically upward. The coefficients k_W and k_N, at least, depend on the relative amounts of water and nonaqueous liquid present and are therefore functions of two moisture contents:

$$k_W = k_W(\theta_W, \theta_N) , \qquad k_N = k_N(\theta_W, \theta_N)$$

In addition to these new functional dependencies there are some new constraints. To begin with, the three fluids (air, water, and nonaqueous liquid) must occupy all of the pore space of the solid matrix. Therefore the fluid content variables θ_A, θ_W, and θ_N, giving volume of fluid per bulk volume of soil, must add together to give the total fraction ofthe matrix that is void:

$$\theta_A + \theta_W + \theta_N = \phi .$$

Moreover, the presence of three fluid phases implies the existence of three distinct pressures. From these pressures there arise two independent pressure differences $p_W - p_A$ and $p_N - p_A$, that is, the differences between the two liquid pressures and the air pressure. These pressure differences, and thus the corresponding pressure heads h_W and h_A, vary with moisture content. Inverting these relationships gives two functional relationships having the forms $\theta_W = \theta_W(h_W)$ and $\theta_N = \theta_N(h_N)$ analogous to the relationship $\theta = \theta(h)$ arising in the single-liquid theory reviewed above.

Using principles from continuum physics to develop governing equations in this way has at least two benefits. First, since these principles have their basis in rigorous physical theory, the resulting flow equations at least have a sound conceptual foundation. The arguments used to derive Equations (4) explicitly

show how multiphase unsaturated flows fit into a general and widely accepted body of physical theory. Second, the resulting set of partial differential equations serves to guide experimental work by indicating new variables and functional dependencies that need to be quantified to allow precise descriptions of the flows in question. Progress in understanding multiphase unsaturated flows urgently needs empirical work, and a sound mechanical framework provides an essential context for the design of experiments.

Work in progress

The numerical solution of Equation (4) is a matter of current research. At this writing, the project has yielded a numerical formulation for two-liquid unsaturated flows in the vertical direction. However, the coding of this formulation is still incomplete. This task has evolved more slowly than expected, for two reasons. First, the simultaneous solution of two coupled, nonlinear, time-dependent partial differential equations is inherently difficult from a numerical point of view. Second, and more important, both of the graduate students who have contributed to this project (Carolyn L. Murphy and Lowell Smylie) have left the University of Wyoming, the first after completing an M.S., the second for personal reasons. There being no funding available for students at this time, responsibility for mathematical analysis, code development, and code testing now rests with the Principal Investigator.

RESULTS

To date, this project generated the following results.

1. A continuum-mechanical formulation of the flow equations for multigrid flows in variably saturated porous media (Allen, to appear).

2. A mass-conserving finite-element collocation method for solving one-dimensional transient vertical flows of a single liquid through variably saturated porous media, together with a Fortran code implementing the method (Allen and Murphy, 1985).

3. An extension of the one-dimensional collocation method to two space dimensions, together with Fortran codes implementing the method for two sample problems (Murphy, 1985; Murphy and Allen, to appear).

Computer codes from items 1 and 2 are available from Myron B. Allen, Department of Mathematics, University of Wyoming, Laramie, Wyoming 82071. Each request should be accompanied by a blank 9-track tape, which will be returned with the appropriate codes and data at a density of 1600 characters per inch, Cyber format.

As discussed above, development of a one-dimensional code using finite-element collocation to solve the flow equations for two liquids in a variably saturated porous media is in progress at this writing.

CONCLUSIONS AND RECOMMENDATIONS

This project has generated theoretical and numerical methods for the modeling of multiphase contaminant flows in the unsaturated zones of porous soils. As mentioned in the introduction, understanding of such flows is vital to the advance of remedial schemes for an ever-growing class of groundwater contamination problems. Specific conclusions drawn here include the following:

1. Mixture theory provides a sound theoretical basis on which to develop the continuum mechanics of multiphase underground flows. As explained in the published work (Allen, to appear), the equations developed in the course of this project reflect certain restrictive assumptions that, while plausible for

most soils, should be examined in any site-specific application.

2. Finite-element collocation furnishes an accurate numerical method for solving the unsaturated flow equations. Given careful attention to the formulation of the discretization, collocation schemes can be forced to guarantee mass conservation, violation of which is a problem afflicting many naive numerical schemes for unsaturated flows. Moreover, a reasonable Newton-like iterative scheme accommodates the nonlinearity inherent in these flow equations in a stable manner. Finally, as our numerical results indicate, the method admits a conceptually simple extension to two space dimensions.

Much remains to be done in this area. Specific recommendations include the following:

1. Work on numerical schemes for two-liquid flows should continue. This is an important emerging area in groundwater engineering, and advances to date have been sparse (see Abriola and Pinder, 1985; Faust, 1985 for the major publications in this area known to the author). Numerical simulation is destined to be an important tool in studies of subsurface contamination, paralleling the now widespread use of simulators in the petroleum extraction industry. Without further research and development, this area of inquiry could become the critical path in the engineering of remedial measures.

2. The basic governing equations developed in this project need to be verified by experiments. While the author is not qualified to design and conduct such experiments, he is willing to cooperate with any efforts in this regard. A potentially important effort in this regard is presently under way at Princeton University under the direction of Professor Chris Milly, Department of Civil Engineering.

3. Before numerical simulation can become a standard, site-specific engineering tool, we must have better methods for characterizing sites. This recommendation involves a plethora of research needs too broad to allow extensive mention here, but some of the major problems in site characterization include the lack of sampling and measuring procedures for multiphase flows in the unconsolidated soils typically found near the surface, the lack of universally accepted sampling and analysis protocol for NAPL in soils, and an incomplete understanding of the roles of such soil features as clay stringers, dessication cracks, and human-built bentonite structures in providing barriers or high-permeability conduits for NAPL migration.

REFERENCES

(Note: asterisks (*) indicate items produced in connection with this project.)

*Abriola, L. M., and Pinder, G. F. (1985), "A multiphase approach to the modeling of porous media contamination by organic compounds 2. Numerical simulation," *Water Res. Research* **21**, 19–26.

Allen, M. B. (1984), *Collocation Techniques for Modeling Compositional Flows in Oil Reservoirs*, Berlin: Springer-Verlag.

*Allen, M. B. (1984), "Why upwinding is reasonable," in J. P. Laible et al., eds., *Proceedings of the Fifth International Conference on Finite Elements in Water Resources*, Burlington, Vermont, June 14–18, Berlin: Springer-Verlag.

*Allen, M. B. (1985), "Numerical modeling of multiphase flows in porous media," presented at the NATO Advanced Study Institute on Fundamentals of Fluid Flow and Transport in Porous Media, Newark, Delaware, July 14–23, 1985; to appear in *Adv. Water Resources.*

*Allen, M. B. (to appear), "Mechanics of multiphase fluid flows in variably saturated porous media," *Int. Jour. Engrg. Sci.*

*Allen, M. B., Ewing, R. E., and Koebbe, J. V. (1985), "Mixed finite-element methods for computing groundwater velocities," *Numer. Meth. for P.D.E.* **3**, 195–207.

*Allen, M. B., and Murphy, C.)1985a), "Modeling contaminant flows in unsaturated soils," presented at Wyoming Water '85, May 2–3, Laramie, Wyoming.

*Allen, M. B., and Murphy, C. L. (1985b), "A finite-element collocation method for variably saturated flows in porous media," *Numer. Meth. for P.D.E.* **3**, 229–239.

Allen, M. B., and Pinder, G. F. (1983), "Collocation simulation of multiphase porous medium flow," *Soc. Pet. Eng. J.*, 135–142.

Allen, M. B., and Pinder, G. F. (1985), "The convergence of upstream collocation in the Buckley-Leverett problem," *Soc. Pet. Eng. J.*, 363–370.

Corapcioglu, M. Y., and Baehr, A. (to appear), "Immiscible contaminant transport in soils and groundwater with an emphasis on petroleum hydrocarbons: system of differential equations vs. single cell model," *Water Science and Technology.*

Eringen, A. C., and Ingraham, J. D. (1965), "A continuum theory of chemically reacting media—I," *Int. J. Engrg. Sci.* **3**, 197–212.

Faust, C. R. (1985), "Transport of immiscible fluids within and below the unsaturated zone: a numerical model," *Water Res. Research* **21**, 587–596.

Huyakorn, P., and Pinder, G. F. (1984), *Computational Methods in Subsurface Flow*, New York: Academic Press.

Milly, P. C. D. (1984), "A mass-conservative procedure for time-stepping in models of unsaturated flow," in *Finite Elements in Water Resources, Proceedings of the Fifth International Conference* (eds. J. P. Laible et al.), London: Springer-Verlag, 103–112.

*Murphy, C. L. (1985), "Finite Element Collocation Solution of the Unsaturated Flow Equations," M.S. thesis, Department of Mathematics, University of Wyoming, Laramie, Wyoming.

*Murphy, C. L., and Allen, M. B. (to appear), "A collocation model of two-dimensional unsaturated flow," in A. Sa da Costa et al., eds., *Proceedings of the Sixth International Conference on Finite Elements in Water Resources*, Lisbon, Portugal, June 1–6, 1986, Southampton, U.K.: CML Publications, Ltd.

Prenter, P. M. (1975), *Splines and Variational Methods*, New York: John Wiley and Sons.

Raats, P. A. C. (1984), "Applications to the theory of mixtures in soil physics," Appendix 5D to C. Truesdell, *Rational Thermodynamics (2nd ed.)*, New York: Springer-Verlag, 326–343.

Richards, L. A. (1931), "Capillary conduction of liquids in porous media," *Physics* **1**, 318–333.

Schwille, F. (1984), "Migration of organic fluids immiscible with water in the unsaturated zone," in *Pollutants in Porous Media* (eds. B. Yarrow et al.), Berlin: Springer-Verlag, 27–49.

van Genuchten, M. Th. (1982), "A comparison of numerical solutions of the one-dimensional unsaturated-saturated flow and mass transport equations," *Adv. Water Resources* **5**, 47–55.

van Genuchten, M. Th. (1983), "An Hermitian finite element solution of the two-dimensional saturated-unsaturated flow equation," *Adv. Water Resources* **6**, 106–111.

APPENDIX: ARTICLES PUBLISHED FROM THIS PROJECT

Attached are the articles, cited in the Introduction to this report, whose publication resulted from work done during this project.

WHY UPWINDING IS REASONABLE

Myron B. Allen

University of Wyoming

INTRODUCTION

Upwind-biased discrete approximations have a distinguished history in numerical fluid mechanics, dating at least to von Neumann and Richtmyer (1950). Lately, however, upwinding has come under fire in water resources engineering. Among the most effective critics of upwind techniques are Gresho and Lee (1980), who take umbrage at the smearing of steep gradients in solutions of partial differential equations. While this viewpoint has cogency, a blanket condemnation of upwinding would be injudicious. There exist fluid flows for which upstream-biased discretizations are not only valid but in fact mathematically more appropriate than central approximations having higher-order accuracy.

Figures 1 and 2 illustrate the source of the controversy. Both plots show numerical solutions to a convection-dominated species transport equation using finite-element collocation. Figure 1, the result of a centered scheme, shows a solution having unrealistic wiggles near the concentration front; Figure 2, from an upwind scheme, exhibits nonphysical smearing. The wiggles in the centered scheme disappear altogether when the spatial step Δx is small enough, whereas the smearing associated with upstream weighting decreases continuously with Δx. Gresho and Lee argue that the wiggles indicate an inappropriate spatial grid and that suppressing them via upwinding eliminates useful symptoms in favor of a less informative flaw, smearing.

Were wiggles the only difficulty with centered schemes, proscribing upwind methods might be in order. However, as we shall see, for certain types of equations centered schemes can fail to converge. This difficulty is not symptomatic of an unsuitable grid; rather, it betrays an inability of centered schemes to impose proper uniqueness criteria. For such equations, upwinding can be reasonable.

SOME UPWINDING TECHNIQUES

Of various discrete methods used in numerical fluid mechanics, finite differences, Galerkin methods, and finite-element collocation have proved to be among the most attractive. A brief review of techniques in each of these

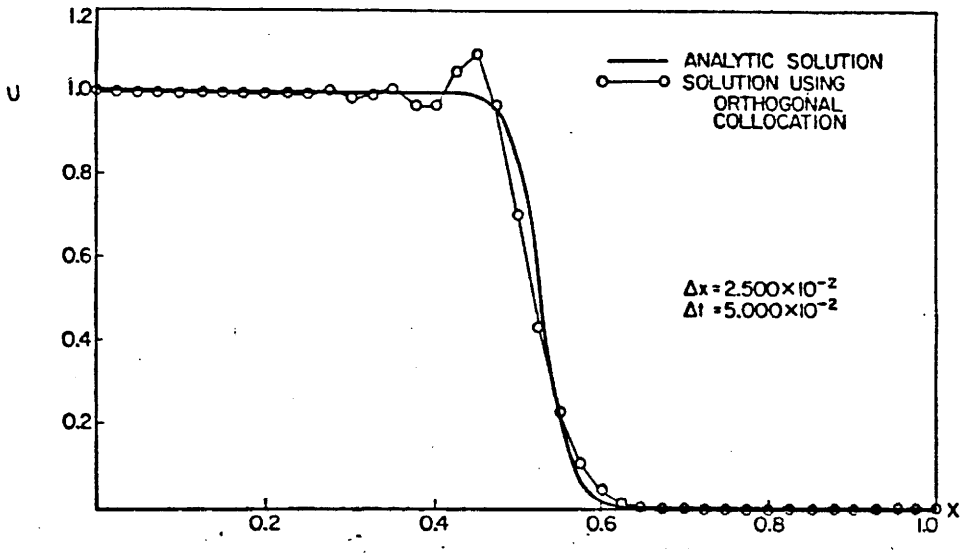

Figure 1. Solution to the convection-diffusion equation using standard collocation on finite elements.

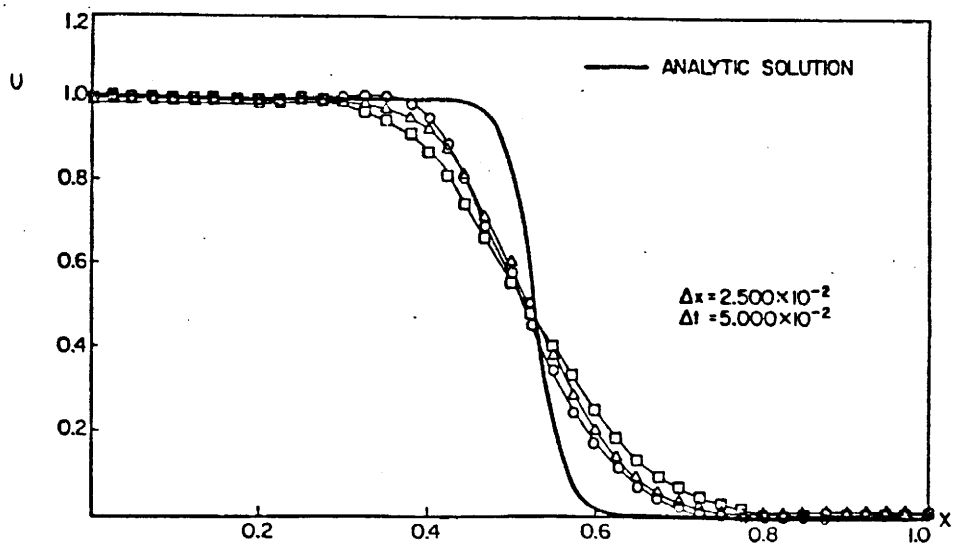

Figure 2. Solutions to the convection-diffusion equation using several choices of upstream collocation points.

make matters concrete, consider as a paradigm of convection-dominated flows the constant-coefficient convection-diffusion problem

$$\begin{aligned} \partial u/\partial t + \partial u/\partial x - Pe^{-1}\partial^2 u/\partial x^2 &= 0 \\ u(x,0) = 0, \quad x \in (0,1) & \\ u(0,t) = 1 \quad \text{and} \quad \partial u(1,t)/\partial x &= 0, \quad t \geq 0 \end{aligned} \tag{1}$$

where x and t are dimensionless space and time coordinates, $u(x,t)$ denotes a normalized concentration, and the Peclet number Pe measures the degree to which convection dominates diffusion.

As commonly implemented, each of the discrete interior methods calls for a partition Δ_N: $0 = x_0 < x_1 < \ldots < x_{N+1} = 1$ of the spatial domain. Suppose for simplicity that Δ_N has uniform mesh Δx. Then the following finite-difference analog of Equation (1) has truncation error $O(\Delta x^2)$:

$$du_i/dt = -(2\Delta x)^{-1}(u_{i+1}-u_{i-1}) + (Pe\ \Delta x^2)^{-1}(u_{i+1}-2u_i+u_{i-1}) \tag{2}$$

where $u_i(t)$ signifies the approximate solution at $x = i\Delta x$ and time t. The problem with Equation (2) is that, unless Δx is sufficiently small, the numerical solution exhibits spurious wiggles near sharp concentration fronts. A desire to avoid these wiggles in favor of smearing prompts many analysts to resort to upwind schemes.

The simplest way to derive an upwind scheme from Equation (2) is to replace the analog of the convective term $\partial u/\partial x$ by a one-sided difference, yielding

$$du_i/dt = -\Delta x^{-1}(u_i-u_{i-1}) + (Pe\ \Delta x^2)^{-1}(u_{i+1}-2u_i+u_{i-1}) \tag{3}$$

The truncation error of Equation (3), $O(\Delta x)$, is larger than that for Equation (2), and writing the lowest error term explicitly shows

$$\begin{aligned} du_i/dt + \Delta x^{-1}(u_i-u_{i-1}) - (Pe\ \Delta x^2)^{-1}(u_{i+1}-2u_i+u_{i-1}) & \\ = \partial u/\partial t + \partial u/\partial x - (Pe^{-1}+\Delta x/2)\partial^2 u/\partial x^2 + O(\Delta x^2) & \end{aligned} \tag{4}$$

where the terms on the right are evaluated at $x = x_i$. It is clear that the upwind difference scheme augments physical diffusion by an amount proportional to Δx. Hence by sacrificing one order of spatial accuracy one can suppress nonphysical wiggles at the cost of numerically induced dissipation.

Upwinding techniques also exist for finite-element Galerkin schemes. One such technique is the use of upstream-biased test functions proposed by Heinrich et al. (1977). Consider the standard Galerkin method applied to Equation (1). This method seeks a trial function

$$\hat{u}(x,t) = u_\partial(x) + \sum_{i=1}^{N} u_i(t)L_i(x)$$

approximating the true solution $u(x,t)$. Here $u_\partial(x)$ is a chapeau function on Δ_N satisfying the boundary conditions and vanishing at each interior node x_i, $i = 1,\ldots,N$, and the functions $L_i(x)$ are elements of the chapeau basis on Δ_N.

To determine the nodal values $u_i(t)$, we force the residual $\partial\hat{u}/\partial t + \partial\hat{u}/\partial x - Pe^{-1}\partial^2\hat{u}/\partial x^2$ to be orthogonal to each basis function $L_j(x)$, $j = 1,\ldots,N$, with respect to the inner product $\langle f,g\rangle = \int_0^1 f(x)g(x)dx$. This requirement leads to a set of N ordinary differential equations for the $u_i(t)$:

$$\sum_{i=1}^{N} (\langle L_i,L_j\rangle du_i/dt + \langle L_i',L_j\rangle u_i + Pe^{-1}\langle L_i',L_j'\rangle u_i) = 0, \quad j = 1,\ldots,N \tag{5}$$

Computing the integrals then gives

$$\frac{\Delta x}{6}\frac{d}{dt}(u_{j-1}+4u_j+u_{j+1}) + \frac{1}{2}(u_{j+1}-u_{j-1}) - (\Delta x\, Pe)^{-1}(u_{j+1}-2u_j+u_{j-1}) = 0 \tag{6}$$

Equation (6) is similar to the centered difference formula, Equation (3), the only difference being a peculiar spatial average of time derivatives in Equation (6). This scheme, like Equation (3), produces wiggles when Δx is too large.

The method advanced by Heinrich et al. modifies Equation (5) by replacing the test functions in the convective term with asymmetric functions $L_j^*(x) = L_j(x) + \alpha A_j(x)$, where

$$A_j(x) = \begin{cases} 2[\Delta x^{-2}(x-x_{j-1})^2 - \Delta x^{-1}(x-x_{j-1})], & x \in [x_{j-1},x_j] \\ -2[\Delta x^{-2}(x-x_j)^2 - \Delta x^{-1}(x-x_j)], & x \in [x_j,x_{j+1}] \\ 0, & x \notin [x_{j-1},x_{j+1}] \end{cases}$$

and $\alpha > 0$. Thus the integral $\langle L_i',L_j^*\rangle$ appears in Equation (5) instead of $\langle L_i',L_j\rangle$, and the upstream-weighted Galerkin scheme differs from Equation (6) by $\alpha\langle L_i',A_j\rangle$. Simple calculation shows

$$\langle L_i',A_j\rangle = \begin{cases} -1/2, & i = j\pm1 \\ 1, & i = j \\ 0, & |i-j| > 1 \end{cases}$$

so the scheme proposed by Heinrich et al. reduces to

$$\frac{\Delta x}{6}\frac{d}{dt}(u_{j-1}+4u_j+u_{j+1}) + \frac{1}{2}(u_{j+1}-u_{j-1}) - \Delta x^{-1}(Pe^{-1}+\alpha\Delta x/2)(u_{j+1}-2u_j+u_{j-1}) \tag{7}$$

Therefore in a manner analogous to Equation (3), Equation (7) augments physical diffusion by an amount proportional to Δx, and this numerical dissipation mitigates wiggles at the expense of smearing.

Shapiro and Pinder (1981) introduce a related upwinding technique for use with finite-element collocation. Their approach entails the use of Hermite cubic interpolating bases (see Prenter, 1975, Chapter 3), except they perturb the trial function in the convective term by a piecewise quartic biased in the upstream direction. Shapiro and Pinder present a detailed Fourier analysis showing the dissipative effects of their upstream weighting on the propagation of sharp fronts.

There is another upwinding technique for finite-element collocation. Consider the standard implementation, in which the trial function has the form

$$\hat{u}(x,t) = u_\partial(x) + \sum_{i=1}^{N} [u_i(t)H_{0i}(x) + u_i'(t)H_{1i}(x)]$$

Here the coefficients $u_i(t)$, $u_i'(t)$ approximate the nodal values $u(x_i,t)$, $\partial u(x_i,t)/\partial x$, respectively, and $\{H_{0i},H_{1i}\}_{i=0}^{N+1}$ is the basis for Hermite cubic interpolation on Δ_N. The standard collocation method, which has truncation error $O(\Delta x^4)$, requires the residual to vanish,

$$\frac{\partial \hat{u}}{\partial t}(\bar{x}_k,t) + \frac{\partial \hat{u}}{\partial x}(\bar{x}_k,t) - Pe^{-1}\frac{\partial^2 \hat{u}}{\partial x^2}(\bar{x}_k,t) = 0 \qquad (8)$$

at each of $2N$ collocation points $\bar{x}_k = x_i + \Delta x/2 \pm \Delta x/\sqrt{3}$, $i = 1,\ldots,N$. As Figure 1 shows, unless Δx is sufficiently small the scheme generates wiggles near sharp fronts (Jensen and Finlayson, 1980).

A technique called upstream collocation (Allen and Pinder, 1983) offers a simple remedy to the wiggles, at the usual cost of smearing as shown in Figure 2. To implement the technique, simply shift the collocation points $\bar{x}_k$ in the convective term of Equation (8) to upstream points $\bar{x}_k^* = \bar{x}_k - \zeta\Delta x$. This gives

$$\frac{\partial \hat{u}}{\partial t}(\bar{x}_k,t) + \frac{\partial \hat{u}}{\partial x}(\bar{x}_k^*,t) - Pe^{-1}\frac{\partial^2 \hat{u}}{\partial x^2}(\bar{x}_k,t) = 0 \qquad (9)$$

in which the differentiated basis-function values $H_{mi}'(\bar{x}_k^*)$ appear in the convective term instead of $H_{mi}'(\bar{x}_k)$. By Taylor's theorem, the difference between these two values is $-\zeta\Delta x\, H_{mi}''(\bar{x}_k) + (\zeta^2\Delta x^2/2)H_{mi}'''(\bar{x}_k)$. Thus, to within $O(\Delta x^2)$, Equation 9 is equivalent to

$$\frac{\partial \hat{u}}{\partial t}(\bar{x}_k,t) + \frac{\partial \hat{u}}{\partial x}(\bar{x}_k,t) - (Pe^{-1} + \zeta\Delta x)\frac{\partial^2 \hat{u}}{\partial x^2}(\bar{x}_k,t) = 0 \qquad (10)$$

It is clear from this equation that numerical diffusion is again the mechanism by which the scheme mitigates wiggles.

Upstream collocation is closely related to an upwind Galerkin scheme introduced by Hughes (1978). This latter scheme involves numerical evaluation of the Galerkin integrals using quadrature points shifted upstream from the Gauss points. In fact, one can show an algebraic correspondence between upstream collocation and a variant of Hughes' method using reduced integration on Hermite trial spaces (Allen, to appear).

A NONLINEAR HYPERBOLIC EQUATION

Numerical dissipation makes upwinding attractive to modelers wishing to avoid wiggles in convection-dominated parabolic flows. It is precisely such motives that provoke justified ire in Gresho and Lee. There is, nevertheless, another motive for using upwind-biased schemes. Many physical systems combine minute dissipation with nonlinearity, obeying governing equations that are effectively hyperbolic. For these systems high-order discrete schemes may be mathematically inappropriate, not because they generate wiggles, but because

they fail to converge. Upwinding techniques then provide reasonable alternatives.

The Buckley-Leverett problem furnishes a simple example of a nonlinear hyperbolic equation for which high-order approximations fail. Consider a typical Cauchy problem for this equation:

$$\frac{\partial S}{\partial t} + \frac{\partial}{\partial x} f(S) = 0, \quad x,t > 0$$
$$S(0,t) = 1 - S_{or}, \quad S(x,0) = S_{wr} \tag{11}$$

Here S stands for water saturation; f(S) is a nonconvex, monotonically increasing function giving the flux of S; and S_{or} and S_{wr} are the minimum oil and water saturations, respectively, for the rock-fluid mixture. Equation (11) models immiscible flows in porous media in which capillarity exerts a negligible influence on fluid velocities. A prime feature of Equation (11) is the propagation of a saturation shock through the porous medium. This problem serves as a prototype for many kinds of nonlinear, hyperbolic or nearly hyperbolic systems of flow equations that occur in applications where convective forces are dominant.

It is widely known that spatially centered approximations to Equation (11) can converge to incorrect solutions. Allen and Pinder (1983), for example, examine the finite-element collocation approximation to this problem using both the conventional formulation and the upstream collocation scheme discussed above. As Figures 3 and 4 show, the conventional method predicts a saturation shock that is too slow and too strong, whereas the upstream method gives good approximations to the true shock. No amount of grid refinement can correct the failure of the conventional scheme. The difficulty here is not one of spurious wiggles; it is a deeper problem concerning the suitability of numerical methods from a mathematical standpoint.

Others have reported results similar to those displayed in Figures 3 and 4. Huyakorn and Pinder (1978) use the upstream-weighted Galerkin scheme reviewed above to overcome convergence difficulties with the standard Galerkin method in solving Equation (11). Mercer and Faust (1977) accomplish the same end by adding an adjustable capillary term to the discrete equations. Shapiro and Pinder (1980) use their upstream-weighted collocation method to produce convergent solutions to Equation (11). Indeed, upstream weighting has become standard practice for immiscible flow modeling in the oil industry (Aziz and Settari, 1979, Chapter 5).

UNIQUENESS AND HYPERBOLIC CONSERVATION LAWS

To see why upwind schemes converge for the Buckley-Leverett equation and similar problems, it is useful to review some mathematical facts about Equation (11). This equation is a quasilinear hyperbolic conservation law. When such equations have nonconvex flux functions like f(S), one cannot expect Cauchy problems for the equations to possess classical solutions. Instead, one may have to settle for weak solutions, defined for Equation (11) by the integral criterion

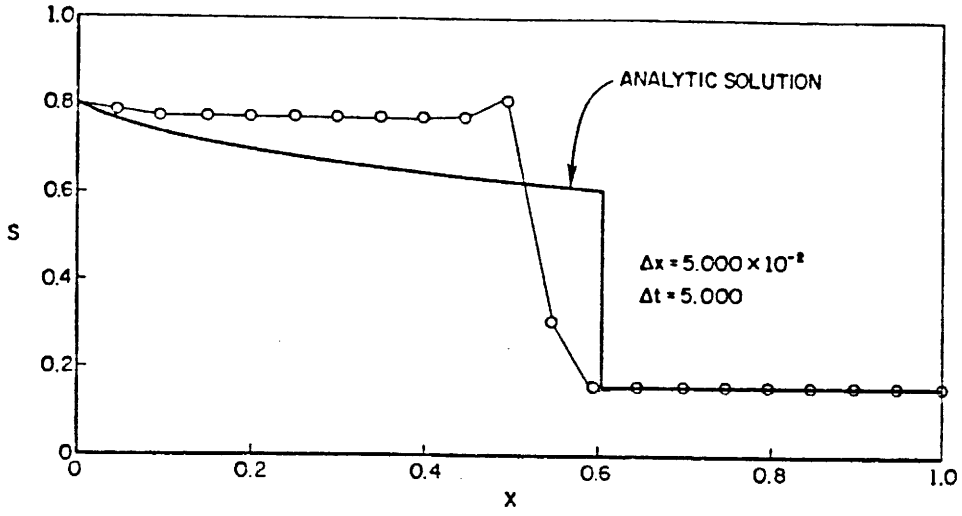

Figure 3. Solution to the Buckley-Leverett problem using standard collocation on finite elements.

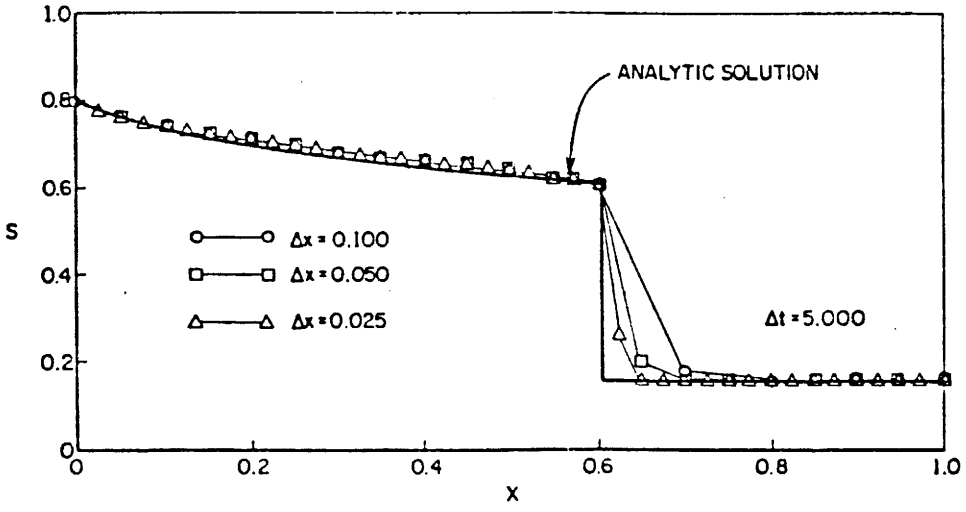

Figure 4. Solutions to the Buckley-Leverett problem using upstream collocation with spatial grids of varying mesh.

$$\int_0^\infty \int_0^\infty \left[S \frac{\partial \phi}{\partial t} + f(S) \frac{\partial \phi}{\partial x} \right] dx\, dt = 0$$

for any C^∞ real-valued function $\phi(x,t)$ with compact support. This criterion reduces to Equation (11) when $S(x,t)$ is continuously differentiable but also admits solutions $S(x,t)$ having shocks.

However, Cauchy problems like Equation (11) may not have unique weak solutions. To guarantee uniqueness for general initial data requires an additional constraint. The correct constraint, or shock condition, requires the weak solution to depend continuously and stably on the initial data. Equivalently, characteristic curves emanating from both sides of a discontinuity must intersect the curve on which the initial data are given. Oleinik (1963) proves a uniqueness condition on weak solutions that is mathematically equivalent to the shock condition but has more immediate implications for discrete approximations. Her criterion essentially states that the solution to the hyperbolic equation must be the limit of solutions, for comparable data, to a parabolic equation differing from the hyperbolic one by a dissipative second-order term of vanishing influence. In gas dynamics, this second-order term is called "vanishing viscosity"; for the Buckley-Leverett problem the term "vanishing capillarity" is perhaps more appropriate.

High-order, spatially centered discretizations of the Buckley-Leverett problem, though formally consistent with Equation (11), yield approximate weak solutions that are physically and mathematically incorrect. From a physical standpoint the neglected capillary term in Equation (11), which has the form

$$- \frac{\partial}{\partial x} \left[F(S) \frac{\partial S}{\partial x} \right], \quad F(S) \geq 0 \tag{12}$$

exerts an important influence in a microscopic region of what appears to macroscopic observers as a saturation shock. Thus while the global effects of capillarity may be legitimately neglected in the macroscopic flow equation, some device must remain to guarantee that the solution $S(x,t)$ respect the microscopic physics. Artificial capillarity is such a device.

It is a relatively simple matter to see how various upwinded approximations contribute artificial capillarity. For example, an upstream-weighted difference approximation to Equation (11) that is analogous to Equation (3) yields a flux term that has the form

$$\begin{aligned} \Delta x^{-1}(f_i - f_{i-1}) &= \frac{\partial f}{\partial x}\bigg|_i - (\Delta x/2) \frac{\partial^2 f}{\partial x^2}\bigg|_i + O(\Delta x^2) \\ &= \frac{\partial f}{\partial x}\bigg|_i - (\Delta x/2) \frac{\partial}{\partial x} \left[f'(S) \frac{\partial S}{\partial x} \right]\bigg|_i + O(\Delta x^2) \end{aligned} \tag{13}$$

Since $f'(S) \geq 0$, it is clear that the lowest error term here mimics the missing physical capillarity of Equation (12), while preserving consistency.

Similarly, the use of upstream-biased test functions in the Galerkin scheme analogous to Equation (7) yields approximations to the flux term of Equation

(11) having an error

$$\langle \partial \hat{f}/\partial x, A_j \rangle = \sum_{i=1}^{N} f_i \alpha \langle L_i', A_j \rangle$$

$$= -(\alpha/2)[f_{j+1} - 2f_j + f_{j-1}] = -(\alpha \Delta x^2/2)\left[\frac{\partial^2 \hat{f}}{\partial x^2}\bigg|_j + O(\Delta x^2) \right]$$

$$= -(\alpha \Delta x^2/2) \frac{\partial}{\partial x}\left[f'(\hat{S}) \frac{\partial \hat{S}}{\partial x} \right]_j + O(\Delta x^2)$$

where $f_i = f(\hat{S}_i(t))$ and $\hat{S}$ is the trial function approximating S. Notice that, parallelling Equation (13), the use of asymmetric test functions adds a numerical capillarity that is $O(\Delta x)$ smaller than the approximations to physical terms in Equation (11).

Upstream collocation also adds artificial capillarity to the Buckley-Leverett problem. In this case we project the flux term of Equation (11) to a Hermite interpolating space and collocate the result $\partial \hat{f}/\partial x$ at points $\bar{x}_k^* = \bar{x}_k - \zeta \Delta x$ upstream of the usual collocation points. A Taylor expansion shows

$$\frac{\partial \hat{f}}{\partial x}(\bar{x}_k^*, t) - \frac{\partial \hat{f}}{\partial x}(\bar{x}_k, t) = -\zeta \Delta x \frac{\partial^2 \hat{f}}{\partial x^2}(\bar{x}_k, t) + O(\Delta x^2)$$

$$= -\zeta \Delta x \frac{\partial}{\partial x}\left[f'(\hat{S}(\bar{x}_k, t)) \frac{\partial \hat{S}}{\partial x}(\bar{x}_k, t) \right] + O(\Delta x^2)$$

Again, the upwind scheme adds the necessary artificial dissipation in the form of a "vanishing capillarity."

Various physics give rise to effectively hyperbolic systems for which uniqueness of weak solutions is an important issue. For such systems formal neglect of dissipation, while arguably valid from an engineering viewpoint, necessitates a device like upwinding to guarantee qualitatively correct numerical solutions. Other examples of interest in water resources engineering include hydraulic jumps (Whitham, 1974, Chapter 13) and wetting fronts in variably saturated soils (Nakano, 1980).

CONCLUSIONS

Upwinding can serve two purposes: it can suppress wiggles or, for certain equations, it can guarantee convergence. As Gresho and Lee observe, the first purpose is largely cosmetic, and the attendant smearing may be a more difficult flaw to recognize than spurious oscillations. However, in the case of conservation laws with discontinuous weak solutions upwinding can be a legitimate practice. The aim in this second case is to formulate consistent approximations that have built-in mechanisms for accommodating the peculiarities of hyperbolic or nearly hyperbolic flows. The lower spatial accuracy inherent in upwind schemes is far preferable to the convergence failures of higher-order schemes. Indeed, in the neighborhood of a discontinuity the very notion of "order of accuracy" can be problematic.

Despite the mathematical validity of upwinding, the problem of smearing remains. While numerical dissipation vanishes with Δx, in practice Δx never vanishes and may be so large that artificial smearing is unacceptable. One of the most promising remedies to this difficulty is adaptive local grid refinement. Here one uses a spatial grid having smaller elements in portions of the flow

field where steep solution gradients drive numerical dissipation. Algorithms combining local grid refinement with upwinding allow both for convergence to correct weak solutions and for the reduction of artificial smearing near sharp fronts. There is no denying the formidable coding difficulties in adaptive local grid refinement; however, progress in this field is encouraging (see Ewing, to appear).

ACKNOWLEDGEMENTS

Partial support for this work came from National Science Foundation grant number NSF-CEE-8111240 and from the Wyoming Water Research Center.

REFERENCES

1. Allen, M.B. (to appear), "How upstream collocation works," Int. J. Num. Meth. Engrg.
2. Allen, M.B., and Pinder, G.F. (1983), "Collocation simulation of multiphase porous-medium flow," Soc. Pet. Eng. J. (February), 135-142.
3. Aziz, K., and Settari, A. (1979), Petroleum Reservoir Simulation, London: Applied Science.
4. Ewing, R. (to appear), "Adaptive mesh refinement in reservoir simulation applications," to be presented at the International Conference on Accuracy Estimates and Adaptive Refinement in Finite Element Computations, Lisbon, Portugal, June, 1984.
5. Gresho, P.M., and Lee, R.L. (1980), "Don't suppress the wiggles--they're telling you something!", in Finite Element Methods for Convection Dominated Flows, ed. by T.J.R. Hughes, New York: American Society of Mechanical Engineers, 37-61.
6. Heinrich, J.C., Huyakorn, P.S., Zienkiewicz, O.C., and Mitchell, A.R. (1977), "An 'upwind' finite element scheme for two-dimensional convective transport equation," Int. J. Num. Meth. Engrg. 11, 131-143.
7. Hughes, T.J.R. (1978), "A simple scheme for developing upwind finite elements," Int. J. Num. Meth. Engrg. 12, 1359-1365.
8. Huyakorn, P.S., and Pinder, G.F. (1978), "A new finite element technique for the solution of two-phase flow through porous media," Adv. Water Resources 1:5, 285-298.
9. Jensen, O.K., and Finlayson, B.A. (1980), " Oscillation limits for weighted residual methods applied to convective diffusion equations," Int. J. Num. Meth. Engrg. 15, 1681-1689.
10. Mercer, J.W., and Faust, C.R. (1977), "The application of finite-element techniques to immiscible flow in porous media," presented at the First International Conference on Finite Elements in Water Resources, Princeton, NJ, July, 1976.
11. Nakano, Y. (1980), "Application of recent results in functional analysis to the problem of wetting fronts," Water Res. Research 16, 314-318.
12. Oleinik, O.A. (1963), "Construction of a generalized solution of the Cauchy problem for a quasi-linear equation of the first order by the introduction of a 'vanishing viscosity'," Am. Math. Soc. Transl. (Ser. 2), 33, 277-283.
13. Prenter, P.M. (1975), Splines and Variational Methods, New York: Wiley.
14. Shapiro, A.M., and Pinder, G.F. (1981), "Analysis of an upstream weighted approximation to the transport equation," J. Comp. Phys. 39,

46-71.

15. Shapiro, A.M., and Pinder, G.F. (1982), "Solution of immiscible displacement in porous media using the collocation finite element method," presented at the Fourth International Conference on Finite Elements in Water Resources, Hannover, FRG, June, 1982.
16. Von Neumann, J., and Richtmyer, R.D. (1950), "A method for the numerical calculations of hydrodynamical shocks," J. Appl. Phys. 21, 232-237.
17. Whitman, G.B. (1974), Linear and Nonlinear Waves, New York: Wiley.

MECHANICS OF MULTIPHASE FLUID FLOWS IN VARIABLY SATURATED POROUS MEDIA

Myron B. Allen

Department of Mathematics

University of Wyoming

Laramie, Wyoming 82071

August, 1984

Revised November, 1984

Abstract

This paper proposes a set of flow equations governing the simultaneous movement of aqueous and nonaqueous liquids in variably saturated soils. The basic principles and balance laws of continuum mixture theory, along with thermodynamically admissible constitutive laws and simplifying kinematic assumptions, yield a formulation for isochoric multiphase flows through a nondeforming porous matrix. Cast in terms of familiar quantities, the governing equations are similar in form to the classic Richards' equation for each liquid phase. The development suggests new rock-fluid properties that must be measured to characterize multiphase flows in the unsaturated zone.

Introduction.

Groundwater contamination by liquids having limited miscibility with water has attracted increasing scientific and legal attention. While studies of groundwater pollution classically have focussed on single-phase flow and transport, many hazardous substances entering our aquifers are relatively insoluble in water and hence flow through porous media as separate, nonaqueous liquid phases. The physics of such flows differ substantially from the physics of single-liquid flows. Especially problematic are simultaneous flows of several liquid phases through the variably saturated zones of soils, which contaminants dumped near the earth's surface often must traverse before reaching saturated aquifers. This paper examines the basic mechanics of multiphase flows in variably saturated soils and proposes an extension of the theory of single-liquid flows to cases where water and nonaqueous liquids flow simultaneously.

Investigations of the mechanics of water flowing in the variably saturated zone date to Richards [1931]. Indeed, Richards' formulation is now the most widely used model of water movement in unsaturated soils. Prominent among subsequent investigations of the dynamics of partially saturated flow are papers by Philip [1954] and Zaslovsky [1964]. Bear et al. [1968] provide an excellent review of the classical literature in this field. Narasimhan and Witherspoon [1977] extend these basic models to include the effects of deformation in the solid porous matrix. More recently, studies by Prévost [1980] and Bowen [1980, 1982] have exploited the continuum theory of mixtures, as developed by Eringen and Ingram [1965, 1967] and reviewed by Atkin and Craine [1976], to derive the partial differential equations governing fluid flows in saturated porous media. The present study also relies on the theory of mixtures but aims at a model of unsaturated media containing two liquid phases under some simplify-

ing assumptions.

In contrast to the physics of saturated porous media and variably saturated media with a single liquid, multi-liquid flows in the unsaturated zone have received fairly scant experimental attention. Thus the development that follows amounts to a proposed model and should not be viewed as an a posteriori explanation of observations.

Kinematics.

Consider a mixture comprising four constituents, which we shall label R (rock), aqueous liquid (W), nonaqueous liquid (N), and air (A). These constituents represent four phases of concern in the simultaneous flow of water and oily contaminants in the vadose zones of soils. Our aim is to describe the movements of these constituents and, ultimately, to derive flow equations governing their dynamics.

Corresponding to each constituent α is a body $\mathcal{B}^\alpha$, which is a collection of material points labeled X^α. The four bodies $\mathcal{B}^R$, $\mathcal{B}^W$, $\mathcal{B}^N$, $\mathcal{B}^A$ form a collection of overlapping continua, so that conceptually each spatial point at which the mixture resides may harbor material points from each of the bodies $\mathcal{B}^\alpha$. Following the standard procedure in mixture theory, let us establish for each body a reference configuration, so that we can label each material point X^α by its spatial position $\underset{\sim}{X}^\alpha$ in that configuration. The motion of the body $\mathcal{B}^\alpha$ is then the function $\underset{\sim}{x} = \underset{\sim}{x}^\alpha(\underset{\sim}{X}^\alpha,t)$ giving the spatial coordinates of any material point $\underset{\sim}{X}^\alpha$ at any time $t \in [0,\infty)$. Under the hypothesis that each motion is a continuously differentiable function with nonzero Jacobian determinant $\det[\partial x_i^\alpha/\partial X_j^\alpha]$, the inverse function theorem guarantees the existence of an inverse motion defined at each time t by $\underset{\sim}{X}^\alpha = \underset{\sim}{X}^\alpha(\underset{\sim}{x},t)$. Given the motions $\underset{\sim}{x}^\alpha$, we can define the Lagrangian and Eulerian velocities

$$\underset{\sim}{v}^{\alpha} = \begin{cases} \dfrac{\partial \underset{\sim}{x}^{\alpha}}{\partial t}(\underset{\sim}{X}^{\alpha},t) = \underset{\sim}{v}^{\alpha}(\underset{\sim}{X}^{\alpha},t) & \text{(Lagrangian)} \\ \dfrac{\partial \underset{\sim}{x}^{\alpha}}{\partial t}(\underset{\sim}{X}^{\alpha}(\underset{\sim}{x}^{\alpha},t),t) = \underset{\sim}{v}^{\alpha}(\underset{\sim}{x}^{\alpha},t) & \text{(Eulerian)} \end{cases}$$

as well as other Lagrangian and Eulerian quantities describing each body's motion.

Also associated with each body $\mathcal{B}^{\alpha}$ is a non-negative scalar function M^{α} defined on measurable subsets V of the spatial configuration $\underset{\sim}{x}(\mathcal{B}^{\alpha})$ at any time $t \geq 0$. Physically, the value $M^{\alpha}(V,t)$ is the mass of phase α contained in the set V of spatial points at time t. If at each time t M^{α} is absolutely continuous with respect to Lebesgue measure on three-dimensional Euclidean space, then by the Radon-Nikodym theorem there must be some scalar function $\xi^{\alpha}: \underset{\sim}{x}(\mathcal{B}^{\alpha}) \times [0,\infty) \to [0,\infty)$ such that

$$M^{\alpha}(V,t) = \int_V \xi^{\alpha}(\underset{\sim}{x},t)\, dv$$

The function ξ^{α} is the bulk mass density of α, giving the mass of phase α per unit volume of mixture.

By analogy with the mass density we can also define the volume fraction occupied by phase α at a given point in the spatial configuration of $\mathcal{B}^{\alpha}$. To each $\mathcal{B}^{\alpha}$ associate a non-negative scalar function F^{α}, whose domain at any time t is the collection of measurable subsets V of $\underset{\sim}{x}(\mathcal{B}^{\alpha})$, such that $F^{\alpha}(V,t)$ gives the volume in V occupied by phase α. It is clear that $0 \leq F^{\alpha}(V) \leq \int_V dv$. If F^{α} is absolutely continuous with Lebesgue measure on Euclidean three-space, then we have a scalar function $\phi^{\alpha}: \underset{\sim}{x}(\mathcal{B}^{\alpha}) \times [0,\infty) \to [0,1]$ such that

$$F^{\alpha}(V,t) = \int_{V} \phi^{\alpha}(\underset{\sim}{x},t)\, dv$$

The function ϕ^{α} is the volume fraction of phase α, and the collection $\{\phi^{R},\phi^{W},\phi^{N},\phi^{A}\}$ must obey the constraint

$$\sum_{\alpha} \phi^{\alpha} = 1$$

Given the functions ξ^{α} and ϕ^{α} for each phase, we can define the intrinsic mass densities. These are $\rho^{\alpha} = \xi^{\alpha}/\phi^{\alpha}$, which are meaningful quantities only where $\phi^{\alpha} \neq 0$, that is, where material from phase α is actually present. The function ρ^{α} gives the mass of phase α per unit volume of phase α. Having established the functions ξ^{α}, ϕ^{α}, and ρ^{α} and the phase velocities $\underset{\sim}{v}^{\alpha}$, we can define a variety of quantities useful in describing the motions of the phases. Table 1 summarizes these definitions.

To describe the rates of change of various quantities with time we need to introduce material derivatives. As is usual in mixture theory, if f is a Lagrangian quantity, so that $f = f(\underset{\sim}{X}^{\alpha},t)$, then the material derivative of f with respect to phase α is the time rate of change of f following a fixed material point $\underset{\sim}{X}^{\alpha}$ in phase α:

$$\overset{\alpha}{\frac{Df}{Dt}}(\underset{\sim}{X}^{\alpha},t) = \frac{\partial f}{\partial t}(\underset{\sim}{X}^{\alpha},t)$$

On the other hand, if f is an Eulerian quantity, implying $f = f(\underset{\sim}{x}^{\alpha},t)$, then

$$\overset{\alpha}{\frac{Df}{Dt}}(\underset{\sim}{x}^{\alpha},t) = \frac{\partial f}{\partial t}(\underset{\sim}{x}^{\alpha},t) + \underset{\sim}{v}^{\alpha}(\underset{\sim}{x}^{\alpha},t) \cdot \nabla f(\underset{\sim}{x}^{\alpha},t)$$

where the operator ∇ signifies the gradient with respect to spatial position; in Cartesian coordinates $\nabla = \left(\frac{\partial}{\partial x_1}, \frac{\partial}{\partial x_2}, \frac{\partial}{\partial x_3}\right)$.

We can also associate with the mixture a barycentric material derivative, given by

$$\frac{D}{Dt} = \frac{\partial}{\partial t} + \underset{\sim}{v} \cdot \nabla$$

where $\underset{\sim}{v}$ is the barycentric velocity defined in Table 1. The operator $\frac{D}{Dt}$ is related to $\overset{\alpha}{\frac{D}{Dt}}$ as follows:

$$\overset{\alpha}{\frac{D}{Dt}} = \frac{D}{Dt} + \underset{\sim}{v}^{\alpha} \cdot \nabla$$

where $\underset{\sim}{v}^{\alpha} = \underset{\sim}{v}^{\alpha} - \underset{\sim}{v}$ is the diffusion velocity, also defined in Table 1. Finally, we shall encounter intensive variables Ψ^{α} appearing in mass-weighted sums over all phases, as in the equation

$$\rho\Psi = \sum_{\alpha} \phi^{\alpha}\rho^{\alpha}\psi^{\alpha}$$

defining the "mixture property" Ψ. When working with sums of this sort we shall find the following identity useful:

$$\rho \frac{D\Psi}{Dt} = \sum_{\alpha} \phi^{\alpha}\rho^{\alpha} \overset{\alpha}{\frac{D\psi^{\alpha}}{Dt}} - \nabla \cdot \sum_{\alpha} \phi^{\alpha}\rho^{\alpha}\psi^{\alpha}\underset{\sim}{v}^{\alpha} \qquad (1)$$

Balance Laws.

The equations governing multiphase contaminant flows in the unsaturated zone arise from the balance laws for mixtures, modified by constitutive assumptions and restrictions imposed by the Clausius-Duhem inequality of thermodynamics. We shall stipulate that the multiphase mixtures of interest are isothermal and have no heat sources, so that it will not be necessary to solve an energy balance equation explicitly. However, the mass, momentum, angular momentum, and energy balances, together with an entropy inequality corresponding to the second law of thermodynamics, are all essential to the complete dynamic specification of the systems. The mixture balance laws, in their primitive form, assert relationships among certain integrals over material volumes and their bounding surfaces. A standard sequence of arguments reduces these integral laws to differential forms involving sums of densities, fluxes, and sources over all constituents in the mixture. Then, by introducing constituent exchange terms, one can reduce the differential balance laws for the mixture to differential laws for each constituent. Since Bowen [1976] reviews this development, the present section simply states the balance laws and gives their particular forms under appropriate assumptions about the mixture.

The differential form of the mass balance for any phase α is

$$\frac{\overset{\alpha}{D}}{Dt}(\phi^{\alpha}\rho^{\alpha}) + \phi^{\alpha}\rho^{\alpha}\nabla\cdot\underset{\sim}{v}^{\alpha} = r^{\alpha}$$

where r^{α} signifies the rate of exchange of mass into phase α from other phases as a result of chemical reactions, phase changes, adsorption, dissolution, and the like. To be consistent with the global mass balance for the mix-

ture, the exchange terms r^α must satisfy $\sum_\alpha r^\alpha = 0$. We shall simplify matters by allowing no interphase mass transfer, so that each $r^\alpha = 0$, and the mass balance reduces to

$$\overset{\alpha}{\frac{D}{Dt}}(\phi^\alpha \rho^\alpha) + \phi^\alpha \rho^\alpha \nabla \cdot \underset{\sim}{v}^\alpha = 0 \ . \tag{2}$$

It is worth noting that exchange terms may be present in many contaminant flows of practical interest, where dissolution and microbial degradation of organic liquids may be significant [Schwille, 1984]. In these cases one must retain r^α in Equation (2).

The primitive differential momentum balance is

$$\overset{\alpha}{\frac{D}{Dt}}(\phi^\alpha \rho^\alpha \underset{\sim}{v}^\alpha) + \phi^\alpha \rho^\alpha \underset{\sim}{v}^\alpha \nabla \cdot \underset{\sim}{v}^\alpha - \nabla \cdot \underset{\approx}{t}^\alpha - \phi^\alpha \rho^\alpha \underset{\sim}{b}^\alpha = \underset{\sim}{\hat{p}}^\alpha$$

Here $\underset{\approx}{t}^\alpha$ denotes the stress tensor for phase α, $\underset{\sim}{b}^\alpha$ signifies the rate at which body forces contribute to the momentum density, and $\underset{\sim}{\hat{p}}^\alpha$ represents the exchange of momentum into phase α from other phases. As in the mass balances, the exchange terms must obey the restriction $\sum_\alpha \underset{\sim}{\hat{p}}^\alpha = \underset{\sim}{0}$. By expanding the primitive momentum balance and eliminating terms that sum to zero according to the mass balance, one finds

$$\phi^\alpha \rho^\alpha \overset{\alpha}{\frac{D\underset{\sim}{v}^\alpha}{Dt}} - \nabla \cdot \underset{\sim}{t}^\alpha - \phi^\alpha \rho^\alpha \underset{\sim}{b}^\alpha = \underset{\sim}{\hat{p}}^\alpha \tag{3}$$

In the mechanics of single continua it is well known that the primitive

balance of angular momentum reduces, in the absence of body couples, to the symmetry of the stress tensor, $\underset{\approx}{t} - \underset{\approx}{t}^T = \underset{\approx}{0}$. Here $\underset{\approx}{t}^T$ denotes the transpose of the stress tensor $\underset{\approx}{t}$. For mixtures, the analogous argument leads to a weaker statement, namely

$$\underset{\approx}{t}^\alpha - (\underset{\approx}{t}^\alpha)^T = \underset{\approx}{M}^\alpha$$

where $\underset{\approx}{M}^\alpha$ stands for the exchange of angular momentum into phase α from other phases. Let us assume that angular momentum exchanges are absent. In this case the angular momentum balance for any constituent α reduces to

$$\underset{\approx}{t}^\alpha - (\underset{\approx}{t}^\alpha)^T = \underset{\approx}{0} ,$$

that is, the stress tensor of each phase is symmetric.

The primitive form of the differential energy balance is

$$\overset{\alpha}{\frac{D}{Dt}}(\phi^\alpha\rho^\alpha E^\alpha + \tfrac{1}{2}\phi^\alpha\rho^\alpha \underset{\sim}{v}^\alpha\cdot\underset{\sim}{v}^\alpha) + \phi^\alpha\rho^\alpha(E^\alpha + \tfrac{1}{2}\underset{\sim}{v}^\alpha\cdot\underset{\sim}{v}^\alpha)\nabla\cdot\underset{\sim}{v}^\alpha$$

$$- \nabla\cdot(\underset{\sim}{q}^\alpha + \underset{\approx}{t}^\alpha\cdot\underset{\sim}{v}^\alpha) - \phi^\alpha\rho^\alpha h^\alpha - \phi^\alpha\rho^\alpha \underset{\sim}{b}^\alpha\cdot\underset{\sim}{v}^\alpha = \varepsilon^\alpha$$

In this equation, E^α is the internal energy of phase α per unit mass; $\underset{\sim}{q}^\alpha$ is the heat flux vector in phase α; and h^α is the rate of contribution to the total energy per unit mass from heat sources. The term $\frac{1}{2}\phi^\alpha\rho^\alpha\underset{\sim}{v}^\alpha\cdot\underset{\sim}{v}^\alpha$ clearly accounts for kinetic energy; $-\nabla\cdot(\underset{\approx}{t}^\alpha\cdot\underset{\sim}{v}^\alpha)$ is the rate of working and heating attributable to stress, and $-\phi^\alpha\rho^\alpha\underset{\sim}{b}^\alpha\cdot\underset{\sim}{v}^\alpha$ represents the rate of working of body forces. The quantity ε^α on the right of the energy balance again stands for

the rate of exchange of energy into phase α from other phases, subject to the restriction $\sum_{\alpha} \varepsilon^{\alpha} = 0$.

As with the momentum balance, it is possible to eliminate certain terms from the primitive energy balance by observing that their sum is proportional to the left side of the mass balance (2). Furthermore, one can notice that several "mechanical energy" terms in the energy balance also appear when one forms the dot product of the momentum balance (3) with $\underset{\sim}{v}^{\alpha}$. Using the mass and momentum balances in this way to simplify the energy balance yields a "thermal energy balance,"

$$\phi^{\alpha}\rho^{\alpha}\frac{\overset{\alpha}{D}E^{\alpha}}{Dt} - \underset{\approx}{t}^{\alpha}:\nabla\underset{\sim}{v}^{\alpha} - \nabla\cdot\underset{\sim}{q}^{\alpha} - \phi^{\alpha}\rho^{\alpha}h^{\alpha} = \varepsilon^{\alpha} - \underset{\sim}{\hat{p}}^{\alpha}\cdot\underset{\sim}{v}^{\alpha} \tag{4}$$

For our purposes the most useful energy balance is not the balance equation for each phase but rather the overall balance for the mixture. To get this equation, simply sum equation (4) over all phases α. Bearing in mind the identity (1) we find, after simplifying,

$$\frac{D}{Dt}\sum_{\alpha}\phi^{\alpha}\rho^{\alpha}E^{\alpha} + (\nabla\cdot\underset{\sim}{v})\sum_{\alpha}\phi^{\alpha}\rho^{\alpha}E^{\alpha} - \sum_{\alpha}\underset{\approx}{t}^{\alpha}:\nabla\underset{\sim}{v}^{\alpha}$$
$$+ \nabla\cdot\sum_{\alpha}(\phi^{\alpha}\rho^{\alpha}E^{\alpha}\underset{\sim}{v}^{\alpha} - \underset{\sim}{q}^{\alpha}) - \sum_{\alpha}\phi^{\alpha}\rho^{\alpha}h^{\alpha} = \sum_{\alpha}\underset{\sim}{p}^{\alpha}\cdot\underset{\sim}{v}^{\alpha}$$

Now define the inner part E_I of the total internal energy as

$$E_I = \frac{1}{\rho}\sum_{\alpha}\phi^{\alpha}\rho^{\alpha}E^{\alpha}$$

and the total heat flux $\underset{\sim}{q}$ and total heat source h as

$$\underset{\sim}{q} = \sum_{\alpha} (\underset{\sim}{q}^{\alpha} - \phi^{\alpha}\rho^{\alpha}E^{\alpha}\underset{\sim}{v}^{\alpha})$$

$$h = \frac{1}{\rho}\sum_{\alpha} \phi^{\alpha}\rho^{\alpha}h^{\alpha}$$

With these definitions, the overall energy balance reduces to

$$\rho\frac{DE_I}{Dt} - \sum_{\alpha} \underset{\approx}{t}^{\alpha}:\underset{\sim}{v}^{\alpha} - \nabla\cdot\underset{\sim}{q} - \rho h = \sum_{\alpha} \underset{\sim}{p}^{\alpha}\cdot\underset{\sim}{v}^{\alpha} \tag{5}$$

Finally, certain thermodynamic restrictions on the behavior of the mixture follow from the Clausius-Duhem inequality governing entropy changes. There is apparently no universally accepted form of this entropy inequality; Atkin and Craine [1976], for example, review the history of this controversy. Passman et al. [1984] also discuss the entropy inequality, noting some of the less satisfactory aspects of the mixture inequality as compared with the entropy inequality valid for single-constituent continua. The version adopted here is essentially that used in Bowen's [1980] development for fluid flow in incompressible porous media. In differential form, this law states that

$$\sum_{\alpha}\left[\frac{D^{\alpha}}{Dt}(\phi^{\alpha}\rho^{\alpha}\eta^{\alpha}) + \phi^{\alpha}\rho^{\alpha}\eta^{\alpha}\nabla\cdot\underset{\sim}{v}^{\alpha} - \frac{1}{T^{\alpha}}\nabla\cdot\underset{\sim}{q}^{\alpha} - \frac{1}{T^{\alpha}}\phi^{\alpha}\rho^{\alpha}h^{\alpha}\right] \geq 0$$

where η^α is the entropy per unit mass in the α phase and T^α is the temperature of the α phase, assumed positive. Let us henceforth assume that the phases in the mixture share a constant, spatially uniform temperature T. By defining the total entropy of the mixture as

$$\eta = \frac{1}{\rho} \sum_\alpha \phi^\alpha \rho^\alpha \eta^\alpha$$

and using the identity (1), we can then rewrite the primitive inequality as

$$\rho \frac{D\eta}{Dt} - \nabla \cdot \sum_\alpha \left(\frac{1}{T} \underset{\sim}{q}^\alpha - \phi^\alpha \rho^\alpha \eta^\alpha \underset{\sim}{v}^\alpha \right) - \sum_\alpha \frac{1}{T} \phi^\alpha \rho^\alpha h^\alpha \geq 0$$

Now we can use the energy balance (5) to substitute for the last term on the left of this inequality. After some simplification, this yields

$$- \sum_\alpha \phi^\alpha \rho^\alpha \frac{DA^\alpha}{Dt} + \sum_\alpha \underset{\approx}{t}^\alpha : \nabla \underset{\sim}{v}^\alpha + \sum_\alpha \hat{\underset{\sim}{p}}^\alpha \cdot \underset{\sim}{v}^\alpha \geq 0 \qquad (6)$$

The quantity A^α appearing in this inequality is the Helmholtz free energy, defined as $A^\alpha = E^\alpha - T\eta^\alpha$.

Constitutive Assumptions.

To apply the balance laws, which have rather general validity, to specific mixtures such as variably saturated porous media, we need to make some assumptions restricting the class of materials to which these laws apply. The restrictions of interest include certain kinematic assumptions regarding the nature of the motions, internal constraints on the possible responses of the bodies, and constitutive laws giving functional relationships between various quantities appearing in the balance equations. The constitutive laws also serve a mathematical purpose in closing the deficit between equations and unknowns in the mechanical formulation of the theory.

Let us assume first that the fluids flow isochorically, so that $\overset{\alpha}{D}\rho^{\alpha}/Dt = 0$ for each fluid phase α. Thus, while some of the fluids occupying the rock's interstices may exhibit significant compressibilities, the velocities of interest are sufficiently small that the effects of compressibility on the flow field are negligible. Since fluid densities must be positive, the assumption that fluid motions are isochoric reduces the mass balance for fluids (2) to

$$\frac{\partial \phi^{\alpha}}{\partial t} + \nabla\cdot(\phi^{\alpha}\underset{\sim}{v}^{\alpha}) = 0 \ , \quad \alpha = W,N,A \ .$$

Second, assume that the rock matrix moves rigidly, so that the Jacobian of its motion is just the identity tensor:

$$\nabla_{\underset{\sim}{X}^{R}} \underset{\sim}{x} = \underset{\approx}{F}^{R} = \underset{\approx}{1} \ .$$

This assumption allows us to affix a rigid Cartesian coordinate system to the rock phase, forcing $\underset{\sim}{v}^{R} = \underset{\sim}{0}$. Also, since a rigid motion must be isochoric,

the rock mass balance becomes

$$\frac{D\phi^R}{Dt}^R = \frac{\partial \phi^R}{\partial t} = 0$$

Now define the porosity of the rock matrix to be $\phi = 1 - \phi^R$, that is, the total volume fraction available to fluids. Since each fluid phase occupies a fraction of the voids, let us call $S^\alpha = \phi^\alpha/\phi$ the saturation of fluid α, where $\alpha = W,N,A$.

As constitutive laws for fluid stresses, let us postulate that each fluid phase $\alpha = W,N,A$ possesses a stress tensor

$$\underset{\approx}{t}^\alpha = -p^\alpha \underset{\approx}{1} + \sum_\beta \lambda^{\alpha\beta} \operatorname{trace}(\underset{\approx}{d}^\beta)\underset{\approx}{1} + \sum_\beta 2\mu^{\alpha\beta}\underset{\approx}{d}^\beta \tag{7}$$

Here the dummy index β ranges over all fluid phases. The tensor $\underset{\approx}{d}^\alpha = \frac{1}{2}[\nabla \underset{\sim}{v}^\alpha + (\nabla \underset{\sim}{v}^\alpha)^T]$ is the deformation rate in fluid phase α; $\lambda^{\alpha\alpha} = \lambda^\alpha$ and $\mu^{\alpha\alpha} = \mu^\alpha$ are the coefficients of viscosity of the fluid α, and $\lambda^{\alpha\beta}$, $\mu^{\alpha\beta}$, $\alpha \neq \beta$, are coefficients of interphase traction between fluids α and β. The parameter p^α is the mechanical pressure in fluid phase α. Equation (7) is essentially a generalized version of Newton's law of viscosity.

For the Helmholtz free energies A^α we shall adopt a constitutive law of the form

$$A^\alpha = A^\alpha(\{\phi^\beta\}, \rho^\alpha, T)$$

where the notation $\{\phi^\beta\}$ signifies the set of volume fractions as β ranges over all phases. The temperature dependence indicated in this law, although formally appropriate, will turn out to be trivial since the mixture is isothermal.

Let us assume that the body forces are entirely attributable to gravity, so that $\phi^\alpha \rho^\alpha \underset{\sim}{b}^\alpha = \rho^\alpha g \nabla Z$, where g is the acceleration of the gravitational field, assumed uniform, and Z denotes depth below some datum. If we locate the origin of our Cartesian coordinate system (x_1, x_2, x_3) at this datum, then $Z = -x_3$. Furthermore, we shall restrict attention to multiphase mixtures in which heat sources are absent $(h^\alpha = 0)$ and heat fluxes are negligible $(\underset{\sim}{q}^\alpha = 0)$.

Finally, we need a constitutive relationship for the momentum exchanges $\underset{\sim}{\hat{p}}^\alpha$. The assumption that is common to most theories of flow in porous media is that the exchanges of momentum between fluids and the rock dominate interfluid exchanges and have the form of Stokes drags:

$$\underset{\sim}{\hat{p}}^\alpha = \phi^\alpha \, (\underset{\approx}{\Lambda}^\alpha)^{-1} \, (\underset{\sim}{v}^R - \underset{\sim}{v}^\alpha) \tag{8}$$

In this equation $\underset{\approx}{\Lambda}^\alpha$ is an invertible transformation giving a tensor relationship between momentum exchanges and relative velocities, guaranteeing that $\underset{\sim}{\hat{p}}^\alpha$ is objective with respect to changes of frame. Since $\underset{\sim}{v}^R = \underset{\sim}{0}$, however, Equation (8) simplifies in our frame of reference to

$$\underset{\sim}{\hat{p}}^\alpha = -\phi^\alpha \, (\underset{\approx}{\Lambda}^\alpha)^{-1} \, \underset{\sim}{v}^\alpha \tag{9}$$

Physically, $\underset{\approx}{\Lambda}^\alpha$ varies with the microscopic configurations of the rock and fluid phases, that is, with both the volume fractions and pore-level geometries of the phases. In practice, however, the pore-level geometries are typically inaccessible to measurement. Therefore we consider $\underset{\approx}{\Lambda}^\alpha$ to be a function of the fractions $\{\phi^\beta\}$ for a given rock-fluid mixture in which the rock geometry is

fixed and the interfacial tensions remain constant. Thus in a sense $\underset{\approx}{\Lambda}^{\alpha}$ is a purely phenomenological variable requiring direct measurement for each system of rock and fluids under investigation.

There are now several mechanisms for the transfer of momentum in the mixture. These include transfers through shear stresses within each fluid, interphase tractions, and direct momentum transfer through fluid drags on the rock matrix. Let us assume that the last of these mechanisms overwhelms the others, so that shear stresses and tractions exert influences on momentum transfers that are negligible compared with the Stokes drag in Equation (9). Thus we need only consider the normal fluid stresses, approximating the constitutive law (7) by

$$\underset{\approx}{t}^{\alpha} = -p^{\alpha}\underset{\approx}{1} , \quad \alpha = W,N,A$$

For each fluid, the mechanical pressure p^{α} in this law may vary as a function of the fluid density in phase α and of the volume fractions $\{\phi^{\beta}\}$. Thus we have an equation of state $p^{\alpha} = p^{\alpha}(\rho^{\alpha},\{\phi^{\beta}\})$, $\alpha = W,N,A$, where the index β ranges over all fluid phases.

The Clausius-Duhem inequality (6) imposes certain thermodynamic restrictions on the functional relationships admissible as constitutive laws. To deduce these restrictions in the general case, one must follow the methodology detailed by Coleman and Noll [1963] and extended to mixtures by Ingram and Eringen [1967]. This procedure involves expanding the inequality (6) in terms of the functional dependencies in the Helmholtz free energy, then reasoning about the values of certain coefficients given that a linear combination of material derivatives having arbitrary sign must be nonnegative. The present

development adopts a less general tack, examining in a similar fashion the restrictions that the Clausius-Duhem inequality imposes on the particular constitutive laws postulated above.

To begin, let us expand the inequality (6) using the chain rule and the functional relationship $A^\alpha = A^\alpha(\{\phi^\beta\},\rho^\alpha T)$:

$$- \sum_\alpha \phi^\alpha \rho^\alpha \left(\frac{\partial A^\alpha}{\partial T} \overset{\alpha}{\frac{DT}{Dt}} + \sum_\beta \frac{\partial A^\alpha}{\partial \phi^\beta} \overset{\alpha}{\frac{D\phi^\beta}{Dt}} + \frac{\partial A^\alpha}{\partial \rho^\alpha} \overset{\alpha}{\frac{D\rho^\alpha}{Dt}} \right)$$

$$- \sum_\alpha \phi^\alpha p^\alpha \nabla \cdot \underset{\sim}{v}^\alpha + \sum_\alpha \underset{\sim}{\hat{p}}^\alpha \cdot \underset{\sim}{v}^\alpha \geq 0 \qquad (10)$$

Now in an isothermal mixture $\overset{\alpha}{DT/Dt} = 0$. Also,

$$\overset{\alpha}{\frac{D\phi^\beta}{Dt}} = \overset{\beta}{\frac{D\phi^\beta}{Dt}} + (\underset{\sim}{v}^\alpha - \underset{\sim}{v}^\beta) \cdot \nabla \phi^\beta$$

$$\overset{\alpha}{\frac{D\rho^\alpha}{Dt}} = 0$$

since each phase's motion is isochoric. What is more, the mass balance for phase α implies

$$\phi^\alpha \nabla \cdot \underset{\sim}{v}^\alpha = - \overset{\alpha}{\frac{D\phi^\alpha}{Dt}}$$

So, (10) becomes

$$- \sum_\alpha \left[\phi^\alpha \rho^\alpha \left(\frac{\partial A^\alpha}{\partial \phi^\alpha} - p^\alpha \right) \overset{\alpha}{\frac{D\phi^\alpha}{Dt}} - \underset{\sim}{\hat{p}}^\alpha \cdot \underset{\sim}{v} \right]$$

$$- \sum_\alpha \sum_{\alpha \neq \beta} \left[\phi^\alpha \rho^\alpha \frac{\partial A^\alpha}{\partial \phi^\beta} \overset{\beta}{\frac{D\phi^\beta}{Dt}} + \frac{\partial A^\alpha}{\partial \phi^\beta} (\underset{\sim}{v}^\alpha - \underset{\sim}{v}^\beta) \cdot \nabla \phi^\beta \right] \geq 0$$

Since this inequality must hold for arbitrary variations in the volume fractions ϕ^β, we must conclude that

$$\frac{\partial A^\alpha}{\partial \phi^\beta} = 0 \ , \quad \alpha \neq \beta$$

and

$$\frac{\partial A^\alpha}{\partial \phi^\alpha} = p^\alpha \tag{11}$$

This last equation identifies the mechanical pressure of fluid phase α as the pore pressure of that phase. Thus our constitutive relationship for the Helmholtz free energy reduces to $A^\alpha = A^\alpha(\phi^\alpha, \rho^\alpha)$, ignoring dependence on temperature in the isothermal mixture.

Equation (11) allows the pressures in different fluids to differ. Thus between any two fluids α and β we can define the difference

$$p_{c\alpha\beta} = p^\alpha - p^\beta = \frac{\partial A^\alpha}{\partial \phi^\alpha}(\phi^\alpha, \rho^\alpha) - \frac{\partial A^\alpha}{\partial \phi^\beta}(\phi^\beta, \rho^\beta)$$

This quantity is the capillary pressure between the two phases. From the definition, it appears that $p_{c\alpha\beta}$ depends on the volume fractions and densities of each phase; however, if the fluids flow isochorically the density dependence becomes trivial. Also, since the rock matrix is rigid we can factor the porosity ϕ out of the volume fractions and thus consider the capillary pressure to be a function of fluid saturations:

$$p_{c\alpha\beta} = p_{c\alpha\beta}(S^\alpha, S^\beta) \tag{12}$$

This functional relationship stands in accord with the usual theories of multiphase flow in porous media. Observe that, in a system where three fluids W,N,A are present, only two capillary pressure functions can be independent.

Flow Equations.

We are now in a position to combine the balance laws and constitutive equations to derive the equations governing the behavior of multiphase flows in variably saturated porous media. To begin with, for each fluid phase α we have a mass balance

$$\frac{\partial}{\partial t}(\phi S^{\alpha}\rho^{\alpha}) + \nabla\cdot(\phi S^{\alpha}\rho^{\alpha}\underset{\sim}{v}^{\alpha}) = 0 \qquad (13)$$

For the rock, rigidity of the matrix and our choice of a coordinate frame in which $\underset{\sim}{v}^{R} = 0$ reduce the mass balance to the equation

$$\frac{\partial \phi}{\partial t} = 0 \ .$$

There is also a momentum balance for each phase. We shall not concern ourselves with the rock momentum balance, however, since the rock is rigid and stationary in our frame. For each fluid phase α, though, our constitutive assumptions for $\underset{\approx}{t}^{\alpha}$, $\underset{\sim}{b}^{\alpha}$, and $\underset{\sim}{\hat{p}}^{\alpha}$ convert Equation (3) to

$$\phi^{\alpha}\rho^{\alpha}\left(\frac{\partial \underset{\sim}{v}^{\alpha}}{\partial t} + \underset{\sim}{v}^{\alpha}\cdot\nabla\underset{\sim}{v}^{\alpha}\right) + \nabla p^{\alpha} - \rho^{\alpha} g \nabla Z = -\phi^{\alpha}(\underset{\approx}{\Lambda}^{\alpha})^{-1}\cdot\underset{\sim}{v}^{\alpha}$$

As is common in porous-media theories, let us assume that the inertial terms in parentheses on the left of this equation contribute negligibly to the fluid motions, being dominated by the effects of normal stresses, gravity, and momentum loss through interactions with the rock matrix. There follows the velocity field equation

$$-\frac{1}{\phi^{\alpha}}\,\underset{\approx}{\Lambda}^{\alpha}\cdot(\nabla p^{\alpha}-\rho^{\alpha}g\nabla Z)=\underset{\sim}{v}^{\alpha}$$

From a phenomenological point of view, the mobility tensor $\underset{\approx}{\Lambda}^{\alpha}$ accounts for the geometry of the rock matrix, the configurations of rock-fluid interfaces, and the flow properties of the fluids. Treating these influences as separable factors leads us to write $\underset{\approx}{\Lambda}^{\alpha}=\underset{\approx}{k}k_{r\alpha}/\mu^{\alpha}$, where $\underset{\approx}{k}$ is the permeability of the rock, having dimensions $[L^2]$; $k_{r\alpha}$ is the dimensionless relative permeability modeling the effects that other fluids have in blocking the flow of phase α, and μ^{α} is the dynamic viscosity of fluid α, having dimensions $[ML^{-1}T^{-1}]$. Thus the velocity field equation becomes

$$\underset{\sim}{v}^{\alpha}=-\frac{\underset{\approx}{k}k_{r\alpha}}{\phi S^{\alpha}\mu^{\alpha}}\,(\nabla p^{\alpha}-\rho^{\alpha}g\nabla Z) \tag{14}$$

which is the familiar form of Darcy's law for multiphase flows.

We need not consider the angular momentum balance explicitly as a governing equation for fluids, since the constitutive law $\underset{\approx}{t}^{\alpha}=-p^{\alpha}\underset{\approx}{1}$ guarantees symmetry of the fluid stresses automatically. Furthermore, we shall not make explicit use of the energy balance, since we assume that the mixture is isothermal with no heat fluxes or heat sources. In a strict sense this neglect is unwarranted, since even when the rock matrix is rigid the loss of fluid momenta to the rock

must be accompanied by concomitant heating of the matrix (and hence the mixture as a whole) via dissipation through the vibrational modes in the solid. By neglecting the energy balance we are therefore excluding from further consideration porous-media flows in which this dissipative heating is significant.

Finally, in addition to the balance laws we have independent functional relationships $p_{c\alpha\beta} = p_{c\alpha\beta}(S^{\alpha},S^{\beta})$ for two of the three capillary pressures and the saturation constraint $S^{W} + S^{N} + S^{A} = 1$.

Substituting the fluid velocity field equation (14) into the mass balance (13) yields a flow equation

$$\frac{\partial}{\partial t}(\phi S^{\alpha}\rho^{\alpha}) = \nabla\cdot\left[\frac{\rho^{\alpha}k_{r\alpha}\overset{\approx}{k}}{\mu^{\alpha}}\cdot(\nabla p^{\alpha} - \rho^{\alpha}g\nabla Z)\right]$$

An equation of this form applies to each fluid phase, $\alpha = W,N,A$. However, in the variably saturated zones of many soils the effects of air flow on the dynamics of the system are limited to the influence of the air saturation S^{A} on relative permeabilities and capillary pressures. Since the details of air movement are likely to hold little interest compared to the movements of the liquid phases, let us therefore neglect the flow equation in the case $\alpha = A$.

For the aqueous and nonaqueous liquids, the assumption that density variations are collinear with pressure variations -- a weaker assumption than we have made in stipulating that the flow is isochoric -- allows us to define a hydraulic head H^{α} in phase α [Hubbert, 1940] as

$$H^{\alpha} = \frac{1}{g}\int_{p^{\alpha}(0)}^{p^{\alpha}(x_3)}\frac{dp^{\alpha}}{\rho^{\alpha}} + \int_{0}^{x_3} dx_3$$

Thus $\nabla H^{\alpha} = (\rho^{\alpha} g)^{-1} \nabla p^{\alpha} - \nabla Z$, and the flow equation for a liquid phase (α = W,N) becomes

$$\frac{\partial}{\partial t}(\phi S^{\alpha} \rho^{\alpha}) = \nabla \cdot (\rho^{\alpha} k_{r\alpha} \underset{\approx}{K}^{\alpha} \cdot \nabla H^{\alpha}) \tag{15}$$

Here $\underset{\approx}{K}^{\alpha} = \rho^{\alpha} g \underset{\approx}{k} / \mu^{\alpha}$ is the hydraulic conductivity of phase α, defined by analogy with the classical single-liquid case.

By expanding the accumulation term on the left side of Equation (15) it is possible to cast the flow equation into a form where the principal unknown is a head. By the product rule,

$$\frac{\partial}{\partial t}(\phi S^{\alpha} \rho^{\alpha}) = \phi S^{\alpha} \frac{\partial \rho^{\alpha}}{\partial t} + \phi \rho^{\alpha} \frac{\partial S^{\alpha}}{\partial t} + \rho^{\alpha} S^{\alpha} \frac{\partial \phi}{\partial t}$$

The last term on the right vanishes since the rock matrix is rigid. Also, if we allow the liquids to be compressible (although they flow isochorically), then

$$\phi S^{\alpha} \frac{\partial \rho^{\alpha}}{\partial t} = \phi S^{\alpha} \frac{d\rho^{\alpha}}{dH^{\alpha}} \frac{\partial H^{\alpha}}{\partial t} = s_s^{\alpha} \rho^{\alpha} S^{\alpha} \frac{\partial H^{\alpha}}{\partial t}$$

where $s_s^{\alpha} = \phi g \, d\rho^{\alpha} / dp^{\alpha}$ represents the specific storage of the liquid α in the matrix. Now for flow fields in which density gradients are very small we may approximate our flow equation by writing

$$\phi \frac{\partial S^{\alpha}}{\partial t} + s_s^{\alpha} S^{\alpha} \frac{\partial H^{\alpha}}{\partial t} = \nabla \cdot (k_{r\alpha} \underset{\approx}{K}^{\alpha} \cdot \nabla H^{\alpha}) \tag{16}$$

In a more general setting where $\partial\phi/\partial t \neq 0$, it is common to assume $\phi = \phi(H^W)$. In this case $\rho^\alpha S^\alpha \partial\phi/\partial t = \rho^\alpha S^\alpha \rho^W g c_W \partial H^W/\partial t$, where $c_W = (\rho^W g\phi)^{-1} d\phi/dH^W$ quantifies the matrix compressibility. When several liquid phases are present, one formally encounters a matrix compressibility $c_\alpha = (\rho^\alpha g\phi)^{-1} d\phi/dH^\alpha$ with respect to each liquid. There is clear mathematical convenience -- and perhaps some physical plausibility -- in assuming $c_W = c_N$. However, for a rigid solid matrix this issue does not arise.

The conventional formulation of single-liquid flows in the variably saturated zone gives the flow equation in terms of pressure head and moisture capacity instead of hydraulic head and saturation [Pinder and Gray, 1977, Section 5.4]. To make our multi-liquid equation conform with the familiar case, let us define the pressure head Φ^α in phase α by the equation

$$\nabla\Phi^\alpha = \frac{1}{\rho^\alpha g} \nabla p^\alpha$$

so that $H^\alpha = \Phi^\alpha - Z$. Also, define the moisture capacity for liquid phase α as $\Theta^\alpha = \phi S^\alpha$. If we observe that $\partial Z/\partial t = -\partial x_3/\partial t = 0$ and $-\nabla Z = \nabla x_3 = \underset{\sim}{e}_3$, the unit vector in the (upward) x_3 direction, and if we call

$$C^\alpha = \phi \frac{d}{d\Phi^\alpha}(\Theta^\alpha) \tag{17}$$

the specific moisture capacity for fluid α, then the flow equation (17) becomes

$$\left(C^\alpha + \frac{\Theta^\alpha s^\alpha_s}{\phi}\right)\frac{\partial\Phi^\alpha}{\partial t} = \nabla\cdot[k_{r\alpha}\underset{\approx}{K}^\alpha\cdot(\nabla\Phi^\alpha + \underset{\sim}{e}_3)] \tag{18}$$

Equation (18) is a natural extension of Richards' [1931] equation for the flow of a single liquid through variably saturated soils. There are several new features to the equation owing to the peculiar physics of multiphase flows in porous media. For one, we must regard the specific moisture capacity, moisture capacity, specific storage, hydraulic conductivity, and pressure head as pertaining to one liquid or the other, so we have the variables C^W, C^N, Θ^W, Θ^N, s_s^W, s_s^N, $\underset{\approx}{K}^W$, $\underset{\approx}{K}^N$, Φ^W, and Φ^N. Also, in the flow equation for each phase there now appears a new parameter $k_{r\alpha}$, the relative permeability of the medium to the liquid phase α. This new parameter will entail a set of measurements of the medium's response over a continuum of liquid saturations S^W and S^N, so we may consider $k_{rW} = k_{rW}(S^W,S^A)$ and $k_{rN} = k_{rN}(S^N,S^A)$ for fluids of unchanging composition. Finally, in addition to the three-phase saturation restriction $S^W + S^N + S^A = 1$ we now have two independent capillarity relationships giving, say, p_{cWA} and p_{cNA} as functions of saturation according to Equation (12). Equation (17) already assumes equivalent relationships in terms of pressure head and moisture capacity, namely $\Theta^\alpha = \Theta^\alpha(\Phi^\alpha)$, whose inverse (provided Θ^α is bijective and exhibits no hysteresis) is $\Phi^\alpha = \Phi^\alpha(\Theta^\alpha)$. Thus, while (18) is formally similar to the classic Richards equation, the extension to multi-liquid flows entails the quantification of additional physical effects.

Conclusions.

The foregoing development shows that the fundamentals of mixture physics, together with some relatively simple assumptions about the behaviors of various phases present, lead to a set of governing equations for multi-liquid flows in variably saturated soils. This formulation serves as a natural extension of Richards' single-liquid theory. The extended model suggests the kinds of meas-

urements that will be necessary to characterize multi-liquid flows and may thus serve as the basis for designing experiments. Indeed, there is a great need for such experiments in light of growing concern over near-surface contamination. Also needed are numerical studies to identify the behavior of systems governed by Equations (18) and to provide a basis for the practical simulations that will be demanded when our understanding of such systems improves.

The formulation of the model presented here identifies several simplifying assumptions that may not apply in all cases of interest. Noteworthy among these limitations are the rigidity of the solid matrix and the isochoricity of the fluid motions. Development of appropriate flow equations under more relaxed assumptions will therefore render a somewhat more general theory.

Notation.

The symbols in square brackets indicate physical dimensions. M stands for mass, L for length, T for time, and θ for temperature.

A	Helmholtz free energy $[L^2T^{-2}]$
$\underset{\sim}{b}$	body force $[LT^{-2}]$
$\mathcal{B}$	material body
c	matrix compressibility $[M^{-2}LT^2]$
C	specific moisture capacity $[L^{-1}]$
$\underset{\approx}{d}$	deformation rate $[T^{-1}]$
$\underset{\sim}{e}$	unit vector in three-space [L]
E	internal energy $[L^2T^{-2}]$
f	generic function
F	volume occupied by a phase $[L^3]$
$\underset{\approx}{F}$	Jacobian of the motion [1]
g	gravitational acceleration $[LT^{-2}]$
h	heat source $[L^2T^{-3}]$
H	hydraulic head [L]
$\underset{\approx}{k}$	permeability $[L^2]$
$\underset{\approx}{K}$	hydraulic conductivity $[LT^{-1}]$
$k_{r\alpha}$	relative permeability of phase α [1]
M	mass [M]
$\underset{\approx}{M}$	interphase angular momentum exchange $[ML^{-1}T^{-2}]$
p	mechanical pressure $[ML^{-1}T^{-2}]$
$\underset{\sim}{\hat{p}}$	interphase momentum exchange $[ML^{-2}T^{-2}]$
$p_{c\alpha\beta}$	capillary pressure between fluids α and β $[ML^{-1}T^{-2}]$

$\underset{\sim}{q}$ heat flux $[MT^{-3}]$

r interphase mass exchange $[ML^{-3}T^{-1}]$

S fluid saturation [1]

s_s specific storage $[L^{-1}]$

t time [T]

$\underset{\approx}{t}$ stress $[ML^{-1}T^{-2}]$

T temperature $[\theta]$

$\underset{\sim}{v}$ velocity $[LT^{-1}]$

V measurable set of spatial points

$\underset{\sim}{x}$ position in spatial coordinates [L]

X material point

$\underset{\sim}{X}$ position in material coordinates [L]

Z depth below datum [L]

ε interphase energy exchange $[ML^{-1}T^{-3}]$

η entropy $[L^{2}T^{-1}\theta^{-1}]$

Θ moisture capacity [1]

ξ bulk mass density $[ML^{-3}]$

λ coefficient of viscosity or interphase traction $[ML^{-1}T^{-1}]$

$\underset{\approx}{\Lambda}$ mobility $[M^{-1}L^{3}T]$

μ coefficient of viscosity or interphase traction $[ML^{-1}T^{-1}]$

$\underset{\sim}{\nu}$ diffusion velocity $[LT^{-1}]$

ϕ volume fraction or porosity [1]

Ψ intensive quantity

Indices

A	air
I	inner part
N	nonaqueous liquid
R	rock
W	water
α	phase index
β	phase index
1,2,3	spatial directions

Acknowledgement.

The author wishes to thank the Wyoming Water Research Center for supporting this work. The reviewer also deserves thanks for helpful comments.

References

Atkin, R. J., and R. E. Craine, Continuum theories of mixtures: basic theory and historical development, Quart. J. Mech. Appl. Math. 29 (2), pp. 209-244, 1976.

Bear, J., Zaslovsky, D., and S. Irway (ed.), Physical Principles of Water Percolation and Seepage, UNESCO, Paris, 1968.

Bowen, R. M., Theory of mixtures, in Continuum Physics, Vol. 3, (A. C. Eringen, ed.), Academic Press, New York, 1976.

Bowen, R. M., Compressible porous media models by use of the theory of mixtures, Int. J. Engng. Sci. 20, pp. 697-735, 1982.

Coleman, B. D., and W. Noll, The thermodynamics of elastic materials with heat conduction and viscosity, Arch. Rat. Mech. Anal. 13, pp. 167-178, 1967.

Eringen, A. C., and J. D. Ingram, A continuum theory of chemically reacting media -- I, Int. J. Engng. Sci. 3, pp. 197-212, 1965.

Hubbert, M. K., The theory of groundwater motion, J. Geol. 48 (8), Pt. 1, pp. 785-944, 1940.

Ingram, J. D., and A. C. Eringen, A continuum theory of chemically reacting media -- II. Constitutive equations of reacting fluid mixtures, Int. J. Engng. Sci. 5, pp. 289-322, 1967.

Narasimhan, T. N., and P. A. Witherspoon, Numerical model for saturated-unsaturated flow in deformable porous media I. Theory, Water Resour. Res. 12 (3), pp. 657-664, 1977.

Passman, S. L., Nunziato, J. W., and E. K. Walsh, A theory of multiphase mixtures, appendix to C. Truesdell, Rational Thermodynamics, 2nd ed., Springer-Verlag, New York, 1984.

Philip, J. R., An infiltration equation with some physical significance, Soil Sci. 77, pp. 153-157, 1954.

Pinder, G. F., and W. G. Gray, Finite Element Simulation in Surface and Subsurface Hydrology, Academic Press, New York, 1977.

Prévost, J. H., Mechanics of continuous porous media, Int. J. Engng. Sci. 18, pp. 787-800, 1980.

Richards, L. A., Capillary conduction of liquids through porous media, Physics 1, pp. 318-333, 1931.

Schwille, F., Migration of organic fluids immiscible with water in the unsaturated zone, in Pollutants in Porous Media, (B. Yaron et al., eds.), Springer-Verlag, Berlin, 1984.

Zaslovksy, D., Theory of unsaturated flow into nonuniform soil profile, Soil Sci. 97, pp. 400-410, 1964.

TABLE 1

DEFINITIONS OF MASS-RELATED QUANTITIES

SYMBOL	DEFINITION	NAME
ρ^{α}	$\xi^{\alpha}/\phi^{\alpha}$	Intrinsic mass density
ρ	$\sum_{\alpha} \phi^{\alpha}\rho^{\alpha}$	Overall mixture density
$\underset{\sim}{v}$	$(1/\rho) \sum_{\alpha} \phi^{\alpha}\rho^{\alpha}\underset{\sim}{v}^{\alpha}$	Barycentric velocity
$\underset{\sim}{\nu}^{\alpha}$	$\underset{\sim}{v}^{\alpha} - \underset{\sim}{v}$	Diffusion velocity
ϕ	$1 - \phi^{R}$	Porosity
S^{α} $(\alpha = W,N,A)$	ϕ^{α}/ϕ	Saturation of fluid α

Numerical modelling of multiphase flow in porous media

Myron B. Allen III

Department of Mathematics, University of Wyoming, Laramie, Wyoming 82071, USA

The simultaneous flow of immiscible fluids in porous media occurs in a wide variety of applications. The equations governing these flows are inherently nonlinear, and the geometries and material properties characterizing many problems in petroleum and groundwater engineering can be quite irregular. As a result, numerical simulation often offers the only viable approach to the mathematical modelling of multiphase flows. This paper provides an overview of the types of models that are used in this field and highlights some of the numerical techniques that have appeared recently. The exposition includes discussions of multiphase, multispecies flows in which chemical transport and interphase mass transfers play important roles. The paper also examines some of the outstanding physical and mathematical problems in multiphase flow simulation. The scope of the paper is limited to isothermal flows in natural porous media; however, many of the special techniques and difficulties discussed also arise in artificial porous media and multiphase flows with thermal effects.

1. INTRODUCTION

1.1 Importance of multiphase flow in porous media

Multiphase flows in porous media occur in a variety of settings in applied science. The earliest applications involving the simultaneous flow of two fluids through a porous solid appear in the soil science literature, where the flow of water in soils partly occupied by air has fundamental importance[1,28]. This unsaturated flow in some ways represents the simplest of multiphase flows. Yet, as we shall see, it exemplifies a fact underlying the continued growth in research in this area: multiphase flows in porous media are inherently nonlinear. Consequently, numerical simulation often furnishes the only effective strategy for understanding their behaviour quantitatively.

Although the earliest studies of multiphase flows in porous media concern unsaturated flows, the most concentrated research in this field over the past four decades has focused on flows in underground petroleum reservoirs. Natural oil deposits almost always contain connate water and occasionally contain free natural gas as well. The simultaneous flow of oil, gas and water in porous media therefore affects practically every aspect of the reservoir engineer's job of optimizing the recovery of hydrocarbons. Here, again, the physics of multiphase fluid flows give rise to nonlinear governing equations. The difficulty imposed by the nonlinearities along with the irregular geometries and transient behaviour associated with typical oil reservoirs make numerical simulation an essential tool in petroleum engineering. The advent of various enhanced oil recovery technologies has added to this field further levels of complexity and hence an even greater degree of reliance on numerical methods.

Accepted August 1985. Discussion closes February 1986

Most recently, multiphase flows have generated serious interest among hydrologists concerned with groundwater quality. There is growing awareness that many contaminants threatening our groundwater resources enter water-bearing rock formations as separate, nonaqueous phases. These oily liquids may come from underground or near-surface storage facilities, land-fills at which chemical wastes are dumped, industrial sites such as oil refineries or wood-treatment plants, or illegal waste disposal. Regardless of the source of the contaminants, our ability to understand and predict their flows underground is crucial to the design of sound remedial measures. This is a fairly new frontier in multiphase porous-media flows, and again the inherent complexity of the physics leads to governing equations for which the only practical way to produce solutions may be numerical simulation.

1.2 Scope of the article

The purpose of this article is to review some of the more salient applications of numerical simultation in multiphase porous-media flows. In light of the history and breadth of these applications, a review of this kind must choose between the impossibly ambitious goal of thoroughness and the risks of narrowness that accompany selective coverage. This article steers toward selective coverage. The aim here is to survey several multiphase flows that have attracted substantial scientific interest and to discuss a few aspects of their numerical simulation that have appeared in the recent technical literature. I confess at the outset that some important multiphase flows receive no attention here at all, and, even for the flows discussed, many potentially far-reaching contributions to numerical simulation get no mention. Perhaps the references given throughout the article can compensate in part for these shortcomings.

In particular, we shall restrict our attention here to underground flows in natural porous media. This

0309-1708/85/040162-26$2.00

restriction excludes many applications in chemical engineering, one notable example being flows in packed beds of catalysts. Also, the article considers only isothermal flows. Therefore we do not discuss steam-water flows in geothermal reservoirs or such thermal methods of enhanced oil recovery as steam injection or fireflooding. Several numerical methods also receive scant or no mention. Among these are integrated finite differences, subdomain finite elements, spectral methods, and boundary-element techniques. Some of these approaches undoubtedly hold promise for future applications in multiphase flows in porous media. For the present, however, we concentrate on developments based on the trinity of more standard discrete approximations: finite differences, Galerkin finite elements and collocation.

2. BACKGROUND

2.1 Definitions

From a quantitative point of view, one of the most fruitful ways of examining multiphase flows in porous media is through the framework of continuum mixture theory. In contrast to a single continuum, a *mixture* is a set of overlapping continua called *constituents*. Any point in a mixture can in principle be the locus of material from each constituent, and each constituent possesses its own kinematic and kinetic variables such as density, velocity, stress and so forth. How one decomposes a physical mixture into constituents depends largely on one's theoretical aims, but in analysing porous media we commonly identify the solid matrix as one constituent and each of the fluids occupying its interstices as another.

In discussions of porous-media physics it is important to distinguish between multi*phase* mixtures and multi*species* mixtures. A mixture consists of several *phases* if, on a microscopic length scale comparable, say, to typical pore apertures, one observes sharp interfaces in material properties. In this sense all porous-media flows involve multiphase mixtures, owing to the distinct boundary between the solid matrix and the interstitial fluids. At this boundary, density, for example, changes abruptly from its value in the solid to that in the fluid. More complicated multiphase mixtures occur, common examples being the simultaneous flows of air and water, oil and water, or oil and gas through porous rock. Here, in addition to rock-fluid interfaces, we observe interfaces between the various immiscible fluids at the microscopic scale. While the detailed structures of these interfaces and the volumes they bound are inaccessible to macroscopic observation, their geometry influences the mechanics of the mixture. This, at least intuitively, is why volume fractions play an important role in multiphase mixture theory. The *volume fraction* ϕ_α of phase α is a dimensionless scalar function of position and time such that $0 \leqslant \phi_\alpha \leqslant 1$, and, for any spatial region $\mathscr{R}$ in the mixture, $\int_{\mathscr{R}} \phi_\alpha \, d\mathbf{x}$ gives the fraction of the volume of $\mathscr{R}$ occupied by phase α. The sum of the fluid volume fractions in a saturated solid matrix is the *porosity* ϕ.

On the other hand, there are mixtures in which no microscopic interfaces appear. Saltwater is an example. Here the constituents are ionic or chemical *species*, and spatial segregation of these constituents is not observable except, perhaps, at intermolecular length scales. Air is another multispecies mixture, consisting of N_2, O_2, CO_2, and some trace gases. Multispecies mixtures differ from multiphase mixtures in that volume fractions do not appear in the kinematics of the former.

It is possible to have multiphase, multispecies mixtures. These *compositional flows* occur in porous-media physics when there are several fluid phases, each of which comprises several chemical species. Such mixtures arise in many flows of practical interest, two important examples being multiple-contact miscible displacement in oil reservoirs and the contamination of groundwater by nonaqueous liquids. In these cases the transfer of chemical species between phases is a salient feature of the mixture mechanics. More detailed treatment of compositional flows appears later in this article.

2.2 Review of the basic physics

While the theory of mixtures dates at least to Eringen and Ingram[61], its foundations are still the focus of active inquiry, as reviewed by Atkin and Craine[17]. Among the applications of mixture theory to multiphase mixtures and porous media are investigations by Prévost[124], Bowen[29,30], Passman, Nunziato and Walsh[112] and Raats[126]. The aims of the present article in this respect are much more limited in scope than those just cited. What follows is a brief review of the basic physics of multiphase flows in porous media, using the language of mixture theory as a vehicle for the development of governing equations[7].

For concreteness, assume that the mixture under investigation has three phases: rock (R) and two fluids (N, W). (The extension of this exposition to mixtures with more fluid phases is straightforward.) Each phase α has its own intrinsic mass density ρ_α, measured in kg/m^3; velocity $\mathbf{v}_\alpha$, measured in m/s; and volume fraction ϕ_α. From their definitions, the volume fractions clearly must obey the constraint $\sum_\alpha \phi_\alpha = 1$. In terms of these mechanical variables, the mass balance for any particular phase α is

$$\frac{\partial}{\partial t}(\phi_\alpha \rho_\alpha) + \nabla \cdot (\phi_\alpha \rho_\alpha \mathbf{v}_\alpha) = r_\alpha \tag{1}$$

where r_α stands for the rate of mass transfer into phase α from other phases. To guarantee mass conservation in the overall mixture, the reaction rates must obey the constraint $\sum_\alpha r_\alpha = 0$.

We can rewrite equation (1) in a more common form by noting that the porosity is $\phi = 1 - \phi_R$ and defining the fluid saturations $S_N = \phi_N/\phi$, $S_W = \phi_W/\phi$. Thus

$$\frac{\partial}{\partial t}[(1-\phi)\rho_R] + \nabla \cdot [(1-\phi)\rho_R \mathbf{v}_R] = r_R$$

for the rock phase, and

$$\frac{\partial}{\partial t}(\phi S_\alpha \rho_\alpha) + \nabla \cdot (\phi S_\alpha \rho_\alpha \mathbf{v}_\alpha) = r_\alpha, \qquad \alpha = N, W \tag{2}$$

for the fluids.

Each phase also obeys a momentum balance. In its primitive form this equation relates the phase's inertia to its stress $\mathbf{t}_\alpha$, body forces $\mathbf{b}_\alpha$, and rate $\mathbf{m}_\alpha$ of momentum exchange from other phases. Thus,

$$\phi_\alpha \rho_\alpha \left(\frac{\partial \mathbf{v}_\alpha}{\partial t} + \mathbf{v}_\alpha \cdot \nabla \mathbf{v}_\alpha \right) - \nabla \cdot \mathbf{t}_\alpha - \phi_\alpha \rho_\alpha \mathbf{b}_\alpha = \mathbf{m}_\alpha - \mathbf{v}_\alpha r_\alpha \tag{3}$$

If we assume that the rock phase is chemically inert, so $r_R = 0$, and fix a coordinate system in which $\mathbf{v}_R = \mathbf{0}$, then the momentum balance for rock reduces to

$$\nabla \cdot \mathbf{t}_R - \phi_R \rho_R \mathbf{b}_R = \mathbf{m}_R$$

Let us assume that each fluid is Newtonian and that momentum transfer via shear stresses within the fluid is negligible compared with momentum exchange to the rock matrix. In this case $\mathbf{t}_\alpha = -p_\alpha \mathbf{1}$, where p_α is the *mechanical pressure* in fluid α and $\mathbf{1}$ is the unit isotropic tensor. If gravity is the only body force acting on fluid phase α, then $\phi_\alpha \mathbf{b}_\alpha = g\nabla Z$, where g stands for the magnitude of gravitational acceleration and Z represents depth below some datum. For the momentum exchange terms, the assumption common to most theories of porous media is that momentum losses to the solid matrix take the form of possibly anisotropic Stokes drags,

$$\mathbf{\Lambda}_\alpha \mathbf{m}_\alpha = \phi(\mathbf{v}_R - \mathbf{v}_\alpha) = -\phi \mathbf{v}_\alpha$$

where $\mathbf{\Lambda}_\alpha$ is a tensor called the *mobility* of phase α. If we assume further that the inertial effects in the fluid are negligible compared with rock-fluid interactions and that there is no interphase mass transfer, then equation (3) yields

$$\mathbf{v}_\alpha = -\frac{\mathbf{\Lambda}_\alpha}{\phi S_\alpha}(\nabla p_\alpha - \rho_\alpha g \nabla Z) \tag{4}$$

which is familiar as Darcy's law.

Clearly, the mobility $\mathbf{\Lambda}_\alpha$ appearing in equation (4) accounts for much of the predictive power of Darcy's law in any particular rock-fluid system. Constitutive laws for mobility are largely phenomenological, the most common versions having the form $\mathbf{\Lambda}_\alpha = \mathbf{k} k_{r\alpha}/\mu_\alpha$, where μ_α is the dynamic viscosity of fluid phase α, $\mathbf{k}$ is the *permeability*, and the *relative permeability* $k_{r\alpha}$ is a coefficient describing the effects of other fluids in obstructing the flow of fluid α.

For a two-fluid system with no interphase mass transfer, the relative permeabilities typically vary with saturation, and the curves $k_{rN}(S_W)$, $k_{rW}(S_W)$ look roughly like those drawn in Fig. 1[102]. The vanishing-point saturations S_{Nr} and S_{Wr} are called *residual* or *irreducible* saturations, and they account for the fact that, for a particular fluid to flow, it must be present at a sufficient degree of saturation to permit the formation of connected flow channels consisting of that phase. Actually, this picture of relative permeabilities is quite simplistic. In nature relative permeabilities often exhibit significant hysteresis, and the verification of the relative-permeability model in the presence of three or more fluid phases[92,144,101] or compositional effects[22,14] is still not clear.

Equation (4) allows each fluid phase to have its own pressure at any point in the reservoir. These pressure differences indeed occur in nature. At the microscopic scale the effects of interfacial tension and pore geometry on the curvatures of fluid-fluid interfaces lead to capillary effects. Leverett[91] uses the classical thermodynamics of Gibbs[75] to describe these effects, while more recent works such as those of Morrow[103] and Davis and Scriven[51] drawn connections with microscopic effects and molecular theories of interfacial tension. These theories imply that, at a macroscopic scale, there will be a pressure difference, or *capillary pressure*, between any two fluid phases in a porous medium. In two-phase systems, for example, there is a single capillary pressure $p_{CNW} = p_N - p_W$. In simple models p_{CNW} is a function of saturation; however, in actual flows the capillary pressure exhibits rather pronounced hysteresis[103,82,134] and dependence on fluid composition[42].

Given velocity field equations such as equation (4), we can expand the mass balances for the fluid phases to get flow equations for each fluid. Using the customary decomposition of the mobility $\mathbf{\Lambda}_\alpha$ and directly substituting equation (4) into equation (2) yields, for a two-phase system,

$$\begin{aligned} &\frac{\partial}{\partial t}(\phi S_N \rho_N) - \nabla \cdot \left[\frac{\rho_N \mathbf{k} k_{rN}}{\mu_N}(\nabla p_W + \nabla p_{CNW} - \rho_N g \nabla Z)\right] = 0 \\ &\frac{\partial}{\partial t}(\phi S_W \rho_W) - \nabla \cdot \left[\frac{\rho_W \mathbf{k} k_{rW}}{\mu_W}(\nabla p_W - \rho_N g \nabla Z)\right] = 0 \end{aligned} \tag{5}$$

Flow equations for systems having more fluid phases will be similar, except that if P phases coexist, then $P-1$ independent capillary pressure functions will appear in the system.

2.3 Early investigations

The picture of multiphase flows in porous media outlined above evolved over several decades beginning in the 1930s. The use of an extended version of the single-phase form of Darcy's law in multiphase flows appears to have begun with Richards[128] in his work on unsaturated flows in the soil physics literature. The explicit use of a separate velocity field equation for each fluid began in the petroleum industry. Here the pioneering work of Muskat *et al.*[104], Wykoff and Botset[161], Buckley and Leverett[34], Fatt and Dykstra[68] and Welge[159], among others, promoted the widespread acceptance of Darcy's equation altered by the incorporation of relative permeabilities. Today this model is the one most widely used in the prediction of multiphase flows in porous media.

Despite its broad appeal in applications, the multiphase version of Darcy's law has some limitations.

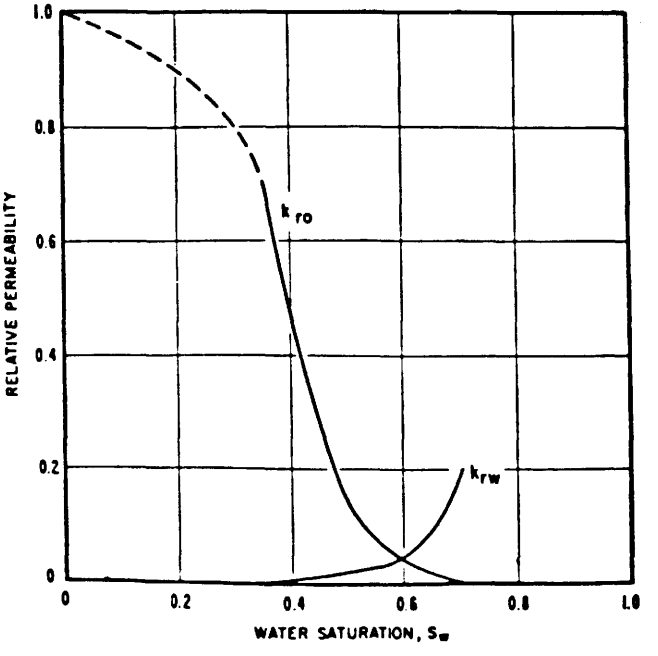

Fig. 1. Typical relative permeability curves[102]

Relative permeabilities are not strictly functions of saturation, the most glaring violation being the phenomenon of hysteresis or dependence on saturation history. Such microscopic phenomena as gas slippage at the solid walls, turbulence, and adsorption can also invalidate the Darcy model in certain flows[33]. These limitations are worthy of consideration in the application of the multiphase Darcy law to any new rock-fluid system.

3. TWO-PHASE FLOWS

The simplest multiphase flows in porous media are those in which two fluids flow simultaneously but do not exchange mass or react with the solid matrix. While many flows of practical interest exhibit more complex physics, two-phase flows have drawn attention in many applications. Among these are unsaturated groundwater flows, salt-water intrusion in coastal aquifers, and the Buckley–Leverett problem in petroleum engineering.

3.1 Unsaturated groundwater flow

In typical soil profiles some distance separates the earth's surface from the water table, which is the upper limit of completely water-saturated soil. In this invervening zone the water saturation varies between 0 and 1, the rest of the pore space normally being occupied by air. Water flow in this *unsaturated zone* is complicated by the fact that the soil's permeability to water depends on its water saturation. Let us derive the common form of the governing equation and examine some of the computational difficulties that arise in its solution.

Most formulations of unsaturated flow rest on the assumption that the motion of air has negligible effect on the motion of water. Therefore one usually neglects the flow equation for air, assuming that the air pressure equals the constant atmospheric pressure at the surface, that is, $p_A = p_{\text{atm}}$. Then we can define the *pressure head* in the water by $\psi = (p_W - p_A)/(\rho_W g)$, having the dimensions of length and being negative in the unsaturated zone where $S_W < 1$. Also, instead of saturation, soil physicists typically refer to the soil's *moisture content*, defined by $\Theta = \phi S_W$. In terms of these new variables the capillary pressure relationship for the air-water system becomes $\psi = \psi(\Theta)$ or, provided ψ is an invertible function, $\Theta = \Theta(\psi)$. From equation (5b), the flow equation for water thus transforms to

$$\frac{\partial}{\partial t}(\Theta \rho_W) = \nabla \cdot [\mathbf{K} \cdot \rho_W (\nabla \psi + \nabla Z)]$$

where $\mathbf{K} = \rho_W g \mathbf{k} k_{rW}/\mu_W$ is the *hydraulic conductivity* of the soil. Notice that $\mathbf{K}$ is a function of ψ, since relative permeability depends on saturation, which varies with ψ according to the capillarity relationship.

In many unsaturated flows the compressibility effects in water are small, so that time derivatives and spatial gradients of ρ_W may be neglected. If this approximation holds, then the flow equation reduces to

$$\frac{\partial \Theta}{\partial t} = \nabla \cdot [\mathbf{K} \cdot (\nabla \psi + \nabla Z)] \tag{6}$$

To get an equation in which ψ is the principal unknown, we simply use the chain rule to expand the time derivative on the left, giving

$$C(\psi)\frac{\partial \psi}{\partial t} = \nabla \cdot [\mathbf{K}(\psi)(\nabla \psi + \nabla Z)]$$

where $C(\psi) = \mathrm{d}\Theta/\mathrm{d}\psi$ is the *specific moisture capacity*. If the flow is essentially one-dimensional in the vertical direction, then this equation collapses to

$$C(\psi)\frac{\partial \psi}{\partial t} = \frac{\partial}{\partial z}\left[K(\psi)\left(\frac{\partial \psi}{\partial z} + 1\right)\right] \tag{7}$$

which is Richards' equation[128].

Several investigators in hydrology have examined the unsaturated flow equation from analytic viewpoints. Philip[119] gives one of the earliest theoretical treatments of Richards' equation, proposing asymptotic solutions for a nonlinear problem. The equation has also attracted interest in the applied mathematics community, including investigations by Aronson[16], Peletier[116] and Nakano[105]. Aronson[16], for example, observes that, while the classical linear heat equation admits solutions in which disturbances propagate with infinite speeds, the nonlinear equation (7) may propagate disturbances with only finite speed. This implies that a moving interface, or *wetting front*, can form between the downward-moving zone of high moisture content Θ and the zone yet uncontacted by the wave of infiltrating water. Under certain initial conditions this moving boundary can exhibit steep spatial gradients in Θ and consequently in ψ. The resulting sharp fronts pose considerable difficulty in the construction of numerical schemes, since the discrete approximations used typically have lowest-order error terms that increase with the norm of the solution's gradient. We shall discuss this difficulty in more detail in Section 6.

Numerical work by a variety of investigators has corroborated the existence of wetting fronts. Much of this work appeared during the 1970s, and it includes articles by Bresler[33], Neuman[107], Reeves and Duguid[127], Narasimhan and Witherspoon[106] and Segol[136]. Van Genuchten[151,152] presents solution schemes for the one- and two-dimensional versions of Richards' equation using both finite differences and finite-element Galerkin methods employing Hermite cubic basis functions. His work furnishes a good comparison of the finite-difference and finite-element approaches to the approximation of wetting fronts.

Van Genuchten's investigation also demonstrates another difficulty in solving Richards' equation numerically. This problem owes its existence to the nonlinear coefficient $C(\psi)$ appearing in the accumulation term of equation (7). Because the equation itself is nonlinear, implicit time-stepping algorithms must incorporate an iterative procedure for advancing the approximate solution from one time step to the next. There then arises a question regarding the proper time level at which to evaluate $C(\psi)$. Van Genuchten demonstrates that evaluating this coefficient in a fully implicit fashion can lead to material balance errors in certain schemes, among them the Galerkin scheme using two-point Gauss quadrature to evaluate the mass and stiffness matrix elements. Figure 2 shows how this scheme produces a wetting front that lags the true solution. Milly[99] advances an iterative method for evaluating $C(\psi)$

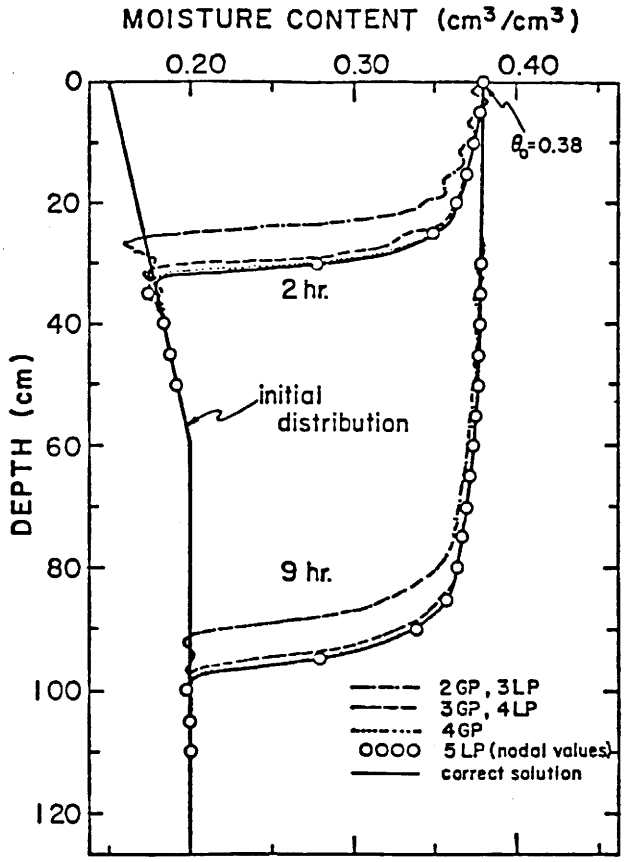

Fig. 2. Solutions to the unsaturated flow equation using various finite-element Galerkin schemes[151]

at the correct time level to guarantee good global material balances.

Allen and Murphy[11] propose another approach to the time-stepping problem in unsaturated flows. While the method is used in connection with finite-element collocation – a technique closely related to the two-point Gauss quadrature scheme mentioned above – the basic idea should be applicable with most spatial discretizations. If we return to the original form of the accumulation term, equation (7) becomes

$$\frac{\partial \Theta}{\partial t} = \frac{\partial}{\partial z}\left[K(\psi)\left(\frac{\partial \psi}{\partial z}+1\right)\right]$$

One can circumvent the difficulties encountered in solving an equation in both Θ and ψ by properly formulating an iterative procedure. Let us approximate the time derivative using implicit finite differences:

$$\frac{\Theta(\psi^{n+1})-\Theta(\psi^n)}{\Delta t} = \frac{\partial}{\partial z}\left[K(\psi^{n+1})\left(\frac{\partial \psi^{n+1}}{\partial z}+1\right)\right]+\mathcal{O}(\Delta t)$$

We can linearize the flux terms in this approximation by establishing an iterative scheme in which $\psi^{n+1,m}$ represents the value of ψ at the most recent known iteration level and $\psi^{n+1,m+1}=\psi^{n+1,m}+\delta\psi^{n+1,m+1}$ represents the value at the sought iterative level:

$$\frac{\partial}{\partial z}\left\{K(\psi^{n+1,m})\left[\frac{\partial}{\partial z}(\psi^{n+1,m}+\delta\psi^{n+1,m+1})+1\right]\right\}$$

This expression allows the nonlinear coefficient $K(\psi^{n+1})$ to lag by an iteration.

In the accumulation term we also lag $\Theta(\psi^{n+1})$, but in addition we linearly project forward to the next iterative level using the Newton-like extrapolation

$$\frac{1}{\Delta t}[\Theta(\psi^{n+1,m})+C(\psi^{n+1,m})\delta\psi^{n+1,m+1}-\Theta(\psi^n)]$$

Here, recall that $C(\psi)=\mathrm{d}\Theta/\mathrm{d}\psi$. The value ψ^n of pressure head at the old time level represents the value furnished by the iterative scheme after convergence, which a computer code can test using either of two criteria. First, one can check whether the iterative increment $\delta\psi^{n+1,m+1}$ is small enough in magnitude or norm to warrant stopping the iteration. Second, one can observe that collecting the terms involving the unknown $\delta\psi^{n+1,m+1}$ on the left and ignoring truncation error leaves the known quantity

$$-\frac{\Theta(\psi^{n+1,m})-\Theta(\psi^n)}{\Delta t}+\frac{\partial}{\partial z}\left[K(\psi^{n+1,m})\left(\frac{\partial \psi^{n+1,m}}{\partial z}+1\right)\right] \equiv -R^{n+1,m}$$

acting as a right-hand side in the linearization. This quantity is precisely the residual to the flow equation at the mth iteration. Whenever $\|R^{n+1,m}\|$ is small in some appropriate norm, the resulting increment $\delta\psi^{n+1,m+1}$ will be small and, more to the point, we shall have solved the time-differenced equation to within a very small error.

It is easy to see why such a scheme conserves mass, at least to within limits imposed by the iterative convergence criteria. If we integrate the residual $R^{n+1,m}(z)$ over the spatial domain Ω of the problem, we find

$$-\int_\Omega \frac{\Theta(\psi^{n+1,m})-\Theta(\psi^n)}{\Delta t}\,\mathrm{d}z + K(\psi^{n+1,m})\left(\frac{\partial \psi^{n+1,m}}{\partial z}+1\right)\Big|_{\partial\Omega} = -\int_\Omega R^{n+1,m}\,\mathrm{d}z$$

If the integral on the right were zero, this equation would be precisely the global mass balance for vertical unsaturated flow. Thus by iterating until $\|R^{n+1,m}\|$ is small, we implicitly enforce the global mass balance to a desired level of accuracy.

3.2 Saltwater intrusion

In coastal aquifers both fresh water and salt water are usually present. Being denser, the salt water underlies the fresh water, the latter forming a lens whose shape and thickness may vary with changes in pumping and recharge. Figure 3 depicts a typical coastal aquifer in cross-section. When the upper portion of the aquifer acts as a source of fresh water, it becomes important to design pumping and recharge strategies that prevent the flow of salt water into production wells.

Strictly speaking, salt water and fresh water are not separate phases. In fact they are completely miscible as fluids, and in a coastal aquifer there exists a zone lying between the two fluids in which salt concentration varies continuously. To be rigorously faithful to the physics of the problem, then, one would solve a single-phase flow equation coupled with a transport equation for salt. Indeed, one of the earliest numerical treatments of

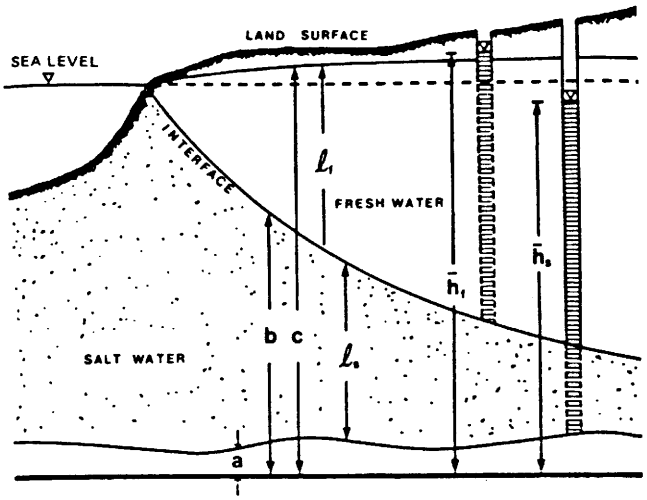

Fig. 3. Schematic cross-section of a coastal aquifer[84]

saltwater intrusion used just this approach[120]. Nevertheless, the transition zone between salt and fresh water is often quite narrow in comparison with the overall thickness of the aquifer, and for computational purposes we may consider it to be a sharp interface. Such a sharp-interface approximation serves as justification for treating saltwater intrusion into coastal aquifers as a multiphase flow.

Let us consider the problem of modelling the areal movement of salt and fresh water. To get vertically averaged flow equations, we first write the equations in terms of *hydraulic heads*, defined in the fresh water (F) and salt water (S) as follows:

$$h_\alpha = \frac{1}{g}\int_{p_{\text{ref}}}^{p_\alpha} \frac{dp'}{\rho_\alpha(p')} + z \qquad \alpha = F \text{ or } S$$

is the effective rate of withdrawal from the freshwater zone, and

$$q_F|_{z=b} = -(\mathbf{v}_F - \phi\mathbf{v}_\Sigma)|_{z=b}\cdot(\mathbf{e}_z - \nabla b)$$

is the effective rate of exchange of freshwater across the interface Σ, which we have assumed to be zero.

A similar development for salt water leads to the vertically averaged flow equation

$$\bar{\nabla}\cdot(T_S\bar{\nabla}\bar{h}_S) + q_S|_{z=b} - q_S|_{z=a} = C_S\frac{\hat{c}\bar{h}_S}{\hat{c}t} + \phi\frac{\partial b}{\partial t} \qquad (10)$$

Here $T_S = K_S l_S$ and $C_S = S_{s,S} l_S$. The sink terms in this equation are

$$q_S|_{z=b} = -(\mathbf{v}_S - \phi\mathbf{v}_\Sigma)|_{z=b}\cdot(\mathbf{e}_z - \nabla b)$$

which represents the effective rate of withdrawal from the saltwater zone, and

$$q_S|_{z=a} = -\mathbf{v}_S|_{z=a}\cdot(\mathbf{e}_z - \nabla a)$$

which gives the effective rate of saltwater leakage into the lower confining layer, whose depth is fixed.

To solve this system we need an equation relating $\bar{h}_F$ and $\bar{h}_S$. In this case, since the two fluids are miscible at the microscopic scale, there will be no head difference between the fluids where they are in contact. Thus the head is continuous across the interface Σ: $h_F = h_S$ at $z = b$. As Huyakorn and Pinder[84] show, this condition allows us to solve for $\partial b/\partial t$ in terms of heads:

$$\frac{\partial b}{\partial t} = \rho_S^*\frac{\hat{c}\bar{h}_S}{\hat{c}t} - \rho_F^*\frac{\partial\bar{h}_F}{\partial t} \qquad (11)$$

where $\rho_\alpha^* = \rho_\alpha/(\rho_S - \rho_F)$. Combining equation (11) with equations (9) and (10) yields the coupled system of flow equations

$$\nabla\cdot\begin{bmatrix} T_F & 0 \\ 0 & T_S \end{bmatrix}\nabla\begin{bmatrix}\bar{h}_F \\ \bar{h}_S\end{bmatrix} + \begin{bmatrix} q_F|_{z=c} \\ q_S|_{z=b} - q_S|_{z=a}\end{bmatrix} = \begin{bmatrix} C_F + \phi\rho_F^* & -\phi\rho_S^* \\ -\phi\rho_F^* & C_S + \phi\rho_S^*\end{bmatrix}\frac{\partial}{\partial t}\begin{bmatrix}\bar{h}_F \\ \bar{h}_S\end{bmatrix} \qquad (12)$$

Let us examine the approximate numerical solution to equation (12) using finite-element Galerkin methods. In these methods we replace the unknown functions $\bar{h}_F(\mathbf{x}, t)$ and $\bar{h}_S(\mathbf{x}, t)$ by *trial functions*

$$\hat{h}_F(\mathbf{x}, t) = h_{F,\hat{c}}(\mathbf{x}, t) + \sum_{i=1}^{I} h_{F,i}(t)N_i(\mathbf{x})$$

$$\hat{h}_S(\mathbf{x}, t) = h_{S,\hat{c}}(\mathbf{x}, t) + \sum_{i=1}^{I} h_{S,i}(t)N_i(\mathbf{x})$$

The functions $h_{F,\hat{c}}$ and $h_{S,\hat{c}}$ satisfy the essential boundary conditions for the problem at hand, and each of the sums on the right satisfies homogeneous boundary conditions. For continuous interpolating trial functions, $h_{F,i}(t)$ and $h_{S,i}(t)$ usually stand for the values of head at the ith spatial node, while the *basis functions* $N_i(\mathbf{x})$ dictate the variation between nodes.

To form the Galerkin equations corresponding to equation (12), we substitute $\hat{h}_F$ and $\hat{h}_S$ for $\bar{h}_F$ and $\bar{h}_S$ in equation (12), multiply each equation by each of the basis functions $N_1(\mathbf{x}), \ldots, N_I(\mathbf{x})$, and force the integral of the result over the spatial domain Ω to vanish. Doing this leads to time evolution equations for the unknown nodal values $h_{F,i}(t)$ and $h_{S,i}(t)$. For the freshwater equation, there results

$$\sum_{i=1}^{I}\left(K_{ij}^F h_{F,i} - Q_{ij}^F h_{F,i} + M_{ij}^{F,1}\frac{dh_{V,i}}{dt} + M_{ij}^{F,2}\frac{dh_{S,i}}{dt}\right) + \int_\Omega q_F|_{z=c}N_j\,d\mathbf{x} = B_j^F \qquad j = 1, \ldots, I$$

where K_{ij}^F, Q_{ij}^F, $M_{ij}^{F,1}$, $M_{ij}^{F,2}$ and B_j^F have the meanings assigned in Table 1.

A similar collection of evolution equations arises from the saltwater flow equation:

$$\sum_{i=1}^{I}\left(K_{ij}^S h_{S,i} - Q_{ij}^S h_{S,i} + M_{ij}^{S,1}\frac{dh_{F,i}}{dt} + M_{ij}^{S,2}\frac{dh_{S,i}}{dt}\right) + \int_\Omega (q_S|_{z=b} - q_S|_{z=a})N_j\,d\mathbf{x} = B_j^S \qquad j = 1, \ldots, I$$

where the definitions of K_{ij}^S, Q_{ij}^S, $M_{ij}^{S,1}$, $M_{ij}^{S,2}$ and B_j^S again appear in Table 1. Rewriting this set of $2I$ evolution equations in matrix form gives a system having the structure

$$[K]\{h\} + [M]\frac{\partial}{\partial t}\{h\} = \{r\} \qquad (13)$$

Table 1. Galerkin integrals appearing in the saltwater intrusion equations

$$K_{ij}^F = \int_\Omega T_F \nabla N_i \cdot \nabla N_j \, d\mathbf{x}$$

$$Q_{ij}^F = \oint_{\partial\Omega} T_F N_j \nabla N_i \cdot \mathbf{n} \, d\mathbf{x}$$

$$M_{ij}^{F,1} = -\int_\Omega (C_F + \phi\rho_F^*) N_i N_j \, d\mathbf{x}$$

$$M_{ij}^{F,2} = \int_\Omega \phi\rho_S^* N_i N_j \, d\mathbf{x}$$

$$B_j^F = -\int_\Omega T_F \nabla h_{F,\partial} \cdot \nabla N_j \, d\mathbf{x} + \oint_{\partial\Omega} N_j T_F \nabla h_{F,\partial} \cdot \mathbf{n} \, d\mathbf{x} + \int_\Omega (C_F + \phi\rho_F^*) N_j \frac{\partial h_{F,\partial}}{\partial t} \, d\mathbf{x} - \int_\Omega \phi\rho_S^* N_j \frac{\partial h_{S,\partial}}{\partial t} \, d\mathbf{x}$$

$$K_{ij}^S = \int_\Omega T_F \nabla N_i \cdot \nabla N_j \, d\mathbf{x}$$

$$Q_{ij}^S = \oint_{\partial\Omega} T_F N_j \nabla N_i \cdot \mathbf{n} \, d\mathbf{x}$$

$$M_{ij}^{S,1} = \int_\Omega \phi\rho_F^* N_i N_j \, d\mathbf{x}$$

$$M_{ij}^{S,2} = -\int_\Omega (C_S + \phi\rho_S^*) N_i N_j \, d\mathbf{x}$$

$$B_j^S = -\int_\Omega T_S \nabla h_{S,\partial} \cdot \nabla N_j \, d\mathbf{x} + \oint_{\partial\Omega} N_j T_S \nabla h_{S,\partial} \cdot \mathbf{n} \, d\mathbf{x} + \int_\Omega (C_S + \phi\rho_S^*) N_j \frac{\partial h_{S,\partial}}{\partial t} \, d\mathbf{x} - \int_\Omega \phi\rho_F^* N_j \frac{\partial h_{F,\partial}}{\partial t} \, d\mathbf{x}$$

where $\{h\}$ signifies a vector containing the $2I$ unknown nodal values of head, $[K]$ and $[M]$ are the stiffness and mass matrices arising from flux and accumulation terms, respectively, and $\{r\}$ is a vector containing known boundary data and withdrawal rates.

The system (13) is nonlinear, owing to the dependence of the zonal thicknesses l_F and l_S on the unknown heads. Thus any temporal discretization of these ordinary differential equations will have to be iterative in nature to guarantee consistency betweeh the numerical solution and the flow coefficients at each time level. Pinder and Page[121] advance one such iterative scheme.

The saltwater interface problem exhibits a peculiar computational difficulty associated with the saltwater-freshwater interface Σ. This problem manifests itself as the saltwater wedge retreats or advances. Under these circumstances the intersection of Σ with the lower confining layer, called the *saltwater toe*, moves horizontally. This moving boundary allows for the possibility that the interface may not exist at some areal locations, and at these locations the free surface condition becomes degenerate[97]. To accommodate this degeneracy, it becomes necessary to track the moving boundary as the flow calculations proceed.

Shamir and Dagan[139] present a finite-difference algorithm for tracking the saltwater toe in a vertically integrated, immiscible setting. By examining a one-dimensional flow, they develop a scheme for regnerating the spatial grid to guarantee that the toe lies on a computational node. Thus on the ocean side of the separating node they solve the simultaneous flow equations for saltwater and freshwater heads, while on the inland side they solve the equation for freshwater head only. This approach obviously involves a great deal of computational complexity in two or three dimensions, since it requires the construction of multidimensional moving finite-difference grids. However, an analogous idea for finite-element grids in two dimensions has proved promising[55].

In another approach, Sá da Costa and Wilson[131] use a fixed, two-dimensional, quadrilateral finite-element grid to model the immiscible flow equations. They devise a toe-tracking algorithm based on the Gauss points used to compute the integrals contributing to the matrix entries in equation (13). At Gauss points inland of the toe the model assigns a very small nonzero saltwater transmissibility T_S. Thus, while the saltwater wedge never actually disappears in the numerical scheme, inland of the toe the flow of salt water is negligible.

3.3 The Buckley–Leverett problem

The Buckley–Leverett problem serves as a fairly simple model of two-phase flow in a porous medium. The problem, introduced by Buckley and Leverett[34], has particular relevance in the petroleum industry, where gas and water injection are two common techniques for displacing oil toward production wells in underground reservoirs. The simplicity of the Buckley–Leverett problem arises from three basic assumptions. First, the total flow rate of oil and displacing fluid (say water) remains constant. Second, the rock matrix and fluids are incompressible. Third, the effects of capillary pressure gradients on the flow field are negligible compared with the pressure gradients applied through pumping. These assumptions are too restrictive to permit widespread application of the Buckley–Leverett model, but, as we shall argue below, the simplified model acts as a paradigm for the numerical difficulties that occur in more complicated models of oil reservoirs.

To derive the Buckley–Leverett model, we begin with equation (5), identifying N as oil and W as water and assuming an isotropic porous medium:

$$\frac{\partial}{\partial t}(\phi S_N \rho_N) - \nabla \cdot [\rho_N \Lambda_N (\nabla p_W + \nabla p_{CNW} - \rho_N g \nabla Z)] = 0$$

$$\frac{\partial}{\partial t}(\phi S_W \rho_W) - \nabla \cdot [\rho_W \Lambda_W (\nabla p_W - \rho_W g \nabla Z)] = 0$$

where $\Lambda_\alpha = k k_{r\alpha}/\mu_\alpha$ is the mobility of fluid α. Coupled to these flow equations are the constraint $S_N + S_W = 1$ and a capillary relationship $p_{CNW} = p_{CNW}(S_W)$. If we restrict our attention to one-dimensional flow in a homogeneous reservoir of uniform cross-section and assume that gravity effects are absent, then the flow equations collapse to

$$\frac{\partial}{\partial t}(\phi S_N \rho_N) - \frac{\partial}{\partial x}\left[\rho_N \Lambda_N \left(\frac{\partial p_W}{\partial x} + \frac{\partial p_{CNW}}{\partial x}\right)\right] = 0$$

$$\frac{\partial}{\partial t}(\phi S_W \rho_W) - \frac{\partial}{\partial x}\left(\rho_W \Lambda_W \frac{\partial p_W}{\partial x}\right) = 0$$

Now we invoke the assumption that capillarity has negligible effect on the flow field-wide, so that

$\partial p_{CNW}/\partial x \simeq 0$. Further, the incompressibility assumption implies that ϕ, ρ_N and ρ_W are constant in time and that the fluid densities are uniform in space, so that

$$\phi \frac{\partial}{\partial t}(1-S_W) - \frac{\partial}{\partial x}\left(\Lambda_N \frac{\partial p_W}{\partial x}\right) = 0 \qquad (14a)$$

$$\phi \frac{\partial S_W}{\partial t} - \frac{\partial}{\partial x}\left(\Lambda_W \frac{\partial p_W}{\partial x}\right) = 0 \qquad (14b)$$

Now observe that $-\Lambda_\alpha \partial p_w/\partial x$ is the Darcy flux q_α of phase α. Also, by assumption, the total flow rate $q = q_W + q_N$ is a constant. Thus we need only solve one of equations (14), using the constant value of q to solve the other equation by subtraction.

Let us solve the water equation (14b). Since $-\Lambda_W \partial p_W/\partial x = q_W = \Lambda_W q/(\Lambda_W + \Lambda_N)$, we arrive at the Buckley–Leverett saturation equation

$$\frac{\partial S_W}{\partial t} + \frac{\partial}{\partial x}\left(\frac{q f_W}{\phi}\right) = 0 \qquad (15)$$

where $f_W = \Lambda_W/(\Lambda_N + \Lambda_W)$ is the *fractional flow* of water. Equation (15) is clearly nonlinear, since f_W depends on the unknown water saturation S_W through the fluid mobilities. While the functional form of $f_W(S_W)$ depends on the particular rock-fluid system being modelled, fractional flow functions typically have an 'S-shaped' profile over their supports $(S_{Wr}, 1-S_{Nr})$, as shown in Fig. 4.

Difficulties in solving Cauchy problems involving equation (15) arise from two sources. First, the equation itself is a nonlinear, hyperbolic conservation law. Its hyperbolicity owes to our neglect of capillary pressure gradients, inclusion of which would have led to an additional second-order term of the form

$$\frac{\partial}{\partial x}\left[\phi^{-1}\Lambda_W p'_{CNW}(S_W)\frac{\partial S_W}{\partial x}\right]$$

Thus equation (15) is, in effect, an approximation to a singularly perturbed parabolic problem in which we have neglected the dissipative effects of capillarity.

Second, the flux function qf_W/ϕ appearing in equation (15) is nonconvex, its S-shaped form implying the existence of an inflection point somewhere in its support. The literature on hyperbolic conservation laws with nonconvex flux functions is quite extensive, including important contributions by Lax[90] and Oleinik[111] and a general discussion by Chorin and Marsden[39]. Of special importance in the present context are the following facts. Cauchy problems based on equation (15) may have no solutions that are classical in the sense of being continuously differentiable over their (x,t)-domains $\Omega \times J$. Instead, such problems may admit only *weak solutions* $S_W(x,t)$. These solutions need only satisfy the integral relation

$$\int_{\Omega \times J}\left[S_W \frac{\partial \varphi}{\partial t} + \frac{q}{\phi} f_W(S_W)\frac{\partial \varphi}{\partial x}\right] dx\, dt = 0 \qquad (16)$$

for all infinitely differentiable functions $\varphi(x,t)$ that vanish on the boundary $\partial(\Omega \times J)$[126]. In contrast to equation (15), equation (16) admits functions $S_W(x,t)$ that have discontinuities, or saturation shocks. Unfortunately, weak solutions may not be unique: there may be several different functions $S_W(x,t)$ that satisfy the integral equation (16).

Nature admits only one solution to the Buckley–Leverett problem. Much of the research into hyperbolic conservation laws has aimed at identifying physically correct weak solutions from among the class of functions obeying equation (16). To specify the physical solution requires an additional constraint known as the *entropy condition*. There are several equivalent forms of this constraint, including the following[13]:

(i) The solution must depend continuously and stably on the initial data, implying that characteristics on both sides of a discontinuity must intersect the initial curve.

(ii) The solution must be the same as that obtained using the method of characteristics with $f_W(S_W)$ replaced by its convex hull.

(iii) The solution must be the limit of solutions, for the same initial data, to a parabolic problem differing from the hyperbolic one by a dissipative second-order term (in this case, capillarity) of vanishing influence.

The tangent construction advanced by Welge[159] explicitly implements condition (ii) while, as Welge shows in his paper, the 'equal-area' rule of Buckley and Leverett[34] imposes this same constraint in a slightly different fashion.

Any numerical scheme for solving the Buckley–Leverett problem, or even more complicated models of multiphase flows that are hyperbolic in character, must respect the entropy condition or else risk producing nonphysical results. Douglas *et al.*[57], for example, propose adding an artificial capillarity to the Buckley–Leverett equation to force convergence to the correct physical solution. An equivalent effect can be achieved by using certain numerical approximations whose lowest-

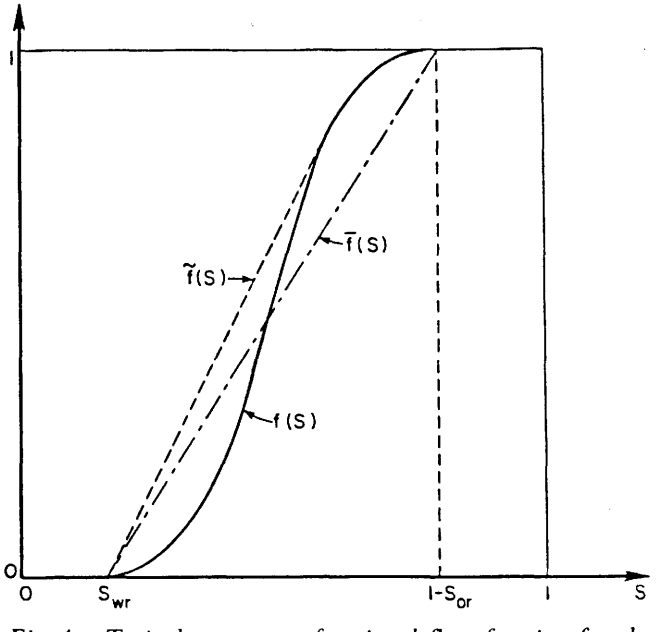

Fig. 4. Typical nonconvex fractional flow fraction f and related convex functions[13]

order error terms mimic the desired dissipative phenomena[8]. This tactic is perhaps easiest to see in finite-difference approximations. Here, an upstream-biased difference analog of the flux term $\partial f/\partial x$ gives

$$\frac{f_i - f_{i-1}}{\Delta x} = \left.\frac{\partial f}{\partial x}\right|_i - \frac{\Delta x}{2}\frac{\hat{c}}{\partial x}\left[f'(S)\frac{\partial S}{\partial x}\right]_i + \mathcal{O}(\Delta x^2)$$

Since $f'(S) > 0$ over the support of f, the lowest-order error term acts like the capillarity term neglected in equation (15) while vanishing linearly as $\Delta x \to 0$. Thus upstream weighting imposes a numerical version of condition (iii) while maintaining consistency in the numerical approximation.

Several investigators have examined upstream-weighted finite-element methods for the Buckley–Leverett problem. Mercer and Faust[96] and Huyakorn and Pinder[83], for example, discuss upstream-weighted Galerkin techniques. Shapiro and Pinder[140] advance a finite-element collocation scheme for the Buckley–Leverett problem using asymmetric basis functions.

Allen and Pinder[12,13] introduce a collocation scheme for the same problem in which upstream biasing of the collocation points leads to the appropriate numerical version of condition (ii). To implement this method, we begin with a continuously differentiable trial function for saturation:

$$\hat{S}(x,t) = \sum_{i=0}^{I} [S_i(t)H_{0,i}(x) + S_i'(t)H_{1,i}(x)]$$

where the basis functions $H_{0,i}(x)$, $H_{1,i}(x)$ are piecewise Hermite cubic polynomials (5). $S_i(t)$, $S_i'(t)$ are the unknown nodal values of S_w and $\partial S_w/\partial x$, respectively. One can similarly represent the nonlinear flux function f_w:

$$\hat{f} = \sum_{i=1}^{I}\left[f_w(S_i)H_{0,i} + \frac{df_w}{dS_w}(S_i)S_i'H_{1,i}\right]$$

In the standard collocation we derive ordinary differential equations for the unknown values S_i, S_i', by setting

$$\frac{\partial \hat{S}}{\partial t}(\bar{x}_k, t) + \frac{q}{\phi}\frac{\partial \hat{f}}{\partial x}(\bar{x}_k, t) = 0$$

at enough points $\bar{x}_k$ in the spatial domain to give one equation for each unknown. Douglas and Dupont[58] show that, on a uniform partition $x_0 < \cdots < x_I = x_0 + I\,\Delta x$, one can achieve $\mathcal{O}(\Delta x^4)$ accuracy in parabolic problems by choosing the Gauss points $x_i - \Delta x/2 \pm \Delta x/\sqrt{3}$, $i = 1, \ldots, I-1$, as the collocation points. As Allen and Pinder[13] demonstrate, however, this highly accurate scheme violates the entropy condition in equation (15). One can force convergence to the correct solution by evaluating the flux term at collocation points upstream of the Gauss points, as in the equation

$$\frac{\partial \hat{S}}{\partial t}(\bar{x}_k, t) + \frac{q}{\phi}\frac{\partial \hat{f}}{\partial x}(\bar{x}_k^*, t) = 0$$

Here, for flow in positive x direction, $\bar{x}_k^* < \bar{x}_k$. Allen[7] presents an error analysis showing how this scheme introduces artificial capillarity. Figures 5 and 6 compare the results of standard collocation and upstream collocation, respectively.

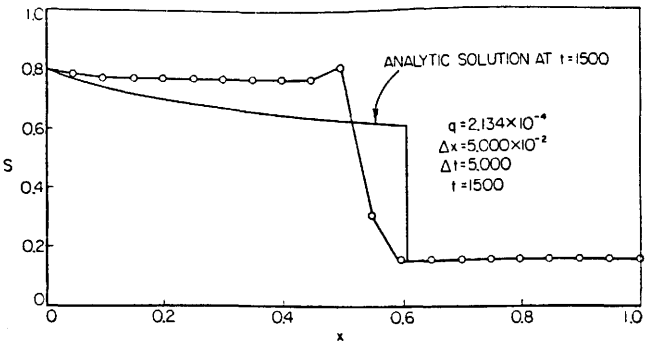

Fig. 5. Solution to the Buckley–Leverett problem generated by orthogonal collocation with $\Delta x = 0.1$[12]

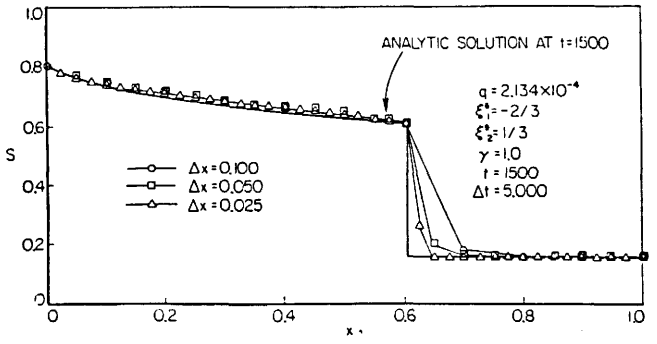

Fig. 6. Solutions to the Buckley–Leverett problem generated by upstream collocation with $\Delta x = 0.1$, 0.05, 0.025[12]

Several investigators have examined the use of upstream weighting in more sophisticated models of multiphase flow. Among the many such studies are those by Peacemen[113], Settari and Aziz[137] and Young[164], each of which offers a good overview of numerical approximations used to model two-phase flows. We shall consider upstream weighting further in Section 4.

One unfortunate aspect of upstream-biased approximations is that their artificially dissipative effects, while guaranteeing convergence, produce unrealistically smeared sharp fronts when the spatial grid mesh is large. What is 'large' in this sense depends on the physics of the problem and not the computational resources of the modeller. Therefore, in some problems, unacceptable smearing on uniform grids can occur even when the grid mesh approaches limits in affordable fineness. One approach to resolving this dilemma is to refine the spatial grid only in the vicinity of the steep front. Since the front itself moves as the flow progresses, such a strategy calls for self-adaptive local grid refinement, a topic discussed in Section 6.

4. FLOWS WITH INTERPHASE MASS TRANSFER

In many multiphase flows of interest in engineering the exchange of chemical species among the fluid phases is crucial to the behaviour of the flows. Historically, concern with the compositional aspects of multiphase flows in porous media originated in the petroleum industry, where the effects of gas dissolution, retrograde condensation, and vaporization and condensation of injected gases have substantial implications in oil recovery operations. As the

complexities of groundwater contamination by organic wastes become more urgent, however, interest in multiphase flows with mass transfer has spread to the hydrology community. In this section we shall focus on the more established modelling efforts in the petroleum industry, leaving discussion of the newer applications in hydrology to Section 5.

4.1 Compositional oil reservoir flows

In compositional flows there are several fluid phases in which some number of chemical species reside. It is therefore necessary to extend the mixture-theoretic formalism to accommodate two different categories of constituents: phases and species. A more detailed exposition of the development given below appears in Allen[7]. For simplicity, let us assume that there are three fluid phases, namely water (W), oil (O) and gas(G) with chemical species indexed by $i=1,\ldots,N+1$. As before, let us label the rock phase by the index R. Conceivably, at least, each species can exist in any phase and can transfer between phases via dissolution, evaporation, condensation and so forth, subject to thermodynamic constraints. We shall assume here that the rock is chemically inert and that there are no intraphase or stoichiometric chemical reactions, although in such applications as enhanced oil recovery by alkaline fluid injection reactions of this kind may be important.

In our new formalism, each pair (i,α), with i chosen from the species indices and α chosen from the phases, is a constituent. Thus, for example, CH_4 in the gas phase is one constituent, CH_4 in oil another and n-C_4H_{10} in oil yet another. Each constituent (i,α) has its own *intrinsic mass density* ρ_i^α, measured as mass of i per unit volume of α, and its own velocity $\mathbf{v}_i^\alpha$. To accommodate the familiar kinematics of phases, we shall still associate with each phase α its volume fraction ϕ_α, and if $\phi=1-\phi_R$ as before, then we define the saturation of fluid phase α as $S_\alpha=\phi_\alpha/\phi$. Using these basic quantities, we define the following variables:

$$\rho^\alpha=\sum_{i=1}^{N}\rho_i^\alpha=\text{intrinsic mass density of phase }\alpha$$

$$\omega_i^\alpha=\rho_i^\alpha/\rho^\alpha=\text{mass fraction of species } i \text{ in phase }\alpha$$

$$\rho=\phi\sum_{\alpha\neq R}S_\alpha\rho^\alpha=\text{bulk density of fluids}$$

$$\omega_i=(\phi/\rho)\sum_{\alpha\neq R}S_\alpha\rho^\alpha\omega_i^\alpha$$
$$=\text{total mass fraction of species } i \text{ in the fluids}$$

$$\mathbf{v}^\alpha=(1/\rho^\alpha)\sum_{i=1}^{N}\rho_i^\alpha\mathbf{v}_i^\alpha$$
$$=\text{barycentric velocity of phase }\alpha$$

$$\mathbf{u}_i^\alpha=\mathbf{v}_i^\alpha-\mathbf{v}^\alpha$$
$$=\text{diffusion velocity of species } i \text{ in phase }\alpha$$

If the index $N+1$ represents the species making up the inert rock phase, then the following constraints hold:

$$\sum_{i=1}^{N}\omega_i=\sum_{i=1}^{N}\omega_i^\alpha=\sum_{\alpha}\phi_\alpha=\sum_{\alpha\neq R}S_\alpha=1$$

where the index α in the second sum can represent any fluid phase, and

$$\sum_{i=1}^{N}\mathbf{u}_i^\alpha=\mathbf{0}$$

Each constituent (i,α) has its own mass balance, given by analogy with equation (1) as

$$\frac{\partial}{\partial t}(\phi_\alpha\rho_i^\alpha)+\nabla\cdot(\phi_\alpha\rho_i^\alpha\mathbf{v}_i^\alpha)=r_i^\alpha$$

where the exchange terms r_i^α must obey the restriction $\sum_{i=1}^{N}\sum_{\alpha\neq R}r_i^\alpha=0$. If we impose the further constraint that there are no intraphase chemical reactions, then we have in addition $\sum_{\alpha\neq R}r_i^\alpha=0$ for each species $i=1,\ldots,N$. Since phase velocities are typically more accessible to measurement than species velocities, it is convenient to rewrite the constituent mass balance as

$$\frac{\partial}{\partial t}(\phi S_\alpha\rho^\alpha\omega_i^\alpha)+\nabla\cdot(\phi S_\alpha\rho^\alpha\omega_i^\alpha\mathbf{v}^\alpha)+\nabla\cdot\mathbf{j}_i^\alpha=r_i^\alpha$$

where $\mathbf{j}_i^\alpha=\phi S_\alpha\rho^\alpha\omega_i^\alpha\mathbf{u}_i^\alpha$ stands for the *diffusive flux* of constituent (i,α). Summing this equation over all fluid phases α and using the restrictions gives a total mass balance for each species i:

$$\frac{\partial}{\partial t}(\rho\omega_i)+\nabla\cdot[\phi(S_W\rho^W\omega_i^W\mathbf{v}^W+S_O\rho^O\omega_i^O\mathbf{v}^O+S_G\rho^G\omega_i^G\mathbf{v}^G)]$$
$$+\nabla\cdot(\mathbf{j}_i^W+\mathbf{j}_i^O+\mathbf{j}_i^G)=0\qquad i=1,\ldots,N$$

To establish flow equations for each species, we need velocity field equations for each fluid phase and some constitutive equations for the diffusive fluxes $\mathbf{j}_i^\alpha$. For the fluid velocities we may postulate Darcy's law, equation (4), assuming in addition that the porous medium is isotropic. For the diffusive fluxes the appropriate assumption is not so clear. In single-phase flows through porous media, the diffusive flux of a species with respect to the fluid's barycentric velocity is called *hydrodynamic dispersion*. As reviewed in Section 5, theories of hydrodynamic dispersion in multiphase flows remain poorly developed. The most common approach in oil reservoir simulation is to assume that hydrodynamic dispersion is a small enough effect that the diffusive fluxes in the mass balance for each species are negligible. Thus we arrive at the flow equation for species i in the fluids:

$$\frac{\partial}{\partial t}[\phi(S_W\rho^W\omega_i^W+S_O\rho^O\omega_i^O+S_G\rho^G\omega_i^G)]$$
$$-\nabla\cdot\left[\frac{kk_{rW}\rho^W\omega_i^W}{\mu_W}(\nabla p_W-\rho^W g\nabla Z)+\frac{kk_{rO}\rho^O\omega_i^O}{\mu_O}(\nabla p_O-\rho^O g\nabla Z)\right.$$
$$\left.+\frac{kk_{rG}\rho^G\omega_i^G}{\mu_G}(\nabla p_G-\rho^G g\nabla Z)\right]=0\qquad i=1,\ldots,N$$

To close this set of equations, we need some supplementary constraints giving relationships among the variables. One class of supplementary constraints consists of the thermodynamic relationships giving phase densities and compositions as functions of pressure and overall fluid mixture composition. Conceptually, these relationships take the forms

$$\rho^\alpha=\rho^\alpha(\omega_1^\alpha,\ldots,\omega_{N-1}^\alpha,p_\alpha)\qquad\alpha=W,O,G\quad i=1,\ldots,N-1$$

$$\omega_i^\alpha = \omega_i^\alpha(\omega_1, \ldots, \omega_{N-1}, p_\alpha) \qquad \alpha = W, O, G$$

$$S_\alpha = S_\alpha(\omega_1, \ldots, \omega_{N-1}, p_\alpha) \qquad \alpha = W, O, G$$

However, it is important from a computational viewpoint to observe that the actual mathematical statements of these relationships may constitute simultaneous sets of nonlinear algebraic equations giving phase densities, compositions and saturations implicitly. This occurs, for example, when one uses equal-fugacity constraints in conjunction with an equation of state to solve for local thermodynamic equilibria, as discussed further below.

The other class of supplementary constraints includes constitutive relationships for the particular rock-fluid system being modelled. These relationships may take the following forms:

$$p_{COW} = p_{COW}(S_O, S_G) \qquad \alpha = W, O, G$$

$$p_{CGO} = p_{CGO}(S_O, S_G)$$

$$k_{r\alpha} = k_{r\alpha}(S_O, S_G)$$

Here, as mentioned in Section 2, we have greatly simplified the physics of many compositional flows by omitting possible dependencies on fluid composition through variations in interfacial tension.

4.2 Black-oil simulation

Black-oil models are special cases of the general compositional equations that allow limited interphase mass transfer, the composition of each phase depending on pressures only. This class of models has become a standard engineering tool in the petroleum industry. As a consequence the literature on the numerics of black-oil simulation, which apparently began in 1948 with a consulting report by John van Neumann[156], has become quite extensive. Indeed, there are now several books in print devoted to black-oil simulation[114,18]. Since any attempt to cover this field in an article of the present scope would be futile, we shall merely review the formulation of the black-oil equations and discuss selected aspects of their numerical solution.

The fundamental premise of the black-oil model is that a highly simplified, three-species system can often serve as an adequate model of the complex mixtures of brine and hydrocarbons found in natural petroleum reservoirs. For practical purposes, petroleum engineers define these three pseudo-species according to what appears at the surface, at stock-tank conditions (STC), after production of the reservoir fluids. Thus, we have the species o, which is stock-tank oil; g, which is stock-tank gas, and w, which is stock-tank water. Underground, at reservoir conditions (RC), these species may partition themselves among the three fluid phases O, G and W in a distribution depending on the pressures in the formation.

Now we impose a set of thermodynamic constraints on this partitioning of species. First, we assume that there is no exchange of water w into the nonaqueous phases O and G, so that $\omega_w^w = 1$, and $\omega_w^O = \omega_w^G = 0$. Second, we allow no exchange of oil o into the vapour phase G or the aqueous liquid W, so that $w_o^O = 1$, and $\omega_o^W = \omega_o^G = 0$. Third, we prohibit the dissolution of gas g into the aqueous liquid W, so that $\omega_g^W = 0$. However, we allow the gas g to dissolve in the hydrocarbon liquid O according to a pressure-dependent relationship called the *solution gas-oil ratio*, defined by

$$R_S(p_O) = \frac{\text{volume of } g \text{ in solution at RC}}{\text{volume of } o}$$

where the volumes refer to volumes at STC.

To facilitate further reference to volumes of species at STC, we relate the phase densities ρ^α at RC to the species densities ρ_i^{STC} at STC by defining the *formation volume factors*. For W and G these definitions are fairly simple:

$$B_W(p_W) = \rho_w^{STC}/\rho^W \qquad B_G(p_W) = \rho_g^{STC}/\rho^G$$

For the hydrocarbon liquid O, however, we must also account for the mass of dissolved gas at RC:

$$B_O(p_O) = (\rho_o^{STC} + R_S \rho_g^{STC})/\rho^O$$

If we substitute these definitions into the flow equations (16) for the species o, g, w and divide through by the constants ρ_i^{STC}, we obtain the three black-oil equations

$$\frac{\partial}{\partial t}\left(\frac{\phi S_W}{B_W}\right) - \nabla \cdot [\lambda_W(\nabla p_W - \gamma_W \nabla Z)] = 0 \qquad (17a)$$

$$\frac{\partial}{\partial t}\left(\frac{\phi S_O}{B_O}\right) - \nabla \cdot [\lambda_O(\nabla p_O - \gamma_O \nabla Z)] = 0 \qquad (17b)$$

$$\frac{\partial}{\partial t}\left[\phi\left(\frac{S_G}{B_G} + \frac{R_S S_O}{B_O}\right)\right] - \nabla \cdot [\lambda_G(\nabla p_G - \gamma_G \nabla Z)] - \nabla \cdot [R_S \lambda_O(\nabla p_O - \gamma_O \nabla Z)] = 0 \qquad (17c)$$

where $\lambda_\alpha = \Lambda_\alpha / B_\alpha$ and $\gamma_\alpha = \rho^\alpha g$.

These equations constitute a system of coupled, nonlinear, time-dependent partial differential equations. Each of the equations is formally parabolic in appearance. However, as suggested by the greatly simplified development in Section 3.3, the system can exhibit behaviour more typical of hyperbolic equations if capillary influences are small. To see this, consider the two-phase version of equation (17) in which gas is absent, porosity is constant and fluid compressibilities and gravity forces have no effect. The flow equations in this case reduce to

$$-\phi \frac{\partial S_W}{\partial t} = \nabla \cdot (\lambda_O \nabla p_O)$$

$$\phi \frac{\partial S_W}{\partial t} = \nabla \cdot (\lambda_W \nabla p_W)$$

Adding these two equations gives a total flow equation $\nabla \cdot \mathbf{q} = 0$, where $\mathbf{q} = -\lambda_O \nabla p_O - \lambda_W \nabla p_W$. Calling $\lambda = \lambda_O + \lambda_W$ and $p = (p_O + p_W)/2$, we can rewrite the total flow equation as

$$\nabla \cdot (\lambda \nabla p) - \left(\frac{\lambda_W - \lambda_O}{2}\right) \nabla p_{COW} = 0$$

If we examine the case when $\nabla p_{COW} \simeq 0$, the total flow equation reduces to an elliptic *pressure equation*

$$\nabla \cdot (\lambda \nabla p) = 0 \qquad (18a)$$

Then, recalling the fractional flow function $f_W = \lambda_W/(\lambda_O + \lambda_W)$, we can rewrite the water flow equation as

$$\phi \frac{\partial S_W}{\partial t} + \mathbf{q} \cdot \nabla f_W(S_W) = 0 \qquad (18b)$$

This *saturation equation* is the hyperbolic analog of the one-dimensional Buckley–Leverett problem.

Several approaches to solving the general system (17) numerically have appeared in the petroleum engineering

literature. We shall review two of the most popular methods: the simultaneous solution (SS) method and the implicit pressure–explicit saturation (IMPES) method.

The SS method, introduced by Douglas, Peaceman and Rachford[59], and further developed by Coats *et al.*[45], treats the flow equations (17) as simultaneous equations for the fluid pressures p_O, p_G and p_W. Inverting the capillarity relationships and imposing the restriction on fluid saturations then yields the saturations S_O, S_G and S_W. For ease of presentation, let us examine the two-phase case, assuming that the vapor phase G does not appear and that the porosity ϕ is constant.

The first step in the formulation is to rewrite the flow equations so that the pressures p_O and p_W appear as explicit unknowns. To do this, we apply the chain rule to the accumulation terms, giving

$$\frac{\partial}{\partial t}\left(\frac{\phi S_W}{B_W}\right)=\phi S_W b_W \frac{\partial p_W}{\partial t}+\frac{\phi S'_W}{B_W}\left(\frac{\partial p_O}{\partial t}-\frac{\partial p_W}{\partial t}\right)$$

$$\frac{\partial}{\partial t}\left(\frac{\phi S_O}{B_O}\right)=\phi S_O b_O \frac{\partial p_O}{\partial t}-\frac{\phi S'_W}{B_O}\left(\frac{\partial p_O}{\partial t}-\frac{\partial p_W}{\partial t}\right)$$

where $b_\alpha=\mathrm{d}(1/B_\alpha)/\mathrm{d}p_\alpha$ and S'_W signifies the derivative of the inverted capillarity relationship $S_W(p_{COW})$. This device allows us to write the system (17) as follows:

$$\phi\begin{bmatrix}(S_W b_W - S'_W/B_W) & (S'_W/B_O)\\ (S'_W/B_O & (S_O b_O - S'_W/B_O)\end{bmatrix}\frac{\partial}{\partial t}\begin{bmatrix}p_W\\ p_O\end{bmatrix}$$
$$-\nabla\cdot\begin{bmatrix}(\Lambda_W/B_W)\nabla & 0\\ 0 & (\Lambda_O/B_O)\nabla\end{bmatrix}\begin{bmatrix}p_W\\ p_O\end{bmatrix}$$
$$+\begin{bmatrix}\rho^W g\nabla Z\\ \rho^O g\nabla Z\end{bmatrix}=\begin{bmatrix}0\\ 0\end{bmatrix} \quad (18)$$

Now we can employ some finite-difference or finite element method to approximate the spatial derivative in equation (18), getting a system of evolution equations having the form

$$[M]\frac{d}{dt}\{p\}+[K]\{p\}=\{f\}$$

Here $[M]$ is the mass matrix, $[K]$ is the stiffness matrix, $\{p\}$ represents the vector of unknown nodal values of oil and water pressure and $\{f\}$ is a vector containing information from the discretized boundary conditions. Since the entries of $[M]$ and $[K]$ vary with the unknown pressures, this system is nonlinear. Therefore the time-stepping approximation must be iterative. As an example, we might use a Newton-like procedure analogous to that presented in Section 3.1, yielding

$$\left(\frac{1}{\Delta t}[M]^{n+1,m}+[K]^{n+1,m}\right)\{\delta p\}^{n+1,m+1}$$
$$=-\left[\frac{1}{\Delta t}[M]^{n+1,m}(\{p\}^{n+1,m}-\{p\}^n)\right.$$
$$\left.-[K]^{n+1,m}\{p\}^{n+1,m}+\{f\}^{n+1,m}\right]=-\{R\}^{n+1,m}$$

In this scheme the notation $\{R\}^{n+1,m}$ suggests that we regard the right side as a residual, iterating at each time step until $\|\{R\}^{n+1,m}\|$ is small enough in some norm.

The formulation presented above is not unique. In fact, several variants of the SS method have appeared, including formulations treating different sets of variables as principal unknowns. Aziz and Settari[18] provide a survey of these alternative approaches.

In the IMPES formulation, the basic idea is to combine the flow equations (17) to get an equation for one of the fluid pressures[32]. Solving the equation implicitly provides the information necessary to update the saturations explicitly at each time step, using an independent set of flow equations and the restriction that saturations sum to unity. Sheldon, Zondek and Cardwell[141] and Stone and Garder[145] introduced this method.

The development follows a line of reasoning paralleling that leading to equations (18). We begin, as in the SS method, by expanding the accumulation terms, this time leaving saturations and pressures as principal unknowns. For the three-phase system, this leads to the following finite-difference approximations

$$\phi\frac{\partial}{\partial t}\left(\frac{S_W}{B_W}\right)=\frac{1}{\Delta t}(C_1\Delta_t S_W+C_2\Delta_t p_W)+\mathcal{O}(\Delta t)$$

$$\phi\frac{\partial}{\partial t}\left(\frac{S_O}{B_O}\right)=\frac{1}{\Delta t}(C_3\Delta_t S_O+C_4\Delta_t p_O)+\mathcal{O}(\Delta t)$$

$$\phi\frac{\partial}{\partial t}\left(\frac{S_G}{B_G}+\frac{R_S S_O}{B_O}\right)$$
$$=\frac{1}{\Delta t}(C_5\Delta_t S_G+C_6\Delta_t p_G+C_7\Delta_t S_O+C_8\Delta_t p_O)+\mathcal{O}(\Delta t)$$

The coefficients $C_1,\ldots,C_8$ appearing here stand for the appropriate derivatives extracted using the chain rule, and $\Delta_t u=u^{n+1}-u^n$ defines the time-difference operator.

The next step involves the crucial assumption that the capillary pressures p_{COW}, p_{CGO} change negligibly over a time step. This assumption implies that $\Delta_t p_O=\Delta_t p_W=\Delta_t p_G$ and, furthermore, that we can treat the capillary contributions to the flux terms explicitly. Thus, our implicit, temporally discrete approximations to equation (17) become

$$C_1\Delta_t S_W+C_2\Delta_t p_O=\Delta t\nabla\cdot[\lambda_W^{n+1}(\nabla p_O^{n+1}-\nabla p_{COW}^n-\gamma_W^{n+1}\nabla Z)] \quad (19a)$$

$$C_3\Delta_t S_O+C_4\Delta_t p_O=\Delta t\nabla\cdot[\lambda_O^{n+1}(\nabla p_O^{n+1}-\gamma_O^{n+1}\nabla Z)] \quad (19b)$$

$$C_5\Delta_t S_G+C_7\Delta_t S_O+(C_6+C_8)\Delta_t p_O$$
$$=\Delta t\nabla\cdot[\lambda_G^{n+1}(\nabla p_O^{n+1}+\nabla p_{CGO}^{n+1}-\gamma_G^{n+1}\nabla Z)$$
$$+R_S^{n+1}\lambda_O^{n+1}(\nabla p_O-\gamma_O^{n+1}\nabla Z)] \quad (19c)$$

To get a single pressure equation from this set, we multiply equation (19c) by the coefficient $B=C_3/(C_7-C_5)$, multiply equation (19a) by $A=BC_5/C_1$, add equations (19a–c), and observe that the saturation differences in the accumulation terms now sum to an expression proportional to $\Delta_t(S_W+S_O+S_G)=0$. Therefore our weighted sum of the time-differenced flow equations yields

$$C^{n+1}\Delta_t p_O=\Delta t\{A^{n+1}\nabla\cdot(\lambda_W^{n+1}\nabla p_O^{n+1})+\nabla\cdot(\lambda_O^{n+1}\nabla p_O^{n+1})$$
$$+B^{n+1}\nabla\cdot[(\lambda_G^{n+1}+R_S^{n+1}\lambda_O^{n+1})\nabla p_O^{n+1}]-\Gamma^{n+1}\} \quad (20)$$

The new parameter Γ is shorthand for the weighted sum of the gravity terms, and $C=AC_2+C_4+B(C_6+C_8)$. Equation (20) is the *pressure equation*.

Now, provided we have an appropriate technique for producing discrete approximations to the spatial derivatives appearing in these equations, we can implement the following time-stepping procedure.

(i) Solve equation (20) implicitly, using some iterative scheme.
(ii) Solve equation (19a) explicitly for $\Delta_t S_W$ and update the water saturation; solve (19b) for $\Delta_t S_O$ and update the oil saturation, setting $S_G^{n+1} = 1 - S_W^{n+1} - S_O^{n+1}$.
(iii) Compute p_{COW}^{n+1} and p_{CGO}^{n+1} using the new saturations; then use these to update p_W and p_G.
(iv) Begin the next time step.

Notice that, in contrast to the SS formulation, the IMPES approach requires the implicit solution of only one flow equation at each time step. As with the SS methods, variants on this development have appeared; see Aziz and Settari[18] for a survey.

The IMPES approach offers the obvious advantage that, with only one implicit equation to solve per time step, the algorithm requires smaller matrix inversions at each iteration. The resulting computational savings can be significant in problems involving large numbers of grid points. On the other hand, because it treats capillary pressures explicitly, the IMPES method suffers instability when the time step Δt exceeds a critical value. This limitation can be inconvenient if the critical value of Δt is unknown or small compared with the life of a field project. The SS method, while requiring more computation per time step, boasts greater stability. This can prove to be a decided advantage when the problem to be solved exhibits strongly nonlinear phenomena, such as coning near wellbores or liquid hydrocarbons passing through bubble points.

The performance of black-oil models is quite sensitive to the treatment of nonlinear coefficients in the discrete flow equations. Consider, for example, the spatial treatment of the flux coefficients λ_α. It is standard practice to use upstream-weighted approximations to these coefficients. To see why, examine the results of Fig. 7, showing predictions of a one-dimensional black-oil model using several midpoint and upstream approximations to λ_α. These plots show that upstream-biased analogs of the flux coefficients force the numerical solution to converge to the correct physical solution when capillarity is small. This result corroborates our discussion of the Buckley–Leverett problem in Section 3.3, since, as we have argued, the black-oil system exhibits similar hyperbolic features.

The temporal weighting of the flux coefficients also affects the solution to the black-oil equations. It is a fairly common practice to treat these coefficients explicitly. As Settari and Aziz show, however, this tactic leads to limits on time steps allowable for stable solutions. The limitation is especially severe in problems with gas percolation, which occurs when the fluid mixture pressure drops below the bubble point. Blair and Weinaug[28] introduce the implicit treatment of the flux coefficients that alleviates this stability problem. As Coats[43] reviews, this highly stable method has proved attractive in simulating other, more complex oil-reservoir flows.

One of the most important problems in black-oil simulation, and in fact in reservoir simulation more generally, is the computational inefficiency associated with the solution of large systems of linear algebraic equations. In either the SS or the IMPES approach, the

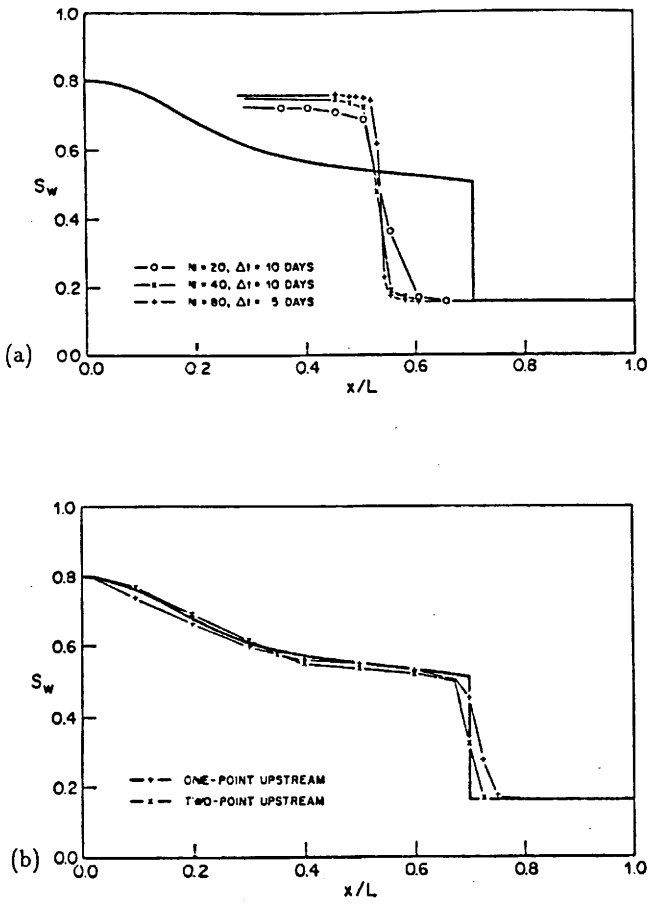

Fig. 7. Black-oil model solutions using (a) midpoint-weighted flux coefficients and (b) upstream-weighted flux coefficients[18]

iterative time-stepping scheme calls for the solution of matrix equations at each iteration of each time step. For simulations at practical scales these calculations alone can tax the storage and CPU-time resources of the largest machines currently available. A great deal of recent research has focused on the development of fast iterative techniques for the solution of the large matrix systems arising in applications.

Among the oldest of these iterative techniques are the *block-iterative* methods. These methods use the blocked, sparse structure of the linear systems to solve the equations iteratively, block-by-block[27]. Block iterative methods, such as block-successive overrelaxation, tend to be quite sensitive to 'tunable' iteration parameters such as overrelaxation coefficients.

Another fairly old class of iterative techniques consists of *alternating direction* methods. These methods, introduced in the context of finite differences by Peaceman and Rachford[115], Douglas and Rachford[60] and Douglas[56], reduce the computational effort in multi-dimensional problems by implicitly solving over one space dimension at a time. While interest in alternating direction techniques for finite differences has waned in recent years, interest in alternating-direction Galerkin and collocation methods has been growing; see, for example, Ewing[62] and Celia and Pinder[36].

In a different approach, Stone[143] proposes the *strongly implicit procedure* (SIP) for solving matrix equations implicitly. The idea here is to replace a matrix equation

having the form $[A]\{p\}=-\{R\}$ by an iterative scheme having the form

$$([A]+[N])\{p\}^{m+1}=([A]+[N])\{p\}^{m}-([A]\{p\}^{m}+\{R\})$$

By properly choosing the matrix $[N]$, one can efficiently factor $([A]+[N])$ into a product of sparse upper- and lower-triangular matrices. This idea gives rise to an algorithm that gives relatively rapid convergence to the solution $\{p\}$ of the original equation.

Finally, much recent interest has focused on *conjugate gradient* methods for solving large matrix equations. These methods have their theoretical roots in the equivalence between linear systems and minimization problems for positive self-adjoint matrices[95]. However, the methods admit extensions to the nonself-adjoint operators that arise in fluid flow problems, especially in conjunction with such preconditioning methods as incomplete LU factorization and nested factorization[15,110,115,122]. The motivation for preconditioning is that, for parabolic flow equations, fine spatial grids can yield iteration equations $[A]\{p\}=-\{R\}$ in which the condition number of $[A]$ is large. By 'preconditioning' $[A]$ with another matrix $[A^*]^{-1}$, one can arrive at an equivalent system

$$[A^*]^{-1}[A]\{p\}=-[A^*]^{-1}\{R\}$$

that is better conditioned. Clever choices of $[A^*]^{-1}$ ensure that $[A^*]^{-1}\{R\}$ will be easy to compute at each iteration, thus promoting computational efficiency. It is reasonable to expect that preconditioned conjugate-gradient methods will play a larger role in oil reservoir simulation as the technology continues to advance.

4.3 Compositional simulation

The most ambitious applications of the equations for compositional flows arise in the simulation of enhanced oil recovery processes. Many of these processes depend for their success on the effects of interphase mass transfer on fluid flow properties. One noteworthy example of such a process is miscible gas flooding. This technology consists of injecting an originally immiscible gas, such as CO_2, into an oil reservoir with the aim of developing a miscible displacement front *in situ*. In successful projects, miscibility develops through continuous interphase mass transfers, leading the fluid mixture toward its critical composition and hence reducing the interfacial tension between the resident oil and the displacing fluid. Compositional modelling serves as an important tool in other oil recovery problems, too, including production from gas condensate reservoirs and recovery of volatile oils.

There are several ways to classify compositional simulators. One way is to characterize the models according to their treatment of fluid-phase thermodynamics. There are at least two forms in which the thermodynamic constraints mentioned in Section 4.1 can appear. The oldest form consists of tabular data for the equilibrium ratios ω_i^G/ω_i^O of species mass (or mole) fractions in the vapour and liquid hydrocarbon phases. Thus, given overall hydrocarbon pressures and compositions at a point in the reservoir, one can compute fluid saturations, densities and compositions by performing 'flash' calculations familiar to chemical engineers[109]. The other form of the thermodynamic constraints is the requirement that vapour and liquid fugacities be equal for each component: $f_i^G=f_i^O$, $i=1,\ldots,N$. This approach is especially attractive when used in conjunction with an equation of state such as that proposed by Peng and Robinson[117]. Equation-of-state methods have the advantage of thermodynamic consistency near fluid critical points, leading to calculations with better convergence properties in models of miscible gas floods. In either the equilibrium-ratio approach or the equation-of-state approach, though, the thermodynamic constraints amount to a system of nonlinear algebraic equations giving fluid saturations, densities and compositions implicitly.

Another way to classify compositional models is according to the manner in which they solve the flow equations (16). Two general schemes have appeared. One of these treats the flow equations sequentially, solving an overall pressure equation and then updating the remaining $N-1$ composition equations and the thermodynamic constraints at each time step or iteration. This approach parallels the IMPES method in black-oil simulation, and, as one might expect, it offers computational speed at the expense of some stability. The other scheme solves the entire system of flow equations and thermodynamic constraints simultaneously at each time step. This approach, analogous to the SS method of Section 4.2, leads to enormous matrix equations at each iteration. However, it enjoys a greater stability than the sequential schemes. Given adequate computers, this *fully implicit* approach is quite attractive, since the compositional equations can exhibit behaviour that is too complex to permit *a priori* estimates of stability constraints.

Among the simulators using sequential methods are those advanced by Roebuck *et al.*[130]; Nolen[109]; Van Quy, Corteville and Simandoux[153]; Kazemi, Vestal and Shank[88]; Nghiem, Fong and Aziz[108]; Watts[158] and Allen[6,7]. Let us examine the time-stepping structure of one such model[7], restricting attention to an oil-gas system in which gravity has no effect. Summing the flow equations over all N species gives an overall fluid mass balance

$$\frac{\partial\rho}{\partial t}=\nabla\cdot(T_T\nabla p_G-T_O\nabla p_{CGO}) \tag{21}$$

where $T_\alpha=kk_{r\alpha}\rho^\alpha/\mu_\alpha$ for each fluid α and $T_T=T_G+T_O$. This leaves $N-1$ independent species balances

$$\frac{\partial(\rho\omega_i)}{\partial t}=\nabla\cdot(\Upsilon_i\nabla p_G-T_O\omega_i^O\nabla p_{CGO}) \quad i=1,\ldots,N-1 \tag{22}$$

where $\Upsilon_i=T_G\omega_i^G+T_O\omega_i^O$. We can regard equation (21) as an equation for the pressure p_G, using equation (22) to solve for the overall species mass fractions ω_i. The thermodynamic constraints then give the saturation, densities and compositions of the liquid and vapour phases.

To solve these equations sequentially, we first discretize the pressure equation (21) in time, using the following Newton-like iterative scheme:

$$\rho^{n+1,m}+\left(\frac{\partial\rho}{\partial p_G}\right)^{n+1,m}\delta p_G^{n+1,m-1}-\rho^n$$
$$=\Delta t\nabla\cdot[T_T^{n+1,m}\nabla(p_G^{n+1,m}+\delta p_G^{n+1,m+1})$$
$$-T_O^{n+1,m}\nabla p_{CGO}^{n+1,m}] \tag{23}$$

This scheme is similar to that used in the unsaturated flow

equation of Section 3.1. After solving for $\delta p_G^{n+1,m+1}$, we update the pressure iterate by setting $p_G^{n+1,m+1} = p_G^{n+1,m} + \delta p_G^{n+1,m+1}$. Then we can update each mass fraction $\omega_1, \ldots, \omega_{N-1}$ using the finite difference approximation

$$\Delta_t \omega_i^{n+1,m+1} = \frac{1}{\rho^{n+1,m-1}} \{\Delta t \nabla \cdot [\Upsilon_i^{n+1,m} \nabla p_G^{n+1,m+1} - (T_O \omega_i^O)^{n+1,m} \nabla p_{CGO}^{n+1,m}] - \omega_i^n \Delta_t p^{n+1,m+1}\} \quad (24)$$

to equation (22), setting $\omega_i^{n+1,m+1} = \omega_i^n + \Delta_t \omega_i^{n+1,m+1}$. This update calls for values of $\rho^{n+1,m+1}$, which are available from the latest iteration of equation (23) as

$$\rho^{n+1,m+1} = \Delta t \nabla \cdot (T_T^{n+1,m+1} \nabla p_G^{n+1,m+1} - T_O^{n+1,m} \nabla p_{CGO}^{n+1,m}) + \rho$$

This iterative sequence requires the solution of a matrix equation only in the spatially discrete analog of equation (23), since equation (24) has an 'explicit' form at each iteration. Notice that, while the scheme is not fully implicit, it calls for implicit treatment of the flux coefficients, which lends to the stability of the formulation. Figure 8 shows a flow chart for the time-stepping algorithm, and Fig. 9 shows a profile of vapour-liquid interfacial tensions in a simulated vaporizing gas drive[7]. The wave of decreasing tensions indicates the development of a zone in which the fluid displacement is very nearly miscible.

With the advent of large, fast digital computers, interest has grown in the fully implicit approach to compositional simulation. Among the models based on this approach are those reported by Fussell and Russell[72], Coats[42], Heinemann[80], and Chien, Lee and Chen[38]. This class of formulations treats the discretized flow equations and thermodynamic constraints as a set of simultaneous

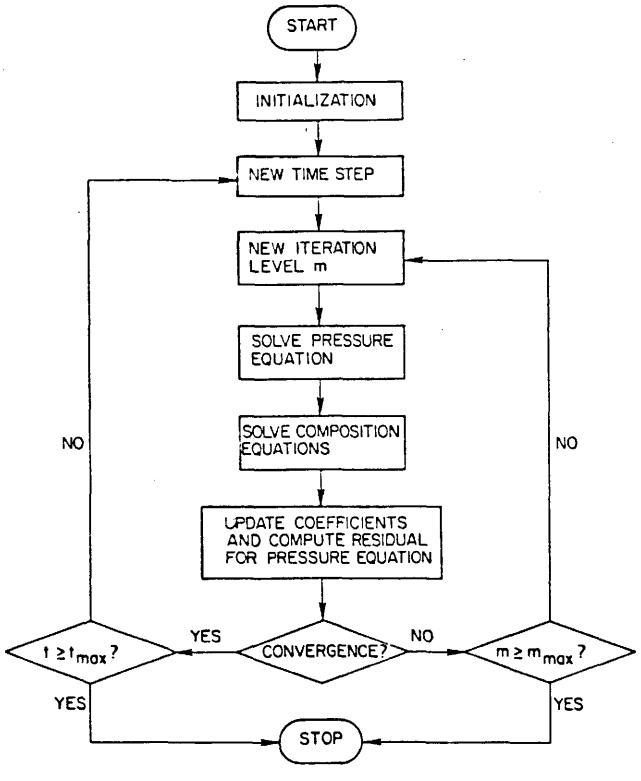

Fig. 8. Flow chart of time-stepping procedure for a sequential compositional simulator[7]

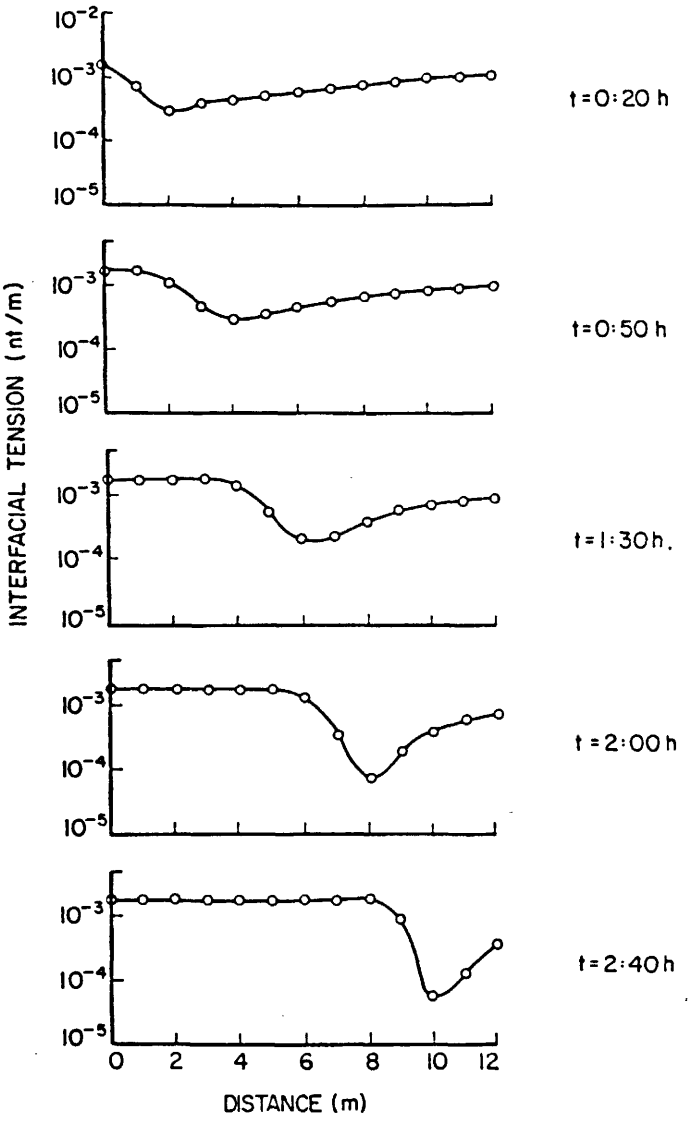

Fig. 9. Interfacial tension profile at various times for a compositional simulation of a vaporizing gas drive[7]

nonlinear algebraic equations, generally using some Newton-like iterative scheme to advance between time steps. The implicit nature of the formulations leads to great stability at the expense of solving large matrix equations of the form $[A]\{y\} = -\{R\}$ at each iteration. Moreover, the iteration matrix $[A]$ typically has less sparseness than the matrices arising from sequential schemes, since simultaneous schemes account for more of the nonlinear coupling between variables. Young and Stephenson[165] present one approach to mitigating this complication by evaluating the flux coefficients explicitly. As should be expected, this scheme reduces the computational effort of the fully implicit approach while sacrificing some of its stability.

There are several areas of difficulty common to practically all compositional simulators. One class of problems concerns the mathematical representation of fluid phase behaviour. Most research in compositional simulation now focuses on methods using cubic equations of state coupled with equal-fugacity constraints to represent the fluid thermodynamics. While this approach guarantees thermodynamic consistency and therefore ensures smooth behaviour of fluid densities, it requires the

solution of highly nonlinear algebraic equations in addition to the discretized flow equations. Furthermore, the numerical solution of these thermodynamic constraints often suffers poor convergence when fluid pressures and compositions approach critical points[129]. While the numerical problems associated with fluid phase behaviour calculations pose serious challenges to the petroleum industry, an extensive discussion of research in this area would carry us far afield.

Another problem affecting compositional simulation is the numerical smearing introduced by upstream weighting. While this source of error affects other numerical models using upstream weighting, it is particularly problematic in compositional simulation. Because compositional models require so much storage and CPU time per spatial node, field-scale simulations often must use relatively few nodes and correspondingly coarser grids. The artifical diffusion that results can introduce large errors in species mass fractions and thus lead to unreal thermodynamics.

Several investigators have proposed methods for alleviating numerical diffusion in compositional simulators. Chase[37], for example, proposes local grid refinement methods for use with Galerkin finite elements. Section 6.4 discusses local grid refinement in more detail. Wilson, Tan and Casinader[160] advance a method for selecting upstream-weighted difference approximations that yield reduced artificial smearing. Ewing and Heinemann[64,65] discuss the use of mixed finite-element methods to reduce smearing in compositional models. These authors propose that inaccurate fluid velocities, obtained by numerically differentiating pressure fields, aggravate numerical smearing. By incorporating mixed methods into their numerical scheme, they compute more accurate velocities and thereby help preserve sharp composition fronts in the numerical solution. Section 6 discusses mixed finite-element methods more thoroughly.

Finally, the growing appeal of the fully implicit approach implies that the computational effort associated with the inversion of large linear systems will become an increasingly important concern. The stakes involved in the linear algebra of compositional modelling are much higher than in black-oil simulation, since a typically fully implicit compositional model must solve the discretized flow equations and equal-fugacity constraints for between seven and ten species. This avenue of research should be active for quite some time to come.

5. OUTSTANDING PROBLEMS: PHYSICS

The next two sections review some of the outstanding problems in simulating multiphase flows in porous media. Roughly speaking, these problems fall into two categories: difficulties arising because our knowledge of the physics of multiphase flows is incomplete and difficulties in devising mathematical methods to capture known physics. The two categories are not as distinct as this description suggests. For some phenomena our lack of physical understanding hinders attempts to model them mathematically. Viscous fingering is an example, as discussed below. For other phenomena, the mathematical difficulties are evidence of physical complications that lead to peculiar behaviour in the governing equations. The occurrence of sharp fronts in immiscible flows is an example of this coupling. Nevertheless, the distinction between physical and numerical difficulties makes some sense if we interpret it as suggesting strategies for future research. In this section we consider several physical problems.

5.1 Viscous fingering

Often, in two-phase flows, the bulk of one fluid lies upstream of the other. In this case we say that the 'upstream' phase displaces the 'downstream' phase, even though there may be large regions where both phases flow simultaneously. The global behaviour of such flows depends strongly on whether the mobility of the displacing fluid is greater or less than that of the displaced fluid. In the latter case, when the *mobility* ratio $\Lambda_{\text{displacing}}/\Lambda_{\text{displaced}} = M < 1$, the flow proceeds stably. This implies that velocity fields and saturations depend continuously on the boundary and initial conditions and well rates. When $M > 1$, however, channels of high displacing-fluid saturation can bypass zones of displaced fluid in a geometrically irregular pattern. These irregularities in the fluid displacement reflect the instability of immiscible displacements at high mobility ratios. The channeling phenomenon is called *viscous fingering*. While this phenomenon occurs in both single-phase and multiphase flows, we shall restrict our attention to the multiphase case.

Viscous fingering is economically important in oil reservoir engineering, where displacement of oil by some injected fluid is common to almost all recovery processes past primary production. In many cases the injected fluid is water, a gas such as CO_2 or N_2, or a surfactant solution. These fluids tend to be more mobile than common crude oils; therefore viscous fingering can occur. As a result, such a displacement scheme may sweep only a small fraction of the oil-bearing rock between an injection well and a production well. This inefficiency motivates reservoir engineers to add mobility control agents, such as hydrolysed polymers, to injected fluids to lower their mobility.

Investigations into the physics of viscous fingering in immiscible displacements began in the late 1950s. Saffman and Taylor[132] investigated an analogy between porous-medium flows and Hele-Shaw flows, confirming that $M > 1$ leads to frontal instability. Chuoke, van Meurs and van der Pol[41] applied perturbation techniques to show the existence of a critical wavelength for unstable fingers. From these early papers through the 1970s the literature on viscous fingering mushroomed. Ewing and George[63] provide a fairly extensive review of this body of work.

Research into viscous fingering has continued in recent years[76,118,163,94,87]. While controversy still exists, there seems to be broad agreement that unstable fingers are triggered by heterogeneities in the porous medium observable at the microscopic scale. However, the macroscopic governing equations based on Darcy's law do not explicitly account for microscopic heterogeneities. Mathematical models based on the macroscopic equations and assuming a macroscopically homogeneous porous medium therefore have no mechanism for initiating fingers. Consequently, the homogeneous model will not exhibit instability, even though it is present in nature. One might, as an analogy, consider the mathematical model of an ideal pendulum hung vertically upward with zero velocity. The idealised model predicts that the pendulum is at equilibrium, whereas a natural pendulum in such a configuration is unlikely to stay there.

This failure to capture microscopic physics has unfortunate implications in numerical simulation. The response of a mathematical method to unstable immiscible displacements depends on the degree of heterogeneity in the data of the problem. Discrete models can represent spatial heterogeneity only within the limits imposed by the fineness of the spatial grid. Hence, models of immiscible displacement in media exhibiting heterogeneity at many scales can produce qualitatively different results depending on the spatial discretization used.

Several articles have appeared reporting efforts to produce better numerical representations of viscous fingering, given the inherent limitations of discrete methods. Among these are papers by Glimm, Marchesin and McBryan[78], who propose the random choice method for solving the flow equations, and Ewing, Russell and Wheeler[66], who examine a mixed method in conjunction with a modified method of characteristics to give accurate approximations of fluid interfaces. Another set of approaches has been to incorporate the 'average' effects of fingering on the mixing of fluids in numerical simulators. This line of research began with Koval[89] and became a common simulation tool with the introduction of a mixing model by Todd and Longstaff[148]. This 'averaging' approach, while currently lacking in rigour, may offer fertile ground for the interaction of sound physical reasoning with the development of numerical techniques.

Finally, there is a great need for more empirical work on viscous fingering. Among the many sources of uncertainty regarding the nature of fingering is the paucity of field-scale data characterizing its effects. As Settari, Price and Dupont[138] asserts

> The study of unstable displacements, particularly viscous fingering, is distingyished by the fact that in no other area of reservoir engineering is there less agreement. There is not even complete agreement on the existence of viscous fingering as a real phenomenon for reservoir conditions, let alone agreement as to the magnitude and interaction of the various mechanisms involved.

5.2 Multiphase hydrodynamic dispersion

As the derivation of the compositional equations in Section 4.1 demonstrates, individual species within a fluid phase need not move with the barycentric velocity of the phase. In porous-media flows, the deviation of species motions with respect to the mean flow of the fluid is called hydrodynamic dispersion. This diffusion-like phenomenon is familiar in the context of single-phase flows such as miscible displacement in petroleum engineering or soluble contaminant transport in groundwater hydrology. However, the literature on hydrodynamic dispersion in multiphase flows is frustratingly sparse.

One likely reason for this sparseness is the difficulty of understanding the physics of hydrodynamic dispersion even in single-fluid flows. Dispersion in porous media actually comprises a set of phenomena, including the following[71]:

(i) molecular diffusion, which to macroscopic observers appears retarded owing to the tortuosity of the solid matrix;
(ii) Taylor diffusion[146], an effect whereby no-slip boundary conditions at the solid walls cause solutes in small-diameter pore channels to spread with respect to their mean motion;
(iii) stream splitting, in which parcels of solute-bearing fluid divide at pore-channel intersections, and
(iv) transit-time deviations, in which the dissimilar tortuosities of adjacent flow paths cause nearby fluid parcels to have different net velocities in the mean flow direction.

Notice that the descriptions of these phenomena belong to the microscopic level of observation, and hence the use of hydrodynamic dispersion to account for their macroscopic effects imposes an inherent loss of information. To modelers, this smearing of small-scale heterogeneities has undesirable implications. Indeed, in models of solute transport in porous media, hydrodynamic dispersion is often the most poorly quantified of all physical parameters fed into the simulator.

Relatively few investigators have ventured to propose quantitative forms for hydrodynamic dispersion in the multiphase setting. Among the earliest laboratory studies of multiphase hydrodynamic dispersion is that of Thomas, Countryman and Fatt[147]. These authors find that, when two phases flow in a porous medium, each fluid alters the effective pore-size distribution available to the other fluid. Thus the degree of saturation of a given phase has pronounced effects on the observed level of dispersion. More recently, Delshad *et al.*[53] confirm the dependence of multiphase dispersion on saturations.

As Section 4.1 mentions, most mathematical models of species transport in multiphase systems ignore hydrodynamic dispersion. There are, however, at least three noteworthy exceptions. The first is the compositional model developed by Young[164], who assumes the second-order tensor form

$$\mathbf{D}_\alpha = (D_{\alpha,\mathrm{mol}} + \alpha_{\alpha,t}|\mathbf{v}^\alpha|)\mathbf{1} + (\alpha_{\alpha,t} - \alpha_{\alpha,t})\frac{\mathbf{v}^\alpha\mathbf{v}^\alpha}{|\mathbf{v}^\alpha|}$$

for each fluid phase α. Here $D_{\alpha,\mathrm{mol}}$ stands for the molecular diffusion coefficient in phase α, and $\alpha_{\alpha,t}$ and $\alpha_{\alpha,t}$ signify the longitudinal and transverse dispersivities, respectively, in phase α. This formulation amounts to a natural extension of the standard hydrodynamic dispersion model to multiphase flows. A model described by Abriola[1] and Abriola and Pinder[2] assumes a related form for dispersion within a phase, namely

$$\mathbf{D}_\alpha = \mathbf{D}_{\alpha,\mathrm{mol}} + \mathbf{D}_1 : \mathbf{v}^\alpha\mathbf{v}^\alpha$$

where $\mathbf{D}_{\alpha,\mathrm{mol}}$ is a second-order tensor adcounting for the effects of molecular diffusion in phase α, modified by the matrix tortuosity, and $\mathbf{D}_1$ is a fourth-order tensor. This form extends the tensor equation proposed by Bear[23] on theoretical grounds. Finally, Baehr and Corapcioglu[20] and Corapcioglu and Baehr[49] derive a set of flow equations for immiscible contaminant transport incorporating a dispersion tensor for each phase; however, they do not postulate a precise tensorial form for dispersion.

Multiphase hydrodynamic dispersion appears to be one area of uncertainty where numerical simulation cannot shed much light. The fundamental questions that plague modelers are the same ones that arise in single-phase flows. What is the mathematical form of dispersion? How can we measure it? Do scale dependencies and asymmetric effects influence dispersion? It seems apparent that these questions address themselves primarily to experimentalists, guided ideally by theoretical studies of continuum mixtures such as that advanced by Bowen[31].

5.3 Multiphase contaminant flows

In recent years interest has arisen in multiphase flows involving immiscible groundwater contaminants. It has long been common practice to store or dispose of hazardous chemicals in near-surface or underground sites, and fluids escaping from these sites pose serious threats to groundwater supplies. Many hazardous chemicals and wastes take the form of nonaqueous-phase liquids, or NAPL. Common examples include gasoline, polychlorinated biphenyls (PCB), chlorinated hydrocarbons, coal tars and creosotes[154]. However, many dumpsites harbour a menagerie of chemical wastes, making it difficult to characterize the NAPL chemically. The multiphase flows that lead to contamination of groundwater are physically quite complex, and, despite the pressing need for predictive tools, numerical simulation of NAPL flows remains in its infancy.

One type of flow that is important in this context is the simultaneous flow of NAPL and water in the unsaturated zone. This soil layer usually lies between near-surface NAPL sources and the water table and therefore acts as the main pathway for groundwater contamination. As we illustrated in Section 3.1, the flow of a single liquid in the unsaturated zone already poses a difficult nonlinear problem, so one might expect that multiliquid flows will be even harder to simulate numerically.

Current efforts in multiphase unsaturated flows focus mainly on developing physical understanding. Schwille[135], for example, discusses the migration of immiscible organics in the unsaturated zone, reviewing such fundamental processes as capillary action, volatilization of the organic species, and microbial degradation. Allen[9] applies continuum mixture theory to develop a set of flow equations for two liquids in the unsaturated zone. By analysing a medium containing air (A), NAPL (N) and water (W), he derives a pair of partial differential equations, each resembling Richards' equation in form:

$$\left(C_\alpha+\frac{\Theta_\alpha S_{s,\alpha}}{\phi}\right)\frac{\partial\psi_\alpha}{\partial t}=\nabla\cdot[k_{r\alpha}\mathbf{K}\cdot(\nabla\psi_\alpha+\nabla Z)] \qquad (25)$$

for $\alpha=N$ or W. Several variables appearing in this equation are analogous to those appearing in the single-liquid case: C_α is the specific moisture capacity of phase α; Θ_α is the moisture content of α; ψ_α is the pressure head in phase α; $\mathbf{K}$ is the soil's hydraulic conductivity and Z is depth below some datum. Also appearing are the variables $S_{s,\alpha}$, which is the specific storage associated with phase α, and $k_{r\alpha}$, signifying the relative permeability of the soil matrix to phase α. The pair of flow equations given by equation (25) constitutes a nonlinear system. Coupling between the equations occurs through the dependence of Θ_α, $S_{s,\alpha}$ and $k_{r\alpha}$ on the pressure heads ψ_α; the capillarity relationships $\psi_\alpha=\psi_\alpha(\Theta_N,\Theta_W)$, and the restriction $\Theta_N+\Theta_W=\phi(1-S_A)$.

In what appears to be the first effort at numerically simulating multiphase unsaturated flows, Faust[69] develops a two-dimensional finite-difference model for the flow of water and NAPL. This model uses a two-equation formulation similar to that given by equation (25). To solve the discretized flow equations, Faust devises a fully implicit scheme akin to the SS method used in black-oil simulation. As with other models of multiphase flows, Faust's simulator uses upstream-weighted relative permeabilities to accommodate possible hyperbolic behaviour, as explained in Section 4.2.

As a practical matter, the simultaneous flow of NAPL and water is only part of the multiphase contamination problem. Groundwater contamination itself occurs because of mass transfer between NAPL and water. Even though NAPL may be immiscible with water, some of its constituent species may dissolve in water at very small concentrations. While highly dilute, the resulting solution of organics in water is often toxic or carcinogenic. Therefore, a complete mathematical description of multiphase contaminant flows ought to incorporate phase-exchange effects more familiar in the setting of compositional reservoir simulators.

Very little work has been done in this area. Baehr and Corapcioglu[20] propose a model consisting of individual flow equations for each species. Since their model aims principally at predicting pollution from gasoline spills, they include in their formulation such effects as microbial degradation, equilibrium partitioning among fluid phases, and adsorption onto the solid phase. Abriola[1] and Abriola and Pinder[2,3] present a finite-difference model of species transport in an air-water-NAPL system. This simulator accommodates interphase mass transfer through the use of equilibrium ratios analogous to those discussed in Section 4.3. The model solves the nonlinear algebraic equations resulting from the finite difference approximation using a scheme patterned after the SS method reviewed in Section 4.2. Considering the range of problems solved and the analyses given of the code's performance, this is perhaps the best documented model of multiphase, multispecies contaminant transport appearing in the literature at this writing.

6. OUTSTANDING PROBLEMS: NUMERICS

Quite a few of the difficulties arising in numerical simulation of multiphase flows concern the limitations of the numerical methods themselves. Here the problem is that the numerical techniques in common use produce approximations that are in some way unrealistic based on our understanding of the flows that they model. In this case the challenge to researchers is to devise new methods or to modify existing approaches to permit more accurate simulations. We shall examine three types of numerical difficulties of topical interest: grid orientation effects, front tracking and local grid refinement.

6.1 Grid-orientation effects

Since the early 1970s, petroleum engineers have recognized that many discrete methods for solving fluid flow equations give qualitatively different results when one changes the orientation of the spatial grid with respect to the geometry of the physical flow. Todd, O'Dell and Hirasaki[149] first reported this phenomenon in a simulator of immiscible flow. They noted that the effects of grid orientation are especially pronounced at large mobility ratios. A severe example occurs in steamflood simulation[44], where solutions generated using different grid orientations apparently converge to different answers. Since these investigations, a substantial body of research has developed in the effort to overcome or mitigate grid-orientation effects in reservoir simulators.

One of the first effective techniques for reducing grid-orientation effects appeared in 1979, when Yanosik and

McCracken[162] presented a nine-point finite-difference scheme that reduces grid-orientation effects for square grids. The nine-point scheme approximates derivatives at a point (x_i, y_i) in two-dimensional domains by using values at all adjacent nodes instead of the corner nodes only. Thus the nine-point analog of the Laplacian on a uniform grid is

$$\nabla^2 u|_{i,j} = \frac{1}{6\Delta x^2}[4(u_{i+1,j}+u_{i-1,j}+u_{i,j+1}+u_{i,j-1}) + (u_{i+1,j-1}+u_{i-1,j-1}+u_{i-1,j+1}+u_{i+1,j-1})-20u_{i,j}]$$

Coats and Ramesh[46] observe that the nine-point formulation exhibits poor behaviour when used on nonuniform spatial grids. Bertiger and Padmanabhan[25] explain this poor performance by demonstrating that the usual nine-point formulation on nonuniform grids yields an inconsistent approximation to ∇^2. These authors then propose a modified nine-point scheme that restores consistency while still reducing the grid-orientation effect. In another approach, Potempa[123] advances a finite-element technique that is closely related to the Yanosik–McCracken nine-point difference scheme but again preserves consistency. Several other investigators have devised modified finite-difference schemes yielding solutions that are largely independent of grid-orientation effects; among them are Vinsome and Au[155]; Frauenthal, di Franco and Towler[70]; Shubin and Bell[142] and Preuss and Bödvarsson[125].

Finite-element techniques also admit variants that reduce grid-orientation effects. Among the more promising groups of finite-element schemes in this regard are mixed methods[50,67,10]. The motivation behind these techniques is to compute accurate Darcy velocities explicitly rather than incurring the loss of accuracy associated with standard schemes requiring the differentiation of fluid pressures. Thus, for example, we factor the second-order pressure equation

$$\nabla\cdot(k\nabla p)=0$$

into two first-order equations

$$\mathbf{v}=-k\nabla p$$

$$-\nabla\cdot\mathbf{v}=0$$

By properly choosing the trial functions for $\mathbf{v}$ and p, we can compute pressures and velocities having the same order of accuracy. In problems involving the effects of species transport the mixed method is especially effective when used in conjunction with time-stepping procedures based on modified methods of characteristics[67]. A variety of numerical experiments reported in the references cited above demonstrate the method's ability to give good numerical results even in problems with highly variable material properties.

6.2 Front-tracking methods

As we have seen in previous sections, several multiphase flows in porous media exhibit sharp fronts that can be modelled as discontinuous fluid interfaces. The salt-water toe and the Buckley–Leverett saturation shock are two examples of such discontinuities. Discrete approximations using fixed finite elements or finite-difference cells have difficulty in capturing the behaviour of these sharp fronts, since the computational procedures tend to smear information over the spatial subregions of the discretizations. Front-tracking methods aim at circumventing this difficulty by assigning computational degrees of freedom to the unknown location of the front. Solving for the frontal locations along with the variables characterizing the smooth parts of the flow allows the modeller to track the front explicitly without introducing numerical diffusion. Since one can concentrate many degrees of freedom at the interface, front tracking methods also hold great promise in the simulation of viscous fingering.

Front-tracking methods have their roots in numerical applications of the method of characteristics in convection-dominated flows. The first applications of this approach in porous-media simulation addressed the miscible transport of solutes in single-phase flows[73,120]. In the method of characteristics, one replaces a partial differential equation by a system of ordinary differential equations valid along curves where the original equation agrees with the chain rule. For example, by comparing the Buckley–Leverett saturation equation

$$\frac{\partial S_w}{\partial t}+\frac{q f_w'(S_w)}{\phi}=0 \tag{26}$$

with the chain rule

$$\frac{dt}{d\xi}\frac{\partial S_w}{\partial t}+\frac{dx}{d\xi}\frac{\partial S_w}{\partial x}=\frac{dS_w}{d\xi}$$

one can see that $dS_w/d\xi=0$ along curves $\xi(x,t)$ in the (x,t)-plane where $dx/dt=qf_w'(S_w)/\phi$. Loci of constant S_w therefore travel with speed $qf_w'(S_w)/\phi$. This fact allows us to compute the position of the constant-saturation shock as it moves across a one-dimensional domain.

Perhaps the most extensively applied front-tracking scheme in the current literature is that of Glimm and his coworkers[77,79,93]. This approach uses an IMPES formulation for two-dimensional immiscible displacements in the absence of capillarity. The scheme solves the pressure equation on a finite-element grid whose element boundaries move to align themselves with the saturation shock. To update saturations, the scheme uses standard interior methods in regions where the saturation is smooth and couples to the smooth solution a Riemann problem propagating the interface. This frontal propagation relies on a method of characteristics akin to the one-dimensional version outlined above, taking advantage of a local coordinate system aligned with the shock to advance the discontinuity in its normal direction. Thus the actual computations required to track the front reduce to locally one-dimensional ordinary differential equations.

Jensen and Finlayson[85,86] introduce an alternative scheme for front-tracking that gives good results in convection-dominated species-transport problems. This method defines a set of moving coordinates based on the method of characteristics for the hyperbolic, or purely convective, part of the partial differential equations. Within this moving coordinate system, the convection-dominated transport problem reduces to a problem of the diffusion type. Jensen and Finlayson construct a finite-element grid attached to the moving coordinates, ensuring that the grid in the vicinity of the sharp front is

sufficiently fine to avoid the occurrence of nonphysical oscillations in the numerical solution.

In a third approach to front tracking, the Mathematics Group at the Lawrence Berkeley Laboratory applies the theory of Riemann problems for first-order hyperbolic systems to solve the immiscible flow equations using the random choice method[47,48,4]. The random choice method, developed as a numerical technique by Chorin[40], is an effective procedure for approximating nonlinear hyperbolic conservation laws such as equation (26). The method replaces the unknown function $S_w(x,t)$ by a piecewise constant approximation $\hat{S}_w(x,t)$ and then solves a sequence of Riemann problems, each advancing the numerical solution by sampling the piecewise constant function $\hat{S}$ to determine initial data. When the solution possesses shocks, the random choice method preserves their sharp fronts, since the sampling at each time step avoids the introduction of spurious intermediate values in the numerical solution. However, the method allows small errors in the shock location since the sampling identifies the frontal position only to within the resolution limits imposed by the spatial grid. Although developed for one-dimensional flows, the random choice method admits extensions to two-dimensional problems. Colella, Concus and Sethian[47] describe the use of operator splitting techniques to decompose a two-dimensional equation into a sequence of one-dimensional equations.

6.3 Adapative local grid refinement

Many problems involving multiphase flows in porous media exhibit behaviour whose structure is localized in small subregions of the spatial domain. We have already encountered such phenomena in the form of wetting fronts and saturation shocks. Similar localized behaviour occurs near wellbores or in the moving concentration fronts found in convection-dominated species transport processes. To capture the essential physics of these features often requires a spatial grid capable of providing high resolution in their vicinity. Grid refinement is especially important in view of the common use of low-order upstream-weighted approximations in near-hyperbolic flows. As frequently applied, these approximations introduce a numerical diffusion error whose magnitude is $\mathcal{O}(\Delta x)$ for grids of mesh Δx. By refining the spatial grid in the vicinity of the front, one reduces numerical diffusion by shrinking Δx, all the while preserving the desirable effects of upstream weighting.

Generating this extra resolution usually poses few difficulties if the locus of highly structured behaviour remains constant in time. However, in the case of moving fronts, for example, the zones where increased resolution is needed move through the spatial domain as time progresses. Under these circumstances the refined portion of the grid must be capable of moving in time to follow the localized structure of the solution. Such schemes fall under the rubric of *adaptive local grid refinement* (ALGR). While ALGR schemes are generally difficult to implement, the technical literature in this area is vast. Therefore the review that follows merely highlights results that appear relevant in multiphase flow simulation.

There are three basic approaches to ALGR. One of these is to increase the polynomial degree of the approximation to the solution in regions needing refinement. Such techniques are called *p-methods*. Another approach is to add computational degrees of freedom in the regions of refinement, keeping the polynomial degree of the approximation constant. These techniques are perhaps most appropriate when used in conjunction with upstream weighting, since they reduce numerical diffusion by shrinking Δx. Such methods are called *h-methods*. Finally, there are several techniques that allow the location of the spatial nodes in the grid to act as variables in the numerical approximation. By solving for the nodal locations and nodal solution values simultaneously, one effectively forces the grid to move in time to accommodate the structure of the solution. These methods are called *moving finite element* (MFE) techniques.

Reports of underground flow simulators using p-methods are not very numerous. Chase[37] describes a chemical flood simulator based on a finite-element Galerkin method that employs hybrid trial functions. These trial functions use C^0 piecewise bilinear Lagrange functions in smooth regions of the flow but insert C^1 piecewise bicubic Hermite functions in the vicinity of steep gradients. Mohsen[100] describes another p-method applied in finite-element collocation solutions of the Buckely–Leverett equation. This approach refines a coarse grid consisting of C^1 piecewise cubic Hermite functions by substituting C^1 piecewise quintic functions near the saturation shock.

The use of h-methods has been more popular. One reason for this fact may be a general aversion to the oscillatory tendencies associated with polynomial approximations of high degree. Another reason is undoubtedly that h-methods fit more naturally into the framework of finite-difference approximations, which do not explicitly use trial functions. Quite a few ALGR schemes for finite differences have appeared; among them are the methods of von Rosenberg[157], Heinemann and van Handelmann[81] and Douglas *et al.*[57], who present both finite-difference and finite-element schemes. A considerable amount of theoretical work and numerical experimentation has focused on finite-element schemes with ALGR[19,52,24,54]. One of the problems that arises in the construction of adaptive refinement codes is the management of the data defining the grid as its structure changes. There are great computational advantages associated with the invention of data structures that can accommodate the dynamic refinement and unrefinement of a grid without destroying the efficiency of matrix solution algorithms[21].

MFE methods adopt a somewhat different approach[35,98,,74,55]. For an equation of the form $\partial u/\partial t - \mathscr{A}u = 0$, where $\mathscr{A}$ is a spatial differential operator, we begin with a piecewise polynomial trial function $\hat{u}$ having unknown time-dependent coefficients $u_1(t), \ldots, u_N(t)$. In addition, we allow the coordinates of the spatial nodes $\bar{\mathbf{x}}_1, \ldots, \bar{\mathbf{x}}_N$ to be variable. By choosing $\{\partial u_i/\partial t, \bar{\mathbf{x}}_i\}_{i=1}^N$ to minimize $\|\partial\hat{u}/\partial t - \mathscr{A}\hat{u}\|_2$ in a Galerkin sense, one can develop a finite-element approximation in which the nodes tend to concentrate around regions where the solution exhibits localized structure. To prevent all of the nodes from accumulating near shocks, however, one must impose certain penalties on the clustering of nodes. A variety of internodal spring functions and viscosity-like devices exist to help preserve good global approximations by maintaining adequate separation between nodes.

ALGR techniques have a wide range of potential applications in general computational mechanics. Fluid flows in particular exhibit highly localized behaviours for

which local refinement is an attractive alternative to globally fine grids. Gas dynamic shocks, hydraulic jumps, moving interfaces, and such singularities as sources, sinks and corners are just a few examples of these features.

7. CONCLUSIONS

Throughout this review we have seen several facets of multiphase flows in porous media reappear in various applications. These physical and computational peculiarities emerge as major themes in the numerical simulation of flows. Let us close by recapitulating these themes.

Every flow we have examined obeys a nonlinear, time-dependent partial differential equation. Nonlinearity is a characteristic feature of multiphase porous-media flows, owing to the fact that the permeability of the rock matrix to one fluid varies with the saturation of any other fluid. Further nonlinearities can arise when storage or compressibility effects imply pronounced dependence on pressure in the accumulation terms or when there is strong coupling within a system of flow equations. The nonlinear governing differential equations generally give rise to nonlinear algebraic equations in the approximating discretizations. These algebraic systems, in turn, demand iterative solution, and therefore one commonly finds Newton–Raphson schemes or related procedures imbedded in implicit time-stepping methods for these problems.

Another common feature in multiphase porous-media flows is the occurrence of sharp fronts or moving boundaries in the fluid system. The Buckley–Leverett saturation shock stands as a classic example. Similar interfaces arise in other contexts: unsaturated flows can give rise to wetting fronts, and the saltwater intrusion problem exhibits a moving boundary in the toe of the saltwater wedge. Sharp fronts pose difficulties to the numerical analyst, since they require high spatial resolution to model and are sometimes associated with uniqueness issues. In certain classes of flows they can also exhibit instability, as when viscous fingering occurs in displacements at adverse mobility ratios. The most natural solutions to these sharp-front difficulties are front-tracking methods and adaptive local grid refinement.

Finally, various numerical aspects of modelling multiphase flows combine to require truly large-scale computations. A typical simulator solves large, sparse matrix equations at every iteration of every time step. When compositional effects are present, the code must solve nonlinear thermodynamic constraints as well. The desirability of local grid enrichment, front-tracking algorithms, or moving grid schemes adds to this scale of calculation both in complexity and in computational effort. Scientists who model multiphase underground flows have every reason to applaud the emerging generation of supercomputers and parallel architectures, since these machines may spell the difference between compromise in the approximation of complex flows and the practical achievement of realistic simulations.

ACKNOWLEDGEMENTS

The Wyoming Water Research Center supported much of this work through a grant to study multiphase contaminant flows. The National Science Foundation provided support through grant number CEE-8404266.

This paper was presented at the NATO Advanced Study Institute on Fundamentals of Transport Phenomena in Porous Media, 14–23 July, 1985, Newark, Delaware, USA.

REFERENCES

1 Abriola, L. M. *Multiphase Migration of Organic Compounds in a Porous Medium*, Springer-Verlag, Berlin, 1984
2 Abriola, L. M. and Pinder, G. F. A multiphase approach to the modelling of porous media contamination by organic compounds 1. Equation development, *Water Resources Research*, 1985, **21**, 11–18
3 Abriola, L. M. and Pinder, G. F. A multiphase approach to the modelling of porous media contamination by organic compounds 2. Numerical simulation, *Water Resources Research*, 1985, **21**, 19–26
4 Albright, N. and Concus, P. On calculating flows with sharp fronts in a porous medium, *Fluid Mechanics in Energy Conservation*, J. D. Buckmaster, ed., Society for Industrial and Applied Mathematics, Philadelphia, Pa., 1980, 172–184
5 Allen, M. B. How upstream collocation works, *International Journal for Numerical Methods in Engineering*, 1983, **19**, 1753–1763
6 Allen, M. B. A collocation model of compositional oil reservoir flows, *Mathematical Methods in Energy Research*, K. I. Gross, ed., Society for Industrial and Applied Mathematics, Philadelphia, Pa., 1984, 157–180
7 Allen, M. B., *Collocation Techniques for Compositional Flows in Oil Reservoirs*, S'ringer-Verlag, Berlin, 1984
8 Allen, M. B., Why upwinding is reasonable, *Finite Elements in Water Resources*, J. P. Laible *et al.*, eds, Springer-Verlag, Berlin, 1984, 13–23
9 Allen, M. B. Mechanics of multiphase fluid flows in variably saturated porous media, *International Journal for Engineering Science*, 1985, to appear
10 Allen, M. B., Ewing, R. E. and Koebbe, J. V. Mixed finite-element methods for computing groundwater velocities, *Numerical Methods for Partial Differential Equations*, 1985, to appear
11 Allen, M. B. and Murphy, C. A finite-element collocation method for variably saturated flows in porous media, *Numerical Methods for Partial Differential Equations*, to appear
12 Allen, M. B. and Pinder, G. F. Collocation simulation of multiphase porous-medium flow, *Society of Petroleum Engineers Journal*, 1983, 135–142
13 Allen, M. B. and Pinder, G. F. The convergence of upstream collocation in the Buckley–Leverett problem, *Society of Petroleum Engineers Journal*, 1985, to appear
14 Amaefule, J. O. and Handy, L. L. The effect of interfacial tensions on relative oil/water permeabilities of consolidated porous media, *Society of Petroleum Engineers Journal*, 1982, 371–381
15 Appleyard, J. R., Cheshire, I. M. and Pollard, R. K. Special techniques for fully-implicit simulators, *Third European Symposoium on Enhanced Oil Recovery*, F. J. Fayers, ed., Elsevier Scientific Publishing Co., Amsterdam, 1981, 395–408
16 Aronson, D. G. Nonlinear diffusion problems, *Free Boundary Prlblems: Theory and Applications*, Fasano, A. and Primicerio, M. (eds), Vol. 1, Pitman Advanced Publishing Program, Boston, Mass., 1983, 135–149
17 Atkin, R. J. and Craine, R. E. Continuum theories of mixtures: Basic theory and historical development, *Quarterly Journal of Applied Mathematics*, 1976, **29**(2), 209–244
18 Aziz, K. and Settari, A. *Petroleum Reservoir Simulation*, Applied Science Publishers, London, 1979
19 Babuska, I. and Rheinboldt, W. C. Error estimates for adaptive finite element computations, *Society for Industrial and Applied Mathematics Journal of Numerical Analysis*, 1978, **15**, 736–754
20 Baehr, A. and Corapcioglu, M. Y. A predictive model for pollution from gasoline in soils and groundwater, *Proceedings*, Petroleum Hydrocarbons and Organic Chemicals in Groundwater: Prevention, Detection and Restoration, Houston, Texas, 1984
21 Bank, R. E. and Sherman, A. H. A refinement algorithm and dynamic data structure for finite element meshes, *Center for Numerical Analysis Technical Report 166*, University of Texas, Austin, Texas, 1980
22 Bardon, C. and Longeron, D. G. Influence of interfacial tensions on relative permeability, *Society of Petroleum Engineers Journal*, 1980, 391–401

23 Bear, J. On the tensor form of dispersion in porous media, *Journal of Geophysical Research*, 1961, **66**, 1185–1197

24 Beiterman, M. A posteriori error estimation and adaptive finite element grids for parabolic equations, *Adaptive Computational Methods for Partial Differential Equations*, Babuska, I. *et al.* (eds), Society for Industrial and Applied Mathematics, Pniladelphia, Pa., 1983, 123–141

25 Bertiger, W. I. and Padmanabhan, L. Finite difference solutions to grid orientation problems using IMPES, *Proceedings*, Seventh Symposium on Reservoir Simulation, Society of Petroleum Engineers, 1983, 163–172

26 Birkkoff, G. Numerical fluid dynamics, *Society for Industrial and Applied Mathematics Review*, 1983, **25**, 1–34

27 Björdammen, J. B. and Coats, K. H. Comparison of alternating direction and successive overrelaxation techniques in simulation of reservoir fluid flow, *Society of Petroleum Engineers Journal*, 1969, 47–58

28 Blair, P. M. and Weinaug, C. F. Solution of two-phase flow problems using implicit finite differences, *Society of Petroleum Engineers Journal*, 1969, 417–424

29 Bowen, R. M. Incompressible porous media models by the use of the theory of mixtures, *International Journal of Engineering Science*, 1980, **18**, 1129–1148

30 Bowen, R. M. Compressible porous media models by the use of the theory of mixtures, *International Journal of Engineering Science*, 1982, **20**, 697–735

31 Bowen, R. M. Diffusion models implied by the theory of mixtures, Appendix 5A to *Rational Thermodynamics*, 2nd ed., by C. A. Truesdell, Springer-Verlag, New York, NY. 1984, 237–263

32 Breitenbach, E. A., Thurnau, D. H. and van Poolen, H. K. Solution of the immiscible fluid flow simulation equation, *Society of Petroleum Engineers Journal*, 1969, 155–169

33 Bresler, E. Simultaneous transport of solutes and water under transient unsaturated flow conditions, *Water Resources Research*, 1973, **9**, 975–986

34 Buckley, S. E. and Leverett, M. C. Mechanism of fluid displacement in sands, *Transactions*, American Institute of Mining, Metallurgical and Petroleum Engineers, 1942, **146**, 107–116

35 Carey, G. F., Mueller, A., Sephehrnoori, K. and Thrasher, R. L. Moving elements for reservoir transport processes, *Proceedings*, Fifth Symposium on Reservoir Simulation, Society of Petroleum Engineers, 1979, 135–144

36 Celia, M. A. and Pinder, G. F. An analysis of alternating-direction methods for parabolic equations, *Numerical Methods for Partial Differential Equations*, 1985, **1**, 57–70

37 Chase, C. A. Variational simulation with numerical decoupling and local mesh refinement, *Proceedings*, Fifth Symposium on Reservoir Simulation, Society of Petroleum Engineers, 1979, 73–94

38 Chien, M. C. H., Lee, S. T. and Chen, W. H. A new fully implicit compositional simulator, *Proceedings*, Eighth Symposium on Reservoir Simulation, Society of Petroleum Engineers, Feb., 1985, 7–30

39 Chorin, A. J. and Marsden, J. E. *A Mathematical Introduction to Fluid Mechanics*, Springer-Verlag, New York, NY, 1979, Chapter 3

40 Chorin, A. J. Random choice solution of hyperbolic systems, *Journal of Computational Physics*, 1976, **22**, 517–533

41 Chuoke, R. L., van Meurs, P. and van der Poel, C. The instability of slow, immiscible, liquid-liquid displacements in permeable media, *Society of Petroleum Engineers Journal*, 1959, 188–194

42 Coats, K. An equation-of-state compositional model, *Society of Petroleum Engineers Journal*, 1980, 363–376

43 Coats, K. Reservoir simulation: State of the art, *Journal of Petroleum Technology*, 1982, 1633–1642

44 Coats, K. H., George, W. D., Chu, C. and Marcum, B. E. Three-dimensional simulation of steamflooding, presented at the Sept. 30–Oct. 3, 1973, Annual Fall Technical Conference and Exhibition of the Society of Petroleum Engineers

45 Coats, K. H., Nielsen, R. L., Terhune, M. H. and Weber, A. G. Simulation of three-dimensional, two-phase flow in oil and gas reservoirs, *Society of Petroleum Engineers Journal*, 1967, 377–388

46 Coats, K. H. and Ramesh, A. B. Effect of grid type and difference scheme on pattern steamflood results, presented at the Sept. 26–29, 1982, Fall Technical Conference and Exhibition of the Society of Petroleum Engineers

47 Colella, P., Concus, P. and Sethian, J. Some numerical methods for discontinuous flows in porous media, *The Mathematics of Reservoir Simulation*, Ewing, R. E. (ed.), Society for Industrial and Applied Mathematics, Philadelphia, Pa., 1983, 161–186

48 Concus, P. Calculation of shocks in oil reservoir modeling and porous flow, *Numerical Methods for Fluid Dynamics*, Morton, K. W. and Baines, M. J. (eds), Academic Press, New York, NY, 1982, 165–178

49 Corapicoglu, M. Y. and Baehr, A. Immiscible contaminant transport in soils and groundwater with an emphasis on petroleum hydrocarbons: System of differential equations vs. single cell model, *Water Sciences and Technology*, 1985, to appear

50 Darlow, B. L., Ewing, R. E. and Wheeler, M. F. Mixed finite element methods for miscible displacement problems in porous media, *Proceedings*, Sixth Symposium on Reservoir Simulation, Society of Petroleum Engineers, 1982, 137–146

51 Davis, H. T. and Scriven, L. E. The origins of low interfacial tensions for enhanced oil recovery, presented at the September 21–24, 1980, Annual Fall Technical Conference and Exhibition of the Society of Petroleum Engineers of AIME

52 Davis, S. and Flaherty, J. An adaptive finite element method for initial-boundary value problems for partial differential equations, *Society for Industrial and Applied Mathematics Journal for Scientific and Statistical Computing*, 1983, **3**, 6–27

53 Delshad, M., MacAllister, D. J., Pope, G. A. and Rouse, B. A. Multiphase dispersion and relative permeability experiments, presented at the Sept., 1982. Society of Petroleum Engineers Annual Fall Technical Conference and Exhibition, held in New Orleans, La

54 Diaz, J. C., Ewing, R. E., Jones, R. W., McDonald, A. E., Uhler, L. M. and von Rosenberg, D. U. Self adaptive local grid refinement in enhanced oil recovery, *Proceedings*, Fifth International Symposium on Finite Elements and Flow Problems, Austin; Texas, Jan. 23–26, 1984, 479–484

55 Djomehri, M. J. and Miller, K. A moving finite element code for general systems of partial differential equations in two dimensions, *University of California Center for Pure and Applied Mathematics Report PAM-57*, Berkeley, Calif., Oct. 1981

56 Douglas, J. Jr., Alternating direction methods for three space variables, *Numerische Mathematik*, 1962, **2**, 91–98

57 Douglas, J. Jr., Darlow, B. L., Wheeler, M. F. and Kendall, R. P. Self-adaptive finite element and finite difference methods for one-dimensional two-phase immiscible flow, *Computer Methods in Applied Mechanics and Engineering*, 1984, **47**, 119–130

58 Douglas, J. Jr. and Dupont, T. A finite-element collocation method for quasilinear parabolic equations, *Mathematics of Computation*, **27**, 17–28

59 Douglas, J. Jr., Peaceman, D. W. and Rachford, H. H. Jr. A method for calculating multidimensional immiscible displacement, *Transactions*, American Institute of Mining, Metallurgical and Petroleum Engineers, 1959, **216**, 297–306

60 Douglas, J. Jr. and Rachford, H. H. Jr. On the numerical solution of heat conduction problems in two and three space variables, *Transactions*, American Mathematical Society, 1956, **82**, 421–439

61 Eringen, A. C. and Ingram, J. D. A continuum theory of chemically reacting media—I. *International Journal of Engineering Science*, 1965, **3**, 197–212

62 Ewing, R. E. Alternating-direction Galerkin methods for parabolic, hyperbolic and Sobolev partial differential equations, *Proceedings of the Special Year in Numerical Analysis*, University of Maryland, College Park, Md., 1981, 123–150

63 Ewing, R. E. and George, J. H. Viscous fingering in hydrocarbon recovery processes, *Mathematical Methods in Energy Research*, Gross, K. I. (ed.), Society for Industrial and Applied Mathematics, Philadelphia, Pa., 1984, 194–213

64 Ewing, R. E. and Heinemann, R. F. Incorporation of mixed finite element methods in compositional simulation for reduction of numerical dispersion, *Proceedings*, Seventh Symposium on Reservoir Simulation, Society of Petroleum Engineers, Nov., 1983, 341–347

65 Ewing, R. E. and Heinemann, R. F. Mixed finite element approximation of phase velocities in compositional reservoir simulation, *Computer Methods in Applied Mechanics and Engineering*, 1984, **47**, 161–176

66 Ewing, R. E., Russell, T. F. and Wheeler, M. F. Simulation of miscible displacement using mixed methods and a modified method of characteristics, *Proceedings*, Seventh Symposium on Reservoir Simulation, Society of Petroleum Engineers, 1983, 71–82

67 Ewing, R. E., Russell, T. F. and Wheeler, M. F. Convergence analysis of an approximation of miscible displacement in porous media by mixed finite elements and a modified method of characteristics, *Computer Methods in Applied Mechanics and Engineering*, 1984, **47**, 73–92

68 Fatt, I. and Dykstra, H. Relative permeability studies, *Transactions*, American Institute of Mining, Metallurgical and Petroleum Engineers, 1951, **192**, 249–256

69 Faust, C. R. Transport of immiscible fluids within and below the unsaturated zone: A numerical model, *Water Resources Research*, 1985, **21**, 587–596

70 Frauenthal, J. C., di Franco, R. B. and Towler, B. F. Reduction of grid orientation effects in reservoir simulation using generalized upstream weighting, *Proceedings*, Seventh Symposium on Reservoir Simulation, Society of Petroleum Engineers, 1983, 7–16

71 Fried, J. J. *Groundwater Pollution*, Elsevier Scientific Publishing Co., Amsterdam, 1975

72 Fussell, L. T. and Fussell, D. D. An iterative technique for compositional reservoir models, *Society of Petroleum Engineers Journal*, 1979, 211–220

73 Garder, A. O., Peaceman, D. W. and Pozzi, A. L. Numerical calculation of multidimensional miscible displacement by the method of characteristics, *Society of Petroleum Engineers Journal*, 1964, 26–36

74 Gelinas, R. J., Doss, S. K. and Miller, K. The moving finite element method: Applications to general partial differential equations with large multiple gradients, *Journal of Computational Physics*, 1981, **40**, 202–221

75 Gibbs, J. W. On the equilibrium of heterogeneous substances, *Transactions*, Connecticut Academy, 1876, **3**, 108–248, and 1878, 343–524

76 Glimm, J., Isaacson, E. L., Lindquist, B., McBryan, O. and Yaniv, S. Statistical fluid dynamics: The influence of geometry on surface instabilities, *The Mathematics of Reservoir Simulation*, Ewing, R. E. (ed.), Society for Industrial and Applied Mathematics, Philadelphia, Pa., 1983, 137–160

77 Glimm, J., Lindquist, B., McBryan, O. and Padmanabhan, L. A front tracking reservoir simulator, five-spot validation studies and the water coning problem, *The Mathematics of Reservoir Simulation*, Ewing, R. E. (ed.), Society for Industrial and Applied Mathematics, Philadelphia, Pa., 1983, 107–135

78 Glimm, J., Marchesin, D. and McBryan, O. Unstable fingers in two-phase flow, *Communications in Pure and Applied Mathematics*, 1981, **34**, 53–75

79 Glimm, J., Marchesin, D. and McBryan, O. A numerical method for two phase flows with an unstable interface, *Journal of Computational Physics*, 1981, **39**, 91–119

80 Heinemann, R. F. Simulation of compositional oil recovery processes, *Mathematical Methods in Energy Research*, Gross, K. I. (ed.), Society for Industrial and Applied Mathematics, Philadelphia, Pa., 1984, 214–235

81 Heinemann, Z. E. and von Hantelmann, G. Using local grid refinement in a multiple application reservoir simulator, *Proceedings*, Seventh Symposium on Reservoir Simulation, Society of Petroleum Engineers, 1983, 205–218

82 Hoa, N. T., Gaudu, R. and Thirriot, C. Influence of the hysteresis effect on transient flows in saturated-unsaturated porous media, *Water Resources Research*, 1977, **13**, 992–996

83 Huyakorn, P. S. and Pinder, G. F. A new finite element technique for the solution of two-phase flow through porous media, *Advances in Water Resources*, 1978, **1**, 285–298

84 Huyakorn, P. S. and Pinder, G. F. *Computational Methods in Subsurface Flow*, Academic Press, New York, NY, 1983

85 Jensen, O. K. and Finlayson, B. A. A solution of the transport equation using a moving coordinate system, *Advances in Water Resources*, 1980, **3**, 9–18

86 Jensen, O. K. and Finlayson, B. A. A numerical technique for tracking sharp fronts in studies of tertiary oil recovery pilots, *Proceedings*, Seventh Symposium on Reservoir Simulation, Society of Petroleum Engineers, 1983, 61–70

87 Jerrauld, G. R., Davis, H. T. and Scriven, L. E. Frontal structure and stability in immiscible displacement, *Proceedings*, Fourth Symposium on Enhanced Oil Recovery, Society of Petroleum Engineers and US Department of Energy, 1984, **2**, 135–144

88 Kazemi, H., Vestal, C. R. and Shank, G. D. An efficient multicomponent numerical simulator, *Society of Petroleum Engineers Journal*, 1978, 355–368

89 Koval, E. J. A method for predicting the performance of unsteady miscible displacement, *Society of Petroleum Engineers*, 11963, 145–154

90 Lax, P. D. Hyperbolic systems of conservation laws II, *Communications in Pure and Applied Mathematics*, 1957, **10**, 537–566

91 Leverett, M. C. Capillary behaviour in porous solids, *Transactions*, American Institute of Mining, Metallurgical and Petroleum Engineers, 1941, **142**, 159–169

92 Leverett, M. C. and Lewis, W. B. Steady flow of gas-oil-water mixtures through unconsolidated sands, *Transactions*, American Institute of Mining, Metallurgical and Petroleum Engineers, 1941, **142**, 107–120

93 McBryan, O. Shock tracking methods in 2-D flows, *Ninth National Applied Mechanics Congress*, Cornell University, Ithaca, NY, 1982

94 McLean, J. W. The fingering problem in flow through porous media, thesis presented to the California Institute of Technology, at Pasadena, Cal., in 1980 in partial fulfillment of the requirements for the degree of Doctor of Philosophy

95 Meijerink, J. A. and Van der Vorst, H. A. An iterative solution method for linear systems of which the coefficient matrix is a symmetric M-matrix, *Mathematics of Computation*, 1977, **31**, 148–162

96 Mercer, J. W. and Faust, C. R. The application of finite element techniques to immiscible flow in porous media, *Finite Elements in Water Resources*, Gray, W. G. *et al.* (eds), London, Pentech Press, 1977, 21–43

97 Mercer, J. W. Larson, S. P. and Faust, C. R. Simulation of salt-water interface motion, *Ground Water*, 1980, **18**, 374–385

98 Miller, K. and Miller, R. N. Continuously deforming finite elements, I, *Society for Industrial and Applied Mathematics Journal of Numerical Analysis*, 1981, **18**, 1019–1032

99 Milly, P. C. D. A mass-conservative procedure for time-stepping in models of unsaturated flow, *Finite Elements in Water Resources*, Laible, J. P. *et al.* (eds), Springer-Verlag, London, 1984, 103–112

100 Mohsen, M. F. N. Numerical experiments using 'adaptive' finite elements with collocation, *Finite Elements in Water Resources*, Laible, J. P. *et al.* (eds), Springer-Verlag, Berlin, 1984, 45–61

101 Molina, N. M. A systematic approach to the relative permeability problem in reservoir simulation, presented at the September 21–24, 1980, Annual Fall Technical Conference and Exhibition of the Society of Petroleum Engineers of AIME

102 Morel-Seytoux, H. J. Introduction to flow of immiscible liquids in porous media, *Flow Through Porous Media*, De Weist, R. J. M. (ed.), Academic Press, New York, NY, 1969, 456–516

103 Morrow, N. R. Physics and thermodynamics of capillary action in porous media, *Symposium on Flow Through Porous Media*, Nunge, R. (ed.), American Chemical Society Publications, Washington, DC, 1969, 83–108

104 Muskat, M., Wykoff, R. D., Botset, H. G. and Meres, M. W. Flow of gas–liquid mixtures through sands, *Transactions*, American Institute of Mining, Metallurgical and Petroleum Engineers, 1937, **123**, 69–96

105 Nakano, Y. Application of recent results in functional analysis to the problem of wetting fronts, *Water Resources Research*, 1980, **16**, 314–318

106 Narasimhan, T. N. and Witherspoon, P. A. Numerical model for saturated-unsaturated flow in deformable porous media 3. Applications, *Water Resources Research*, 1978, **14**, 1017–1033

107 Neumann, S. P. Saturated-unsaturated seepage by finite elements, *Journal of the Hydraulics Division of ASCE*, 1073, **99**, 2233–2251

108 Ngheim, L. X., Fong, D. K. and Aziz, K. Compositional Modelling with an equation of state, *Society of Petroleum Engineers Journal*, 1981, 687–698

109 Nolen, J. S. Numerical simulation of compositional phenomena in petroleum reservoirs, *Proceedings*, Third Symposium on Reservoir Simulation, Society of Petroleum Engineers, Jan., 1973, 269–284

110 Northrup, E. J. and Woo, P. T. Application of preconditioned conjugate-gradient-like methods in reservoir simulation, *Proceedings, Eighth Symposium on Reservoir Simulation*, Society of Petroleum Engineers, Feb., 1985, 375–386

111 Oleinik, O. A. Uniqueness and stability of the generalized solution to the Cauchy problem for a quasi-linear equation, *American Mathematical Society Translations, Series 2*, 1973, **33**, 285–290

112 Passman, S. L., Nunziato, J. W. and Walsh, E. K. A theory of multiphase mixtures, Appendix 5C to *Rational Thermodynamics*, 2nd ed., by C. A. Truesdell, Springer-Verlag, New York, NY, 1984, 286–325

113 Peaceman, D. W. Numerical solution of the nonlinear equations for two-phase flow through porous media, *Nonlinear Partial Differential Equations: A Symposium on Methods of Solution*,

Ames, W. F. (ed.), Academic Press, New York, NY, 1967, 171–191
114 Peaceman, D. W. *Fundamentals of Numerical Reservoir Simulation*, Elsevier Scientific Publishing Co., Amsterdam, 1977
115 Peaceman, D. W. and Rachford, H. H. Jr. The numerical solution of parabolic and elliptic differential equations, *Journal of the Society for Industrial and Applied Mathematics*, 1955, **3**, 28–41
116 Peletier, L. A. The porous medium equation. *Applications of Nonlinear Analysis in the Physical Sciences*, Amann, H. *et al.* (eds), Pitman Advanced Publishing Program, Boston, Mass., 1981, 229–240
117 Peng, D.-Y. and Robinson, D. R. A new two-constant equation of stage, *Industrial and Engineering Chemistry: Fundamentals*, 1976, **15**, 53–64
118 Peters, E. J. and Flock, D. L. The onset of instability during two-phase immiscible displacement in porous media, *Society of Petroleum Engineers Journal*, 1981, 249–258
119 Philip, J. R. Numerical solution of equations of the diffusion type with diffusivity concentration dependent. II. *Australian Journal of Physics*, 1957, **10**, 29–40
120 Pinder, G. F. and Cooper, H. H. Jr. A numerical technique for calculating the transient position of the saltwater front, *Water Resources Research*, 1970, **6**, 875–882
121 Pinder, G. F. and Page, R. F. Finite element simulation of salt water intrusion on the South Fork of Long Island, *Finite Elements in Water Resources*, Gray, W. G. *et al.* (eds), Pentech Press, Plymouth, UK, 1977, 2.51–2.69
122 Ponting, D. K., Foster, B. A., Naccache, P. F., Nichols, M. O., Pollard, R. K., Rae, J., Banks, D. and Walsh, S. K. An efficient fully implicit simulator, *Society of Petroleum Engineers Journal*, 1983, 544–552
123 Potempa, T. Finite element methods for convection dominated transport problems, thesis presented to Rice University, at Houston, Texas, in 1982 in partial fulfillment of the requirements for the degree of Doctor of Philosophy
124 Prévost, J. H. Mechanics of continuous porous media, *International Journal of Engineering Science*, **18**, 787–800
125 Preuss, K. and Bödvarsson, G. S. A seven-point finite difference method for improved grid orientation in pattern steamfloods, *Proceedings*, Seventh Symposium on Reservoir Simulation, Society of Petroleum Engineers, 1983, 175–184
126 Raats, P. A. C. Applications of the theory of mixtures in soil physics, Appendix 5D to *Rational Thermodynamics*, 2nd ed., by C. A. Truesdell, Springer-Verlag, New York, NY, 1984, 326–343
127 Reeves, M. and Duguid, J. O. Water movement through saturated-unsaturated porous media: A finite-element Galerkin model, *Oak Ridge National Laboratories Report 4927*, Oak Ridge, Tenn., 1975
128 Richards, L. A. Capillary conduction of liquids in porous media, *Physics*, 1931, **1**, 318–333
129 Risnes, R., Dalen, V. and Jensen, J. I. Phase equilibrium calculations in the near-critical region, *Proceedings*, Third European Symposium on Enhanced Oil Recovery, Fayers, F. J. (ed.), Elsevier Scientific Publishing Co., Amsterdam, 1981, 329–350
130 Roebuck, I. F., Henderson, G. E., Douglas, J. and Ford, W. T. The compositional reservoir simulator: Case I—The linear model, *Society of Petroleum Engineers Journal*, 1969, 115–130
131 Sá da Costa, A. A. G. and Wilson, J. L. Coastal seawater intrusion: A moving boundary problem, *Finite Elements in Water Resources*, Wang, S. Y. *et al.* (eds), University of Mississippi, Oxford, Miss., 1980, 2.209–2.218
132 Saffman, P. G. and Taylor, G. I. The penetration of a fluid into a porous medium or Hele-Shaw cell containing a more viscous liquid, *Proceedings of the Royal Society of London* A, 1958, **245**, 312–329
133 Scheidegger, A. E. *The Physics of Flow Through Porous Media*, 3rd ed., University of Toronto Press, Toronto, 1974
134 Schiegg, H. O. Experimental contribution to the dynamic capillary fringe, *Symposium on Hydrodynamic Diffusion and Dispersion in Porous Media*, Pavia-Italia, Rome, 1977
135 Schwille, F. Migration of organic fluids immiscible with water in the unsaturated zone, *Pollutants in Porous Media*, Yaron, B., Dagan, G. and Goldshmid, J. (eds), Springer-Verlag, Berlin, 1984, 27–49
136 Segol, G. A three-dimensional Galerkin-finite element model for the analysis of contaminant transport in saturated-unsaturated porous media, *Finite Elements in Water Resources*, Gray, W. G. *et al.* (eds), Pentech Press, London, 1977, 2.123–2.144
137 Settari, A. and Aziz, K. Treatment of the nonlinear terms in the numerical solution of partial differential equations for multi-phase flow in porous media, *International Journal of Multiphase Flow*, 1975, **1**, 817–844
138 Settari, A., Price, H. S. and Dupont, T. Development and application of variational methods for simulation of miscible displacement in porous media, *Society of Petroleum Engineers Journal*, 1977, 228–246
139 Shamir, V. and Dagan, G. Motion of the seawater interface in a coastal aquifer: A numerical solution, *Water Resources Research*, 1971, **7**, 644–647
140 Shapiro, A. M. and Pinder, G. F. Solution of immiscible displacement in porous media using the collocation finite element method, *Finite Elements in Water Resources*, Holz, K. P. *et al.* (eds), Springer-Verlag, Berlin, 1982, 9.61–9.70
141 Sheldon, J. W., Zondek, B. and Cardwell, W. T. One-dimensional, incompressible, non-capillary two-phase flow in a porous medium, *Transactions*, American Onstitute of Mining, Metallurgical and Petroleum Engineers, 1959, **216**, 290–296
142 Shubin, G. R. and Bell, J. B. An analysis of the grid orientation effect in numerical simulation of miscible displacement, *Computer Methods in Applied Mechanics and Engineering*, 1984, **47**, 47–72
143 Stone, H. L. Iterative solution of implicit approximations of multidimensional partial differential equations, *Society for Industrial and Applied Mathematics Journal of Numerical Analysis*, 1968, **5**, 530–568
144 Stone, H. L. Estimation of three-phase relative permeability and residual oil data, *Journal of Canadian Petroleum Technology*, 1973, **12** (4), 53–61
145 Stone, H. L. and Garder, A. O. Jr. Analysis of gas-cap or dissolved-gas reservoirs, *Transactions*, American Institute of Mining, Metallurgical and Petroleum Engineers, 1961, **222**, 92–104
146 Taylor, G. I. Dispersion of soluble matter in solvent flowing slowly through a tube, *Proceedings*, Royal Society of London, Series A, 1953, **219**, 186–203
147 Thomas, G. H., Countryman, G. R. and Fatt, I. Miscible displacement in a multiphase system, *Society of Petroleum Engineers Journal*, 1963, 189–196
148 Todd, M. R. and Longstaff, W. J. The development, testing and application of a numerical simulator for predicting miscible flood performance, *Journal of Petroleum Technology*, 1972, 874–882
149 Todd, M. R., O'Dell, P. M. and Hirasaki, G. J. Methods for increased accuracy in numerical reservoir simulators, *Society of Petroleum Engineers Journal*, 1972, 515–530
150 Towler, B. F. and Killough, J. E. Comparison of preconditioners for the conjugate gradient method in reservoir simulation, *Proceedings*, Sixth Symposium on Reservoir Simulation, Society of Petroleum Engineers, Feb., 1982, 7–14
151 van Genuchten, M. Th. A comparison of numerical solutions of the one-dimensional unsaturated-saturated flow and mass transport equations, *Advances in Water Resources*, 1982, **5**, 47–55
152 van Genuchten, M. Th. An Hermitian finite element solution of the two-dimensional saturated-unsaturated flow equation, *Advances in Water Resources*, 1983, **6**, 106–111
153 Van Quy, N., Simandoux, P. and Corteville, J. A numerical study of diphasic multicomponent flow, *Society of Petroleum Engineers Journal*, 1972, 171–184
154 Villaume, J. F. Investigations at sites contaminated with dense, nonaqueous phase liquids (NAPLs), *Ground Water Monitoring Review*, Spring, 1985, 60–74
155 Vinsome, P. K. and Au, A. One approach to the grid orientation problem in reservoir simulation, presented at the Sept. 23–26, 1979, Annual Fall Technical Conference and Exhibition of the Society of Petroleum Engineers
156 von Neumann, J. First report on the numerical calculation of flow problems, *Collected Works*, Taub, A. H. (ed.), Vol. 5, The MacMillan Co., New York, NY, 1963, 664–712
157 von Rosenberg, D. U. Local mesh refinement for finite difference methods, presented at the Sept. 26–29, 1982, Fall Technical Conference and Exhibition of the Society of Petroleum Engineers
158 Watts, J. W. A compositional formulation of the pressure and saturation equations, *Proceedings*, Seventh Symposium on Reservoir Simulation, Society of Petroleum Engineers, Nov., 1983, 113–138
159 Welge, H. J. A simplified method for computing oil recovery by gas or water drive, *Transactions*, American Institute of Mining, Metallurgical and Petroleum Engineers, 1952, **195**, 91–98
160 Wilson, D. C., Tan, T. C. and Casinader, P. C. Control of numerical dispersion in compositional simulation, *Third European Symposium on Enhanced Oil Recovery*, Fayers, F. J.

(ed.), Elsevier Scientific Publishing Co., Amsterdam, 1981, 425–440

161 Wykoff, R. D. and Botset, H. G. The flow of gas–liquid mixtures through unconsolidated sands, *Physics*, 1936, **7**, 325–345

162 Yanosik, J. L. and McCracken, T. A. A nine point finite difference simulator for realistic prediction of adverse mobility ratio displacements, *Society of Petroleum Engineers Journal*, 1979, 253–262

163 Yortsos, Y. C. and Huang, A. B. Linear stability of immiscible displacement including continuously changing mobility and capillary effects, *Proceedings*, Fourth Symposium on Enhanced Oil Recovery, Society of Petroleum Engineers and US Department of Energy, 1984, **2**, 145–162

164 Young, L. C. A study of spatial approximations for simulating fluid displacements in petroleum reservoirs, *Computer Methods in Applied Mechanics and Engineering*, 1984, **47**, 3–46

165 Young, L. C. and Stephenson, R. E. A generalized compositional approach for reservoir simulation, *Society of Petroleum Engineers Journal*, 1983, 727–742

NOMENCLATURE

Capital letters

A	coefficient
$[A]$	system matrix
$\mathscr{A}$	spatial operator
B	formation volume factor; coefficient
B_j	(see Table 1)
C	specific moisture capacity; compressibility; coefficient
D	diffusion coefficient
$\mathbf{D}$	hydrodynamic dispersion tensor
H_0	Hermite cubic of the first kind
H_1	Hermite cubic of the second kind
I	number of nodes
J	temporal domain
K	hydraulic conductivity scalar
$\mathbf{K}$	hydraulic conductivity tensor
K_{ij}	(see Table 1)
$[K]$	stiffness matrix
M	mobility ratio
M_{ij}	(see Table 1)
$[M]$	mass matrix
N	basis function; number of species
$[N]$	SIP matrix
$\mathcal{O}$	order symbol
P	number of phases
Q_{ij}	(see Table 1)
R	residual
R_S	solution gas–oil ratio
$\{R\}$	residual vector
$\mathscr{R}$	spatial region
S	saturation
S_s	specific storage
T	transmissibility (defined variously)
Z	depth below datum

Lower case letters

a	z-coordinate of confining layer
b	z-coordinate of interface; derivative of $1/B$
$\mathbf{b}$	body force
c	z-coordinate of free surface
$\mathbf{e}$	unit vector
f	fractional flow; fugacity
$\{f\}$	boundary data vector
g	gravitational acceleration
h	hydraulic head
$\{h\}$	vector of hydraulic heads
$\mathbf{j}$	diffusive flux
k	permeability scalar
k_r	relative permeability
$\mathbf{k}$	permeability tensor
l	vertical thickness
$\mathbf{m}$	momentum exchange rate
p	pressure
$\{p\}$	vector of pressures
q	flux; flow rate
$\mathbf{q}$	flow rate vector
r	mass exchange rate
$\{r\}$	right-hand side vector
s_y	specific yield
t	time
$\mathbf{t}$	stress tensor
u	unknown function
$\mathbf{u}$	diffusion velocity vector
$\mathbf{v}$	velocity vector
x	horizontal space coordinate
$\mathbf{x}$	spatial position vector
$\mathbf{y}$	vector of unknowns
z	vertical space coordinate

Capital greek letters

Δ_t	time-difference operator
Δt	time increment
Δx	space increment
Θ	moisture content
Λ	mobility scalar
$\mathbf{\Lambda}$	mobility tensor
Σ	interface
Υ	compositional flux coefficients
Φ	free surface
Ω	spatial domain

Lower case greek letters

α	dispersity
γ	gravity coefficient
δ	iterative increment operator
ξ	curve in (x, t)-plane
λ	flux coefficient
μ	dynamic viscosity
ρ	density
ϕ	volume fraction; porosity
φ	test function
ψ	pressure head
ω	mass fraction

Subscripts and superscripts

A	air
atm	atmospheric
C	capillary
F	freshwater
G	gas phase
g	gas species
i, j	node indices; species indices
k	collocation point index
l	longitudinal
m	iteration level
mol	molecular
N	nonaqueous liquid phase
n	time level
O	oil phase
o	oil species
R	rock phase

RC	reservoir conditions
ref	reference
S	saltwater
STC	stock-tank conditions
T	total
t	transverse
W	water phase
w	water species
z	z-direction
α	phase index
∂	boundary

Special symbols

$\underline{\ }$	average; collocation point
$\hat{\ }$	approximation
$'$	derivative; dummy variable
*	dimensionless; upstream; preconditioner

Mixed Finite Element Methods for Computing Groundwater Velocities

M. B. Allen, R. E. Ewing, and J. V. Koebbe
Department of Mathematics, University of Wyoming, Laramie, Wyoming 82171

Central to the understanding of problems in water quality and quantity for effective management of water resources is the development of accurate numerical models to stimulate groundwater flows and contaminant transfer. We discuss several important difficulties arising in modeling of subsurface flow and present promising numerical procedures for alleviating these problems. Furthermore, we describe mixed-finite element techniques for accurately approximating fluid velocities, and review computational results on a variety of hydrologic problems.

I. INTRODUCTION

In the past decade, water quality problems have assumed increasing importance in water resources engineering. An emerging awareness that our groundwater supplies face the threat of contamination from various sources has prompted vigorous research into mathematical methods for predicting contaminant movements in underground water. In many respects the task of simulating contaminant flows in porous media is computationally more demanding than the more traditional problem of resolving supply issues. The fundamental reason for this increased difficulty is that in contaminant flows, the fluid velocity plays a crucial role, while water supply problems more typically concern a scalar field such as head or pressure. According to Darcy's law, one must differentiate heads or pressures to get velocities, and this leads to at least two related mathematical problems. First, any pathologic behavior in pressure or head manifests itself in even more severe behavior in velocity. Thus, for example, the relatively mild logarithmic singularities in pressure or head that occur at pumped wells appear as simple poles in the velocity field. Second, standard numerical solutions of the flow equations commonly produce discrete approximations to the pressure or head, and in differentiating these approximations to compute velocities one incurs a loss of accuracy that is typically one order in the spatial grid mesh.

These difficulties are significant, for they can lead, in the first case, to nonconvergent approximations to velocities near wells and, in the second case, to inferior predictions of the very aspect of groundwater motion that is most crucial in forecasting contaminant transport. In this paper we examine a mixed finite element method for the groundwater flow equations that mitigates these difficulties. The essential idea of the mixed method is that, by solving the second-order equation governing groundwater flow as a set of coupled first-order equations in velocity and head, one can compute both fields explicitly without sacrificing accuracy in the velocity through differentiation. The method

Numerical Methods for Partial Differential Equations, 3, 195–207 (1985)
 CCC 0749-159X/85/030195-13$04.00

also admits natural choices of interpolating polynomials for the trial functions to guarantee the highest accuracy for a given number of degrees of freedom. Furthermore, in problems involving pumped wells, one can incorporate appropriate singularities in the trial functions for velocity. The singular parts, being known, then contribute to the inhomogeneous terms in the systems of algebraic equations that arise through spatial discretization. This approach circumvents convergence difficulties near wells and leads to good global error estimates.

Proper choice of trial functions is an essential feature of the mixed method presented here. In particular, the trial space used for the fluid velocity must yield an approximation whose divergence lies in the trial space for head; otherwise the favorable convergence rates cited below are no longer valid. Thus, the methods advanced here are distinct from other formulations that also treat velocity and head as principal unknowns but use trial functions belonging to the same continuity class for both [1].

II. REVIEW OF THE MIXED METHOD

Let us examine a model equation arising in the simulation of steady-state flow in a two-dimensional, horizontal, leaky aquifier. This type of problem is representative of the sorts of flow equations that need to be solved in conjunction with species transport equations in groundwater contamination studies. The governing equation is

$$\nabla \cdot (T\nabla h) - \frac{K}{b}(h - h_a) + Q = 0 \tag{1}$$

where h is the unknown head in the aquifier, T is the transmissivity, K is the hydraulic conductivity in the aquitard overlying the leaky aquifier, b is the thickness of the aquitard, h_a is the head in the aquitard, and Q represents internal sources or sinks. If the sources or sinks are all wells, then we can idealize them as points:

$$Q = \Sigma_{\ell=1}^{L} Q_\ell \delta(\mathbf{x} - \mathbf{x}_\ell) .$$

Here Q_ℓ stands for the strength of the ℓ-th source (negative for producing wells), and $\delta(\mathbf{x} - \mathbf{x}_\ell)$ is the Dirac distribution centered at spatial position $\mathbf{x}_\ell$. The leakage term in (1) has the linear form proposed by Charbeneau and Street [2].

In the mixed finite-element method we factor Darcy's law from Eq. (1), giving a coupled set of first-order equations:

$$\mathbf{u} + T\nabla h = 0 \tag{2a}$$

$$-\nabla \cdot \mathbf{u} - \frac{K}{b}(h - h_a) + Q = 0 \tag{2b}$$

where $\mathbf{u}$ is the superficial or Darcy velocity of the water. In typical boundary-value problems we solve Eqs. (2) on a bounded open set $\Omega \subset \mathbf{IR}^2$ subject to boundary data of the form

$$\mathbf{u}(\mathbf{x}) \cdot \boldsymbol{\nu}(\mathbf{x}) = 0, \qquad \mathbf{x} \in \partial\Omega_N \tag{3a}$$

$$h(\mathbf{x}) = h_\partial(\mathbf{x}), \qquad \mathbf{x} \in \partial\Omega_D . \tag{3b}$$

Thus the orientable boundary $\partial\Omega$, having unit outward normal vector $\boldsymbol{\nu}$, admits a decomposition $\partial\Omega_N \cup \partial\Omega_D$ into no-flow and prescribed-head segments. $\partial\Omega_N$ is a locus of points where normal fluid velocities vanish, while $\partial\Omega_D$ is the boundary segment along which heads are known.

The boundary-value problem formed by Eqs. (2) and (3) has a variational form that underlies the finite-element approximations. Let $L^2(\Omega)$ be the space of square-integrable functions on Ω, and define the trial spaces:

$$V = \{\mathbf{v} \in L^2(\Omega) \times L^2(\Omega) \,|\, \nabla \cdot \mathbf{v} \in L^2(\Omega) \text{ and } \mathbf{v} \cdot \nu = 0 \text{ on } \partial\Omega_N\}$$

being the space of vector-valued velocity trial functions, and

$$W = \{w \in L^2(\Omega) \,|\, w = h_\partial \text{ on } \partial\Omega_D\}$$

being the space of trial functions for the head. Observe that functions belonging to V not only obey the no-flux boundary conditions but also have divergences lying in $L^2(\Omega)$. This inclusion, which is a natural mathematical feature of the problem, must be preserved in discrete analogs to ensure good error estimates. The variational version of our boundary-value problem is a set of integral equations obtained using the inner products $(f, g) = \int_\Omega fg\, dv$ and $(\mathbf{f}, \mathbf{g}) = \int_\Omega \mathbf{f} \cdot \mathbf{g}\, dv$: we seek $\mathbf{u} \in V$ and $h \in W$ such that

$$(T^{-1}\mathbf{u} + \nabla h, \mathbf{v}) = 0 \quad \text{for all } \mathbf{v} \in V$$

$$\left(-\nabla \cdot \mathbf{u} - \frac{K}{b}(h - h_a) + Q, w\right) = 0 \quad \text{for all } w \in W .$$

Integrating by parts and observing the boundary values of the trial functions gives

$$(T^{-1}\mathbf{u}, \mathbf{v}) - (h, \nabla \cdot \mathbf{v}) = -\int_{\partial\Omega_D} h\mathbf{v} \cdot \boldsymbol{\nu}\, ds \quad \text{for all } \mathbf{v} \in V \tag{4a}$$

$$(\nabla \cdot \mathbf{u}, w) + \left(\frac{K}{b}h, w\right) = \left(\frac{K}{b}h_a + Q, w\right) \quad \text{for all } w \in W . \tag{4b}$$

Finite-element approximations to the boundary value problem given in Eqs. (2) and (3) are analogs of Eqs. (4) posed on finite-dimensional subspaces V_k and W_k of the trial spaces V and W. In particular, we choose subspaces of piecewise polynomial interpolating functions on Ω. The index k therefore indicates the mesh of partitions for finite-element interpolation.

To define the specific subspaces used in this paper, we need to introduce some notation. For simplicity let us choose Ω to be a rectangle, $\Omega = I \times J$, where $I = (a, b)$ and $J = (c, d)$ are open intervals in x and y, respectively. Consider partitions Δ_x: $a = x_0 < \cdots < x_M = b$ and Δ_y: $c = y_0 < \cdots < y_N = d$ of I and J having mesh:

$$k = \max_{\substack{1 \le i \le M \\ 1 \le j \le N}} \{x_i - x_{i-1}, y_j - y_{j-1}\} .$$

We define piecewise polynomial space M_q^p on a given partition Δ of any interval S to be the space of q-times continuously differentiable functions that, when restricted to a single interval in the partition, reduce to polynomials of degree not greater than p: $M_q^p(\Delta) = \{\psi \in C^q \mid \psi$ is a polynomial of degree at most p on each subinterval of $\Delta\}$. Thus, for example, M_{-1}^0 is a space of piecewise constant functions that may be discontinuous between subintervals, while M_0^1 is a space of continuous, piecewise linear functions.

For our trial spaces, we choose tensor-product Raviart-Thomas [3] subspaces on the rectangle $I \times J$. In the lowest-degree case, we pick

$$W_k = \{w_k \in M_{-1}^0(\Delta_x) \otimes M_{-1}^0(\Delta_y) \mid w_k = h_\partial \text{ on } \partial\Omega_D\}$$

$$V_k = \{\mathbf{v}_k \in [M_0^1(\Delta_x) \otimes M_{-1}^0(\Delta_y)] \times [M_{-1}^0(\Delta_x) \otimes M_0^1(\Delta_y)] \mid \mathbf{v}_k \cdot \boldsymbol{\nu} = 0 \text{ on } \partial\Omega_N\}.$$

In this case our trial function for the head h will be piecewise constant in the x and y directions. The trial function for velocity $\mathbf{u}$ will have two components: the x-component will be piecewise linear and continuous in the x direction and piecewise constant with jump discontinuities in the y direction, while the y-component will be piecewise constant in x and piecewise linear in y. For the next highest degree of approximation we choose

$$W_k = \{w_k \in M_{-1}^1(\Delta_x) \otimes M_{-1}^1(\Delta_y) \mid wk = h_\partial \text{ on } \partial\Omega_D\}$$

$$V_k = \{\mathbf{v}_k \in [M_0^2(\Delta_x) \otimes M_{-1}^1(\Delta_y)] \times [M_{-1}^1(\Delta_x) \otimes M_0^2(\Delta_y)] \mid \mathbf{v}_k \cdot \boldsymbol{\nu} = 0 \text{ on } \partial\Omega_N\}.$$

Notice that the degrees of the polynomials have increased by 1 over the first-order spaces, but the degrees of continuity remain the same.

Having chosen our trial spaces, we derive finite-element analogs of Eqs. (4) by forming trial functions $\hat{h}_k \in W_k$ and $\hat{\mathbf{u}}_k \in V_k$ whose values at the nodes (x_i, y_j) of the partition $\Delta_x \times \Delta_y$ are unknown. To solve for these unknown coefficients, we impose the Galerkin criteria:

$$(T^{-1}\hat{\mathbf{u}}, \mathbf{v}_k) - (h_k, \nabla \cdot \mathbf{v}_k) = -\int_{\partial\Omega_D} h_k \mathbf{v}_k \cdot \boldsymbol{\nu}\, ds \quad \text{for all } \mathbf{v}_k \in V_k \tag{5a}$$

$$(\nabla \cdot \mathbf{u}_k, w_k) + \left(\frac{K}{b} h_k, w_k\right) = \left(\frac{K}{b} h_a + Q, w_k\right) \quad \text{for all } w_k \in W_k. \tag{5b}$$

These equations are just finite-dimensional analogs of the variational equations derived earlier.

In problems having pumped wells in Ω the velocity field will possess poles of order one. Error estimates relying on smoothness in the approximated solution fail near these singularities, and as a result many standard finite-element approximations to fluid velocity do not converge near wells. To avoid poor polynomial approximations near wells we modify the trial function for the velocity to accommodate the singularities. Hence, we decompose $\hat{\mathbf{u}}_k$ into a regular part and a singular part: $\hat{\mathbf{u}}_k = \hat{\mathbf{u}}_r + \hat{\mathbf{u}}_s$. Since we know the strengths, locations, and local forms of the singularities, we can write

$$\hat{\mathbf{u}}_s = \frac{1}{2\pi}\sum_{l=1}^{L} Q_l \nabla \log|\mathbf{x} - \mathbf{x}_l|$$

and therefore treat $\hat{\mathbf{u}}_s$ as known. In this case Eqs. (5) become

$$(T^{-1}\hat{\mathbf{u}}_r, \mathbf{v}_k) - (h_k, \nabla \cdot \mathbf{v}_k) = \int_{\partial\Omega_D} h_k \mathbf{v}_k \cdot \boldsymbol{\nu}\, ds - (T^{-1}\hat{\mathbf{u}}_s, \mathbf{v}_k) \quad \text{for all } \mathbf{v}_k \in V_k \tag{6a}$$

and

$$(\nabla \cdot \hat{\mathbf{u}}_r, w_k) + \left(\frac{K}{b} h_k, w_k\right) = \left(\frac{K}{b} h_a + Q, w_k\right) - (\nabla \cdot \hat{\mathbf{u}}_s, w_k) \quad \text{for all } w_k \in W_k. \tag{6b}$$

Evaluating the integrals appearing in these equations leads to a set of linear algebraic equations in the unknown nodal coefficients of $\hat{\mathbf{u}}_r$ and $\hat{h}$.

III. THEORY

As mentioned earlier, the class of methods just described has two advantages over traditional finite-element formulations: they retain high-order accuracy in the velocities by obviating differentiation, and they eliminate convergence difficulties near wells through the subtraction of singularities from trial functions. These advantages have their bases in theoretical error estimates. For the more traditional, straightforward projections of the variational analog of Eq. (1) onto interpolating subspaces, fluid velocities must be computed from heads as $\mathbf{u} = -T\nabla h$. Standard approximation theory [4] reveals that a piecewise polynomial method furnishing $O(k^r)$ approximations to h yields approximations to ∇h that are only $O(k^{r-1})$ as $k \to 0$. Thus improvements in the accuracy of $\mathbf{u}$ require greater refinement of the finite-element partition than comparable improvements in the accuracy of h. In contrast, the mixed method suffers no such disparity. Douglas, Ewing, and Wheeler [5] show that, in regions where the source term Q is smooth, the mixed method using the first- and second-order trial spaces described above has global error bounds of the form

$$\|\hat{\mathbf{u}} - \mathbf{u}\|_2 \le M_1 k$$
$$\|\hat{h} - h\|_2 \le M_2 k$$

and

$$\|\hat{\mathbf{u}} - \mathbf{u}\|_2 \le M_3 k^2$$
$$\|\hat{h} - h\|_2 \le M_4 k^2$$

respectively, where M_1, M_2, M_3, M_4 are constants for a given boundary value problem and $\|\cdot\|_2$ signifies the norm associated with the inner product $(\cdot,\cdot)$. Thus refining the spatial partition in the mixed method yields comparable improve-

ments in both heads and velocities. As Douglas, Ewing, and Wheeler [5] demonstrate, however, the inclusion relationship between the divergence of the velocity trial space and the head trial space is an essential fact in deriving these error estimates.

The error estimates have implications for problems involving nonhomogeneous media. In standard formulations with spatially heterogeneous transmissivities the calculation $\mathbf{u} = -T\nabla h$ calls for the multiplication of a function, T, that may be rapidly varying for physical reasons, with another, ∇h, that may vary rapidly simply by virtue of its being the gradient of a spatially varying approximation. Such a product of rapidly varying functions may be quite poorly behaved in numerical models. The mixed method avoids the numerical noise associated with differentiation of heads and therefore does not compound physical fluctuations with artificial ones.

Douglas, Ewing, and Wheeler [5] also give theoretical justification to the subtraction of singularities. In this case both the first- and second-order schemes give global error estimates of the form

$$\|\hat{\mathbf{u}} - \mathbf{u}\|_2 \leq M_5 k \log(k^{-1})$$
$$\|\hat{h} - h\|_2 \leq M_6 k \log(k^{-1})$$

where, again, M_5 and M_6 are constants for a given boundary-value problem. These estimates ensure that the velocities predicted by the mixed method will converge to the exact velocities near pumped wells when the trial function $\hat{\mathbf{u}}$ explicitly incorporates simple poles at the wells.

IV. COMPUTATIONAL EXAMPLE

To illustrate the effectiveness of the mixed method we shall examine a simple numerical example. Consider the equation

$$\nabla^2 h - (h - 1) + Q = 0$$

on $\Omega = (0, 1) \times (0, 1)$ with $Q = \delta(\mathbf{x} - (1, 1))$ and $\mathbf{u} \cdot \boldsymbol{\nu} = 0$ on $\partial\Omega$. We shall examine various pressure and velocity solutions for this boundary-value problem.

Before discussing the numerical results, however, it is worth reviewing our choice of bases for the trial spaces V_k and W_k. For convenience let us temporarily use the variable z to stand for either x or y, let the partition in the z-direction be Δ_z: $z_0 < \cdots < z_\Lambda$, and call $\Delta z_\lambda = z_\lambda - z_{\lambda-1}$, $\lambda = 1, \ldots, \Lambda$. Define the functions $\{v_\gamma\}_{\gamma=1}^{2\Lambda}$ as follows. If γ is even, v_γ is the standard piecewise linear chapeau function having $v_\gamma(z_\beta) = \delta_{\gamma\beta}$. If γ is odd, say $\gamma = 2\lambda - 1$, then v_γ is the piecewise quadratic given by

$$v_{2\lambda-1}^{(z)} = \begin{cases} 4(z - z_{\lambda-1})(z_\lambda - z)/(\Delta z)^2, & z \in [z_{\lambda-1}, z_\lambda] \\ 0, & \text{otherwise} \end{cases}.$$

Now take $M^1_{-1}(\Delta_z) = \text{span}\{v_\gamma\}_{\gamma=1}^{2\Lambda}$. To get a basis for $M^2_0(\Delta_z)$ define the functions $\{w_{\lambda 0}, w_{\lambda 1}\}_{\lambda=1}^{\Lambda}$ as follows:

$$w_{\lambda 0}(z) = \begin{cases} \dfrac{z_{\lambda-1} + \sigma_2 \Delta z_\lambda - z}{(\sigma_2 - \sigma_1)\Delta z_\lambda}, & z \in (z_{\lambda-1}, z_\lambda) \\ 0, \quad \text{otherwise} \end{cases}$$

$$w_{\lambda 1}(z) = \begin{cases} \dfrac{z - z_{\lambda-1} - \sigma_1 \Delta z_\lambda}{(\sigma_2 - \sigma_1)\Delta z_\lambda}, & z \in (z_{\lambda-1}, z_\lambda) \\ 0, \quad \text{otherwise} \end{cases}$$

where σ_1, σ_2 are the Gauss points $(1 \pm \sqrt{3}^{-1})/2$ in the unit interval $(0, 1)$. Then $M^2_0 = \text{span}\ \{w_{\lambda 0}, w_{\lambda 1}\}_{\lambda=1}^{\Lambda}$. With these definitions, we can form tensor-product bases for the spaces W_k and V_k introduced in Section II.

Using these bases we can compute the matrix equation representing the discrete Galerkin approximation to the model problem. It happens that, while the matrix is sparse, positive-definite, and invertible, it is not particularly well

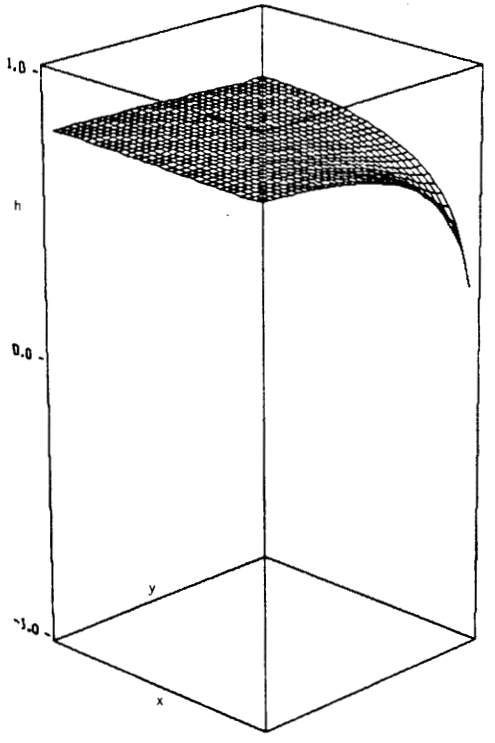

FIG. 1. Head distribution computed using first-order elements on a square grid having 32 elements on a side.

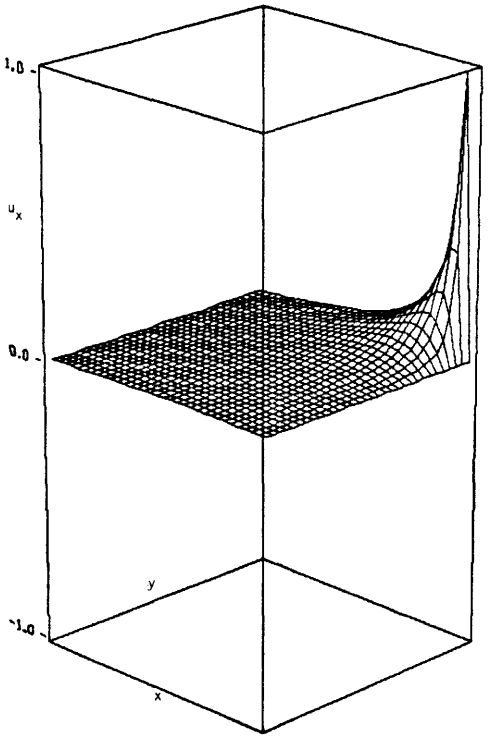

FIG. 2. x-velocity distribution computed using first-order elements on a square grid having 32 elements on a side.

conditioned. Ewing and Koebbe [6] describe an application of preconditioned conjugate-gradient techniques to overcome the poor conditioning and speed the iterative solution of the linear system.

Figure 1 shows the pressure or head distribution over Ω computed using the lowest degree (first-order) elements on a square grid having 32 elements on a side. Figure 2 shows the corresponding field for the x-component of water velocity. These solutions exhibit a logarithmic drawdown in head near the producing well together with a concomitant pole in u_x. Figures 3 and 4 shows the head and x-velocity distributions computed for the same problem using the second-order trial space on a square grid having 16 elements on a side. Since the second-order method requires approximately twice as many degrees of freedom per element in each coordinate direction, the number of nodal unknowns needed to generate Figures 3 and 4 is comparable to the number needed in Figures 1 and 2. The two pairs of plots are quite similar, as one might expect considering the parity in computational effort between the two cases.

The method also performs well in problems with heterogeneous medium properties. Figure 5, for example, shows the x-velocity distribution that results

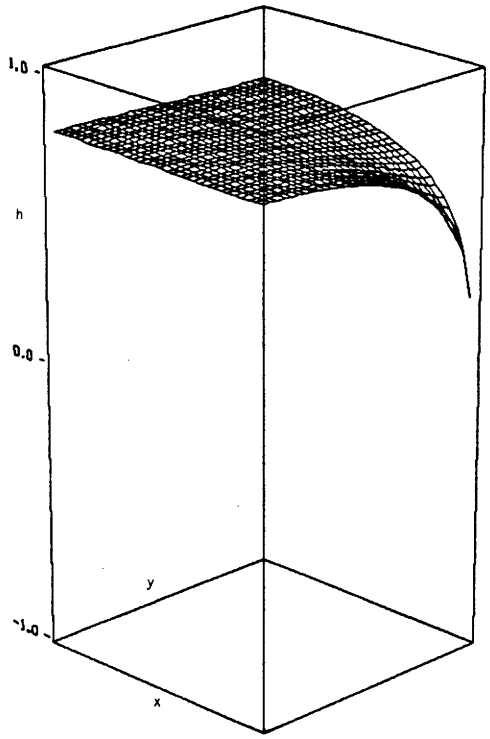

FIG. 3. Head distribution computed using second-order elements on a square grid having 16 elements on a side.

when we use first-order elements and impose a nonuniform transmissivity having the form

$$T(x,y) = \begin{cases} 1, & y \geq x \\ 0.01, & y < x. \end{cases} \tag{7}$$

Thus T suffers a jump discontinuity along a line running diagonally through Ω into the wellbore. The x-velocity away from the wellbore therefore remains small for $y < x$ but increases rapidly toward the wellbore near the edge of the domain where $y = 1$.

Figure 6 illustrates the x-velocity that results from using second-order elements and a discontinuous aquitard head h_a of the form

$$h_a(x,y) = \begin{cases} 1.0, & x \leq 0.5 \\ 0.01, & x > 0.5. \end{cases} \tag{8}$$

The contour plot of u_x in Figure 7 shows more clearly the radial flow dominant near the well and the "ridgeline" pattern prevailing away from the well. While

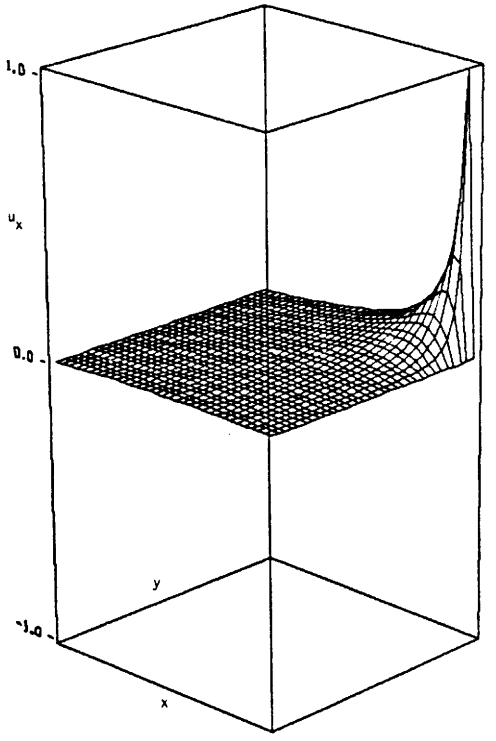

FIG. 4. x-velocity distribution computed using second-order elements on a square grid having 16 elements on a side.

heterogeneities of the forms given in Eqs. (7) and (8) are highly idealized, they provide simple yet relatively strenuous tests of the mixed method's ability to model problems with nonuniform material properties.

V. CONCLUSIONS

We have seen that the mixed finite-element method is an attractive approach for solving groundwater flow equations, especially in contaminant transport problems where accurate water velocities are paramount. The method gives velocities that have the same order of accuracy as heads, affording rapid error reductions on grid refinement compared with the traditional finite-element approach. Further advantages accrue through the explicit incorporation of source and sink singularities in the trial functions for velocity. Here the improvement over traditional discrete methods is more dramatic: the mixed method with subtracted singularities converges at wells, while traditional schemes do not.

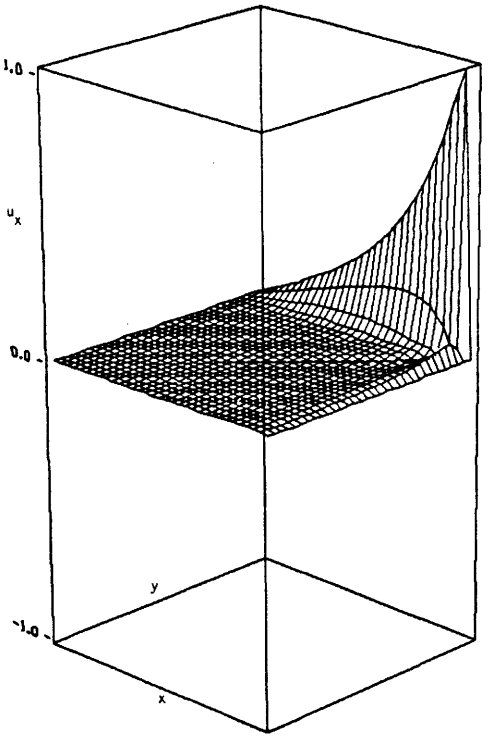

FIG. 5. x-velocity distribution computed using first-order elements on a problem in which the transmissivity has a discontinuity along $y = x$.

Finally, the mixed method gives good numerical results even in problems with rather severe heterogeneities in medium properties.

This research is supported in part by Contract No. DAAG29-84-K-002 from the Army Research Office, by Grant No. CEE-8404266 from the National Science Foundation, and by a grant from the Wyoming Water Research Center.

References

[1] G. Segol and G. F. Pinder, "Transient simulation of saltwater intrusion in southeastern Florida." *Water Res. Research* **23**:65–70 (1976).

[2] R. J. Charbeneau and R. L. Street, "Modeling groundwater flow fields containing point singularities: a technique for singularity removal." *Water Res. Research* **15**:583–599 (1979).

[3] P. A. Raviart and J. M. Thomas, *A Mixed Finite Element Method for Second-Order Elliptic Problems: Mathematical Aspects of the Finite Element Method*. Springer-Verlag, Heidelberg, 1977.

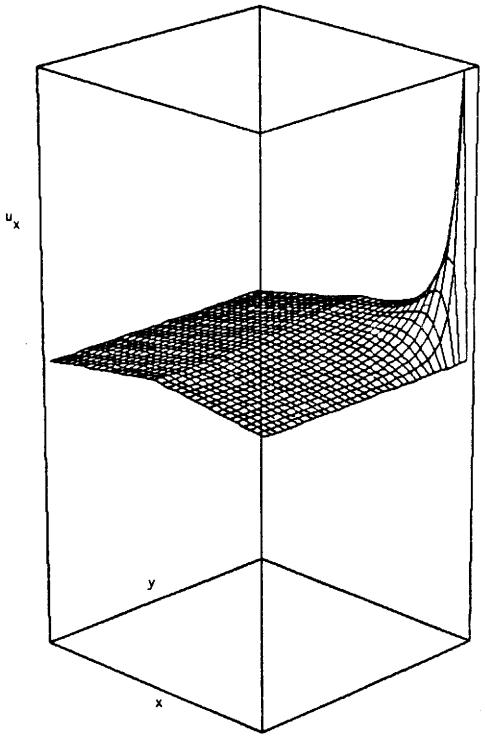

FIG. 6. x-velocity distribution computed using second-order elements on a problem where the acquitard head h_a has a discontinuity along $x = 0.5$.

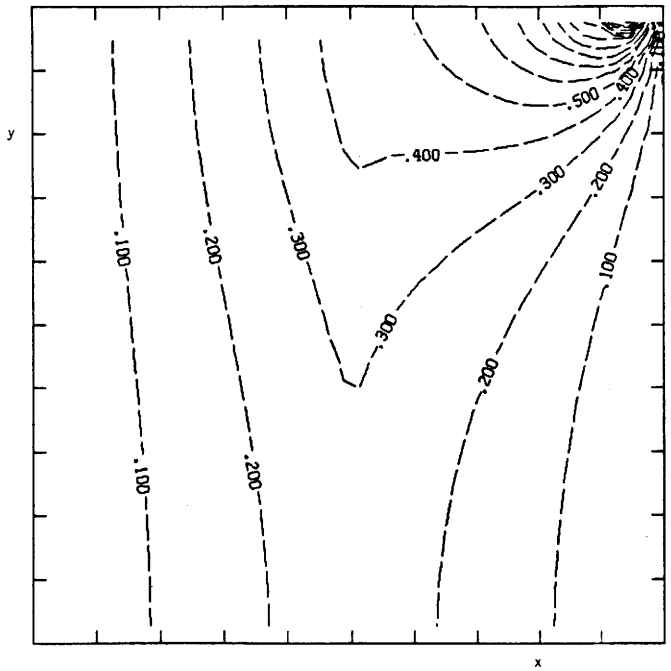

FIG. 7. Contour plot of x-velocities shown in Figure 6.

[4] P. M. Prenter, *Splines and Variational Methods*. John Wiley & Sons, New York, 1975.

[5] J. Douglas, R. E. Ewing, and M. F. Wheeler, "The approximation of the pressure by a mixed method in the simulation of miscible displacement." *RAIRO Analyse Numerique* **17**:17–34 (1983).

[6] R. E. Ewing and J. V. Koebbe, "Mixed finite element methods for groundwater flow and contaminant transport," in *Proceedings of the Fifth IMACS International Symposium on Computer Methods for Partial Differential Equations*, Bethlehem, Pennsylvania, June 19–21, 1984, p. 106–113.

A Finite Element Collocation Method for Variably Saturated Flows in Porous Media

Myron B. Allen and Carolyn Murphy
Department of Mathematics, University of Wyoming, Laramie, Wyoming 82071 U.S.A.

One common formulation of Richard's equation for variably saturated flows in porous media treats pressure head as the principal unknown and moisture content as a constitutive variable. Numerical approximations to this "head-based" formulation often exhibit mass-balance errors arising from inaccuracies in the temporal discretization. This article presents a finite-element collocation scheme using a mass-conserving formulation. The article also proposes a computable index of global mass balance.

I. INTRODUCTION

The ability to model water flows in variably saturated soils is importnt to several problems in water resources engineering, among them the prediction of water table contamination from sources at or near the earth's surface. The partial differential equations governing such flows are difficult to solve owing to their nonlinearity, and it is generally necessary to use numerical techniques such as finite differences or finite elements to produce approximate solutions. However, even with numerical schemes there remain difficulties, notably the conservation of mass. Discrete analogs to some formulations of variably saturated flow fail to produce approximate solutions that respect the global mass balance law, even though the original differential equation is derived from this law. We introduce an approach to this problem using finite element collocation. The key to the success of this approach is the choice of a formulation of the flow equation whose temporal discretization is a differential form of the global mass balance for each time interval. Thus the only mass-balance errors in the numerical solution are those arising from the use of a nonzero convergence criterion in the iterations used to advance between time levels. The use of finite element collocation to discretize the space derivatives guarantees approximations of high-order spatial accuracy while obviating the costs of integration and formal matrix assembly associated with other finite-element techniques.

II. SETTING OF THE PROBLEM

The equation governing one-dimensional water flows in variably saturated soils has the form [1]

$$\frac{\partial}{\partial x}\left[K(h)\frac{\partial h}{\partial x} - K(h)\right] = C(h)\frac{\partial h}{\partial t}. \tag{1}$$

Numerical Methods for Partial Differential Equations, 3, 229–239 (1985)
 CCC 0749-159X/85/030229-11$04.00

Here h stands for pressure head, measured in meters; K represents the hydraulic conductivity of the soil, measured in meters/second; and C is called the specific moisture capacity of the soil, measured in meters^{-1}. The specific moisture capacity C accounts for the variation in the soil's dimensionless moisture content θ in response to changes in pressure head; specifically, $C = d\theta/dh$. In practice one uses experimental data to quantify the constitutive relationships $\theta(h)$ and $K(h)$.

Equation (1) casts the pressure head h as the dependent variable, leaving θ and K as nonlinear coefficients. As an alternative to this *h-based* formulation, we can pose the problem in terms of the moisture content θ as follows:

$$\frac{\partial}{\partial x}\left[D(\theta)\frac{\partial \theta}{\partial x} - K(\theta)\right] = \frac{\partial \theta}{\partial t}. \tag{2}$$

Here K appears as a function of θ, and $D = K\,dh/d\theta$ is the soil's hydraulic diffusivity, measured in meters^2/second. This is the *θ-based* formulation. Although Eq. (1) and (2) are equivalent by the chain rule, modelers prefer the h-based formulation in most practical problems, where spatial variations in soil properties and sharp gradients in θ can lead to poor behavior in the θ-based formulation [2].

As a model problem we shall solve the initial-boundary value problem for variably saturated flow posed by Warrick et al. [3]. Let a soil column [0, 1.25] have an initial water saturation described by

$$\theta(x,0) = \begin{cases} 0.15 + x/12, & 0 < x \le 0.6 \\ 0.2, & 0.6 < x < 1.25 \end{cases}, \tag{3a}$$

where x stands for depth in meters from the surface. Assume that the pressure head at the surface is atmospheric, that is

$$h(0,t) = -0.14495\,, \tag{3b}$$

and that the pressure head gradient vanishes at the outflow,

$$\frac{\partial h}{\partial x}(1.25,t) = 0\,. \tag{3c}$$

For the constitutive relationships $K(h)$ and $C(h)$ we use the functions measured by Warrick et al. [3], which in SI units are

$$K(h) = \begin{cases} 1.157 \times 10^{-7}(19.34 \times 10^5|100h|^{-3.4095}), & h \le -0.29484 \\ 1.157 \times 10^{-7}(516.8|100h|^{-0.97814}), & h > -0.29484 \end{cases}$$

$$\theta(h) = \begin{cases} 0.6829 - 0.09524\ \ln|100h|, & h \le -0.29484 \\ 0.4531 - 0.02732\ \ln|100h|, & h > -0.29484 \end{cases}$$

Thus the prescribed atmospheric pressure head at $x = 0$ corresponds approximately to a moisture content $\theta(0,t) = 0.38$.

The numerical solution of this problem using finite elements is not entirely straightforward. The nonlinearities in the h-based flow equation can lead to poor global mass balance and thus to unacceptable numerical approximations.

Van Genuchten [4] demonstrates this difficulty quite clearly by comparing several Galerkin approximations to Eq. (1) with the auxiliary data (3). Figure 1 shows some of his results. Notice in particular that the wetting front in the solution using a Hermite cubic trial function with two-point Gauss quadrature on each element (marked "2GP, 3LP" in Fig. 1) lags the correct wetting front by a significant distance. This poor approximation apparently bodes ill for finite-element collocation on Hermite cubic spaces, since there is a direct algebraic correspondence between such collocation schemes and Galerkin's method on Hermite cubics with two-point quadrature [5]. We shall examine the difficulties with collocation in the next section.

Recognizing the importance of mass-balance errors, Milly [6] examines the effect of temporal discretization on the accuracy of the accumulation term $C\,\partial h/\partial t$ in Eq. (1). He proposes a global mass-balance criterion of the form

$$\frac{1}{\Delta t}\int_{\Omega}(\theta^{n+1}-\theta^{n})\,dx = \int_{\Omega}\left(K\frac{\partial h}{\partial x}-K\right)dx \tag{4}$$

where $\Omega = [0, 1.25]$ is the spatial domain of the flow, Δt is the discrete time interval, and $n, n+1$ signify successive time levels. Milly attributes the mass balance errors plaguing various discrete analogs to failures to evaluate the coefficient $C(h)$ in a way that reflects the average behavior of the soil over each time interval. He advances an iterative scheme for approximating $C(h)$ that leads to arbitrarily good mass balance in the sense of Eq. (4), given a sufficient number of iterations.

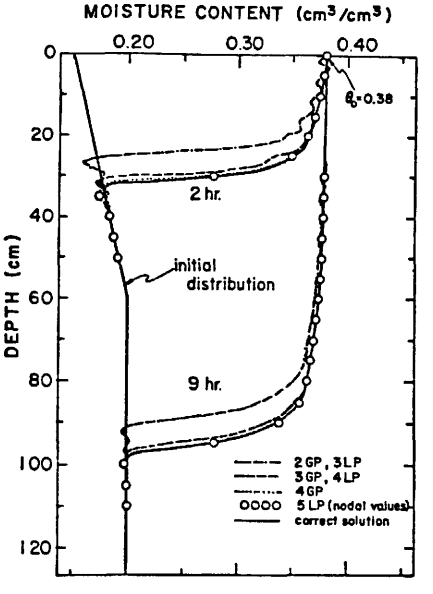

FIG. 1. Numerical moisture-content profiles computed from the h-based formulation using the Galerkin method on Hermite cubics with various quadrature schemes (from Reference [4]).

We propose a finite element collocation scheme for variably saturated flows that conserves mass by a somewhat simpler device. Before describing this scheme, however, let us examine in detail the difficulties that arise in the straightforward application of collocation approximation to Eq. (1).

III. COLLOCATION USING THE *h*-BASED FORMULATION

To construct a collocation approximation to Eq. (1), we can follow an approach that is analogous to Van Genuchten's [4]. Let us begin by discretizing Eq. (1) in time using an implicit Euler difference scheme:

$$K^{n+1}\frac{\partial^2 h^{n+1}}{\partial x^2} + \frac{\partial K^{n+1}}{\partial x}\frac{\partial h^{n+1}}{\partial x} - \frac{\partial K^{n+1}}{\partial x} - C^{n+1}\frac{h^{n+1} - h^n}{\Delta t} = 0 \qquad (5)$$

Here, as in Eq. (4), the superscripts $n, n+1$ indicate successive time levels and Δt is the time interval between them. This approximation imposes a truncation error that is $O(\Delta t)$.

Since the coefficients K^{n+1}, C^{n+1} depend on the unknown h^{n+1}, it is necessary to use an iterative method to advance Eq. (5) from one time level to the next. We can effect a Newton-like iteration scheme as follows:

$$K^{n+1,m}\frac{\partial^2}{\partial x^2}(h^{n+1,m} + \delta h) + \frac{\partial K^{n+1,m}}{\partial x}\frac{\partial}{\partial x}(h^{n+1,m} + \delta h) - \frac{\partial K^{n+1,m}}{\partial x} - \frac{C^{n+1,m}}{\Delta t}(h^{n+1,m} + \delta h - h^n) = 0. \qquad (6)$$

In this scheme, the variable $h^{n+1,m}$ signifies the known approximation to the new pressure head h^{n+1} at the m-th iterative level; $K^{n+1,m}$ and $C^{n+1,m}$ stand for $K(h^{n+1,m})$ and $C(h^{n+1,m})$, respectively, and the unknown δh represents an increment that must be added to $h^{n+1,m}$ to produce an improved approximation $h^{n+1,m+1}$. At each time level the iterative scheme begins with the initial value $h^{n+1,0} = h^n$ and ends by assigning $h^{n+1} = h^{n+1,m+1}$ when either the increment δh or the residual

$$K^{n+1,m+1}\frac{\partial^2 h^{n+1,m+1}}{\partial x^2} + \frac{\partial K^{n+1,m+1}}{\partial x}\frac{\partial h^{n+1,m+1}}{\partial x} - \frac{\partial K^{n+1,m+1}}{\partial x} - \frac{C^{n+1,m+1}}{\Delta t}(h^{n+1,m+1} - h^n) = R^{n+1,m+1}$$

is sufficiently small.

To construct a collocation analog of this discrete-time scheme, let us approximate the unknown δh by a piecewise Hermite cubic finite element representation:

$$\delta\hat{h}(x) = \sum_{i=1}^{N}[\delta_i H_{0,i}(x) + \delta_i' H_{1,i}(x)]. \qquad (7)$$

In this equation $H_{0,i}(x)$ and $h_{1,i}(x)$ are elements of the Hermite cubic basis for C^1 polynomial interpolation on a partition of Ω, and δ_i and δ_i' stand for the

values of $\delta\hat{h}$ and $\partial(\delta\hat{h})/\partial x$, respectively, at node i of the partition [7]. Once we have solved for the coefficients $\{\delta_i, \delta_i'\}_{i=1}^N$ in Eq. (7), we can compute a new iterative approximation to the pressure head in the obvious way:

$$\hat{h}^{n+1,m+1}(x) = \sum_{i=1}^{N} [(h_i^{n+1,m} + \delta_i)H_{0,i}(x) + (h_i'^{n+1,m} + \delta_i')H_{1,i}(x)].$$

There are several ways to represent the coefficients K and C. One approach that seems to produce well-behaved approximations is simply to interpolate between the nodal values $K(h_i)$ or $C(h_i)$. If we use linear interpolation, then the representations become

$$\hat{K}(x) = \sum_{i=1}^{N} K(h_i)L_i(x)$$

$$\frac{\partial \hat{K}}{\partial x}(x) = \sum_{i=1}^{N} K(h_i)\frac{dL_i}{dx}(x)$$

$$\hat{C}(x) = \sum_{i=1}^{N} C(h_i)L_i(x)$$

where $\{L_i\}_{i=1}^N$ is the Lagrange basis for C^0 linear interpolation on the partition of Ω [7].

If we substitute all of these finite element approximations into the discrete-time equation (6), there remains the task of solving for the $2N$ unknowns $\{\delta_i, \delta_i'\}_{i=1}^N$. Since the boundary conditions translate to $h_0 = h(0,t)$ and $h_N' = \partial h/\partial x(1.25, t)$, we know that $\delta_1 = \delta_N' = 0$. To solve for the remaining $2N - 2$ unknowns, we collocate the finite-element approximation to Eq. (6). That is, we force

$$\hat{K}^{n+1,m}(\bar{x}_k)\frac{\partial^2}{\partial x^2}[\hat{h}^{n+1,m}(\bar{x}_k) + \delta\hat{h}(\bar{x}_k)] + \frac{\partial \hat{K}^{n+1,m}}{\partial x}(\bar{x}_k)\frac{\partial}{\partial x}[\hat{h}^{n+1,m}(\bar{x}_k) + \delta\hat{h}(\bar{x}_k)]$$
$$- \frac{\partial \hat{K}^{n+1,m}}{\partial x}(\bar{x}_k) - \frac{\hat{C}^{n+1,m}(\bar{x}_k)}{\Delta t}[\hat{h}^{n+1,m}(\bar{x}_k) + \delta\hat{h}(\bar{x}_k) - \hat{h}^n(\bar{x}_k)] = 0$$

at $2N - 2$ values $\bar{x}_k \in \Omega$. Douglas and Dupont [5] show that, if the finite element partition of Ω is uniform, then the optimal collocation points are the Gauss points

$$\bar{x}_k = x_i + \left(\frac{1}{2} \pm \frac{1}{\sqrt{3}}\right)\Delta x, \qquad i = 1, \ldots, N - 1$$

where Δx is the mesh of the partition. This scheme produces approximate solutions with a spatial error that is $O(\Delta x^4)$.

Figure 2 shows the numerical pressure head profiles at two and nine hours using this scheme with $\Delta x = 0.05$, $\Delta t = 240$, and an iterative convergence criterion requiring that the maximum residual $\max\{R^{n+1,m+1}(\bar{x}_k)\}_{k=1}^{2N-2}$ be less than 5.0×10^{-6}/s. Figure 3 depicts the corresponding moisture content distributions at two and nine hours, computed from the constitutive relationship $\theta(h)$. Observe that the wetting front at two hours lies at approximately $x =$

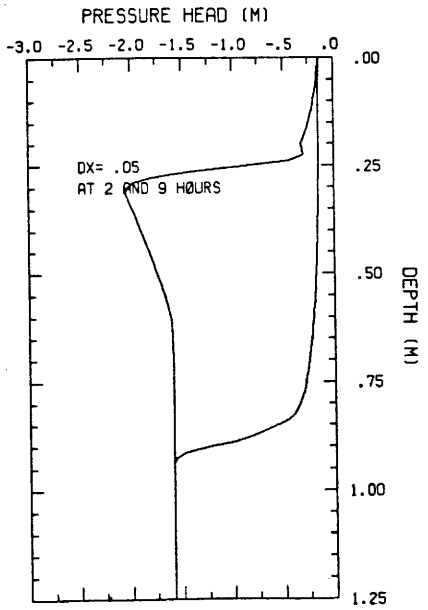

FIG. 2. Numerical pressure-head profiles computed from the h-based formulation using finite-element collocation.

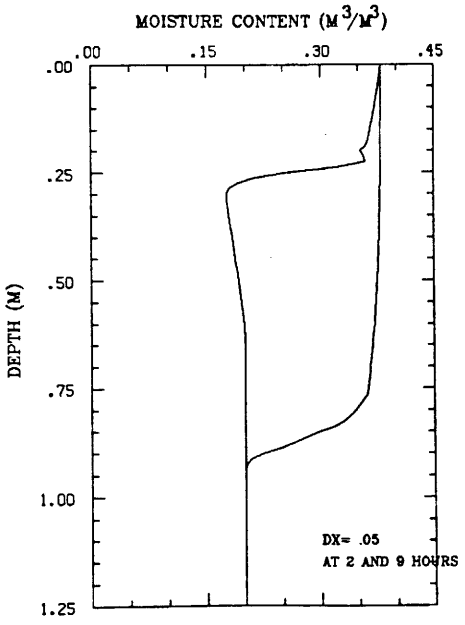

FIG. 3. Numerical moisture-content profiles computed from the h-based formulation using finite-element collocation.

0.24, which is very close to that in Van Genuchten's solution in Figure 1 using Hermite cubics with two-point Gauss quadrature on each element. Thus the collocation method outlined above exhibits mass-balance errors similar to those of the Galerkin method with two-point quadrature, as we expected on the strength of the theoretical correspondence between the two methods.

IV. AN ALTERNATIVE COLLOCATION SCHEME

One can generate a mass-conserving collocation scheme by discretizing a differential equation derived directly from the global mass balance, Eq. (4), in the limit $\Delta t \to 0$. This yields a governing equation of the form

$$\frac{\partial}{\partial x}\left[K(h)\frac{\partial h}{\partial x} - K(h)\right] = \frac{\partial \theta}{\partial t}(h) \tag{8}$$

provided the integrands in the global equation are continuous. Since the left side of this equation is exactly the same as the left side of the h-based formulation (Eq. (1)), while the right side is simliar to that appearing in the θ-based formulation (Eq. (2)), we might call Eq. (8) a *hybrid* formulation.

Let us discretize Eq. (8) in a fashion analogous to our treatment of Eq. (1). First, replace the time derivative by an implicit difference scheme having truncation error $O(\Delta t)$:

$$K^{n+1}\frac{\partial^2 h^{n+1}}{\partial x^2} + \frac{\partial K^{n+1}}{\partial x}\frac{\partial h^{n+1}}{\partial x} - \frac{\partial K^{n+1}}{\partial x} - \frac{\theta^{n+1} - \theta^n}{\Delta t} = 0.$$

Here θ^{n+1}, θ^n stand for $\theta(h^{n+1}), \theta(h^n)$, respectively. Next, to accommodate the nonlinearities in K and θ, assume an iterative method of the form

$$K^{n+1,m}\frac{\partial^2}{\partial x^2}(h^{n+1,m} + \delta h) + \frac{\partial K^{n+1,m}}{\partial x}\frac{\partial}{\partial x}(h^{n+1,m} + \delta h) - \frac{\partial K^{n+1,m}}{\partial x} - \frac{1}{\Delta t}\left(\theta^{n+1,m} + \frac{d\theta^{n+1,m}}{dh}\,\delta h - \theta^n\right) = 0 \tag{9}$$

for updating the implicit coefficients from one time level to the next. Finally, project the unknowns δh to Hermite cubic subspaces and the coefficients K and $d\theta/dh = C$ to Lagrange linear subspaces as in Section III above.

There remains the question of a finite-element representation of θ. We have found through numerical experiments that a Hermite cubic expansion of θ gives superior results. To effect such a representation, we use the chain rule to compute the nodal gradients in θ:

$$\hat{\theta}(x) = \sum_{i=1}^{n}\left[\theta(h_i)H_{0,i}(x) + \frac{d\theta}{dh}(h_i)h_i' H_{1,i}(x)\right].$$

Then, using the finite element spatial discretizations together with the iterative time-stepping scheme in Eq. (9), we collocate at the $2N - 2$ Gauss points as before to advance the iterations from one time level to the next.

Figure 4 shows the pressure head profiles at two and nine hours using the new scheme with the same $\Delta x, \Delta t$, and convergence criteria as used in producing Figure 2. Figure 5 displays the corresponding profiles for moisture content. Notice that the wetting front at two hours in this plot falls at about $x = 0.30$, which agrees with the location of the wetting front that Van Genuchten identifies as the correct solution in Figure 1. Finite element collocation applied to the hybrid formulation in Eq. (8) apparently furnishes approximate solutions that more closely respect the balance of mass.

It is useful in checking a coded algorithm for this type of problem to have a computable technique for checking global mass balance. For the collocation method presented in this section we can readily derive such a technique. We wish to verify at any time level that Eq. (4) holds to a good approximation. It happens that each of the integrals in this equation can be rapidly computed using information that is already available from the collocation solution at each time step. Consider first the flux integral on the right side of Eq. (4). Since $\hat{h} \in C^1(\Omega)$ and $\hat{K} \in C^0(\Omega)$, the differential flux $(\hat{K}(\partial\hat{h}/\partial x) - \hat{K}) \in C^0(\Omega)$ and hence the fundamental theorem of calculus yields

$$\int_\Omega \frac{\partial}{\partial x}\left(\hat{K}\frac{\partial \hat{h}}{\partial x} - \hat{K}\right) dx = K(h_N)(h'_N - 1) - K(h_1)(h'_1 - 1).$$

Now look at the accumulation integral on the left side of Eq. (4). This can be written as

$$\frac{1}{\Delta t}\int_\Omega (\hat{\theta}^{n+1} - \hat{\theta}^n)\, dx = \frac{1}{\Delta t}\sum_{i=1}^{N-1}\int_{x_i}^{x_{i+1}} (\hat{\theta}^{n+1} - \hat{\theta}^n)\, dx$$

But the integrand in each term in this decomposition is a cubic function of x, and so two-point Gauss quadrature suffices for the exact calculation of these integrals. Since the Gauss points are precisely the collocation points, the computation of the accumulation integral reduces to a sum of previously computed values:

$$\frac{1}{\Delta t}\int_\Omega (\hat{\theta}^{n+1} - \hat{\theta}^n)\, dx = \frac{\Delta x}{2\Delta t}\sum_{k=1}^{2N-2} (\hat{\theta}^{n+1} - \hat{\theta}^n)\Big|_{\bar{x}_k}$$

where each $\bar{x}_k$ is a collocation point.

Now we can define a mass balance index as the ratio of the accumulation integral to the flux integral:

$$I_{MB} = \frac{1}{K(h_n)(h'_n - 1) - K(h_1)(h'_1 - 1)}\,\frac{\Delta x}{2\Delta t}\sum_{k=1}^{2N-2} (\hat{\theta}^{n+1} - \hat{\theta}^n)\Big|_{\bar{x}_k}$$

For a perfectly conservative numerical scheme $I_{MB} = 1$. For real schemes, however, the necessity of stopping the time-stepping procedure after a finite number of iterations will generally prohibit an exact mass balance. Figure 6 exhibits ranges of values of I_{MB} computed from the hybrid collocation scheme using several spatial meshes Δx. The plots show that the new formulation gives

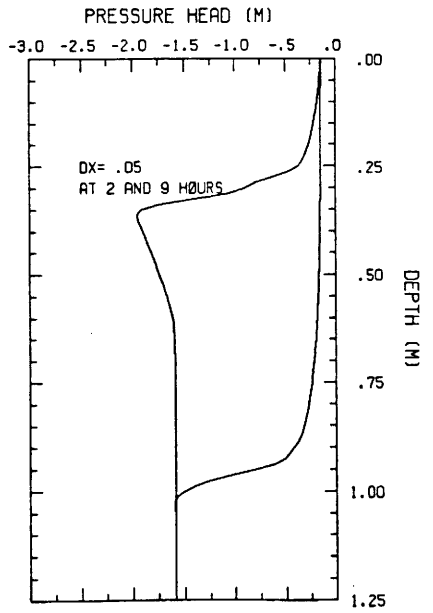

FIG. 4. Numerical pressure-head profiles computed from the hybrid formulation using finite-element collocation.

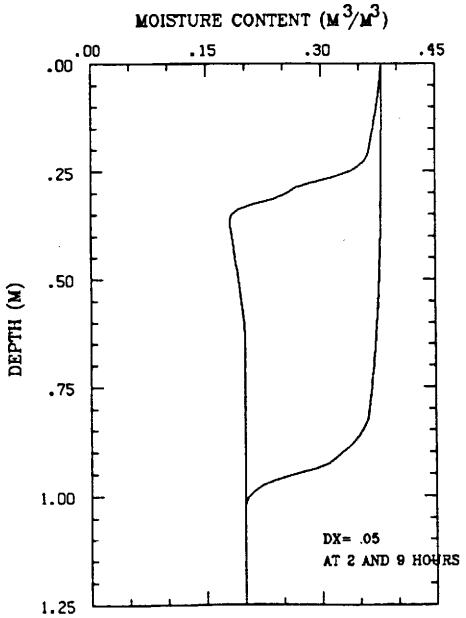

FIG. 5. Numerical moisture-content profiles computed from the hybrid formulation using finite-element collocation.

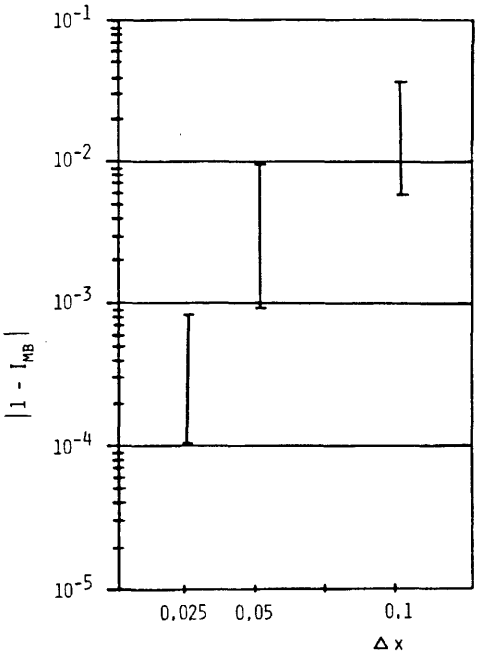

FIG. 6. Mass-balance error $|1 - I_{MB}|$ in the hybrid formulation using finite-element collocation with various spatial meshes.

reasonable global mass balances that improve upon refinement of the spatial partition. These results corroborate the good agreement between the profiles shown in Figure 5 and Van Genuchten's "correct solutions" plotted in Figure 1.

V. CONCLUSIONS

The collocation scheme presented here gives numerical solutions to the variably saturated flow equation that enjoy high-order spatial accuracy and stand in quantifiable agreement with the principle of global mass balance. The choice of a hybrid formulation incorporating features of both the h-based and θ-based flow equations proves instrumental in forcing mass conservation, since this formulation is directly descended from the global mass balance criterion. The direct projection of the accumulation term $\partial\theta/\partial t$ onto Hermite cubic interpolation polynomials avoids the delicate problem of choosing representative values for the time-varying coefficient that arises on applying the chain rule to this term. When one imposes an iterative time-stepping scheme upon this hybrid form in conjunction with finite element collocation, the individual collocation equations drive the mass-balance error at each collocation point toward zero as the iterations proceed.

The authors thank the Wyoming Water Research Center and the National Science Foundation (grant number CEE 8404266) for their support of this work.

References

[1] L. A. Richards, "Capillary conduction of liquids through porous media," *Physics*, **1**, 318–333 (1931).

[2] P. S. Huyakorn, and G. F. Pinder, *Computational Methods in Subsurface Flow*, Academic Press, New York, 1983.

[3] A. W. Warrick, J. W. Biggar, and D. R. Nielsen, "Simultaneous solute and water transfer for unsaturated soil," *Water Resourc. Res.*, **7**:5, 1216–1225 (1971).

[4] M. Th. Van Genuchten, "A comparison of numerical solutions of the one-dimensional unsaturated-saturated flow and mass transport equations," *Adv. Water Resources*, **5**, 47–55 (1982).

[5] J. Douglas, and P. Dupont, "A finte-element collocation method for quasilinear parabolic problems," *Math. Comp.*, **27**:121, 17–28 (1973).

[6] P. C. D. Milly, "A mass-conservative procedure for timestepping in models of unsaturated flow," in *Finite Elements in Water Resources, Proceedings of the Fifth International Conference*, J. P. Laible et al, Eds., Springer-Verlag, London, 1984, 103–112.

[7] P. M. Prenter, *Splines and Variational Methods*, John Wiley, New York, 1975.

A COLLOCATION MODEL OF TWO-DIMENSIONAL UNSATURATED FLOW

Carolyn L. Murphy* and Myron B. Allen

University of Wyoming, Laramie, Wyoming 82071, U.S.A.
*now at Edwards Air Force Base, California 93532, U.S.A.

ABSTRACT

This paper introduces a numerical scheme for solving the equation governing two-dimensional flow in a variably saturated porous medium. The scheme uses a mass-conserving time-stepping method together with a computationally efficient collocation formulation of the spatial derivatives. A Newton-like iteration gives a temporally stable implicit scheme. The paper examines a sample problem involving subsurface irrigation in the unsaturated zone.

INTRODUCTION

This paper presents a new numerical scheme for simulating variably saturated flows in two space dimensions. The scheme, based on finite-element collocation, is an extension of a one-dimensional formulation presented earlier (Allen and Murphy, 1985). In that paper we discussed some of the computational advantages of collocation and examined the issue of mass conservation that arises in many numerical approaches to variably saturated flows.

The equation we solve is

$$\nabla \cdot [K(\nabla h - \mathbf{e}_z)] - \frac{\partial \theta}{\partial t} = 0 \qquad (1)$$

where, in two dimensions, $\nabla \equiv (\partial/\partial x, \partial/\partial z)$ with z measuring distance above some datum, and $\mathbf{e}_z$ is the unit vector in the z-direction. In this equation, $h(x,z,t)$ is the pressure head (m), K stands for the soil's hydraulic conductivity (m/s), and θ signifies the moisture content of the soil (dimensionless). Typically, the physics of variably saturated flows dictate that K and θ vary with h, and the relationships $K(h)$ and $\theta(h)$ make Equation (1) nonlinear. Murphy (1985) gives a derivation of this equation.

In the following section we discuss a finite-element formulation of Equation (1) incorporating iterative time-stepping to accommodate the nonlinearity. Then we describe a collocation scheme for obtaining algebraic analogs to the differential equation and review an application to a sample problem.

FINITE-ELEMENT FORMULATION

Our first task in numerically solving two-dimensional unsaturated flows is to discretize the governing equation (1). To do this, we first expand the spatial derivatives using the product rule and use a backward Euler difference scheme to approximate the time derivative on a uniform temporal grid $0 < \Delta t < 2\Delta t < \cdots < n\Delta t < \cdots$:

$$\frac{\partial K^{n+1}}{\partial x}\frac{\partial h^{n+1}}{\partial x} + \frac{\partial K^{n+1}}{\partial z}\frac{\partial h^{n+1}}{\partial z} + K^{n+1}\left(\frac{\partial^2 h^{n+1}}{\partial x^2} + \frac{\partial^2 h^{n+1}}{\partial z^2}\right) - \frac{\partial K^{n+1}}{\partial z} - \frac{\theta^{n+1} - \theta^n}{\Delta t} = 0 \tag{2}$$

This equation furnishes an implicit time-stepping scheme for the approximate pressure head $h^n(x,z) \approx h(x,z,n\Delta t)$, which we regard as the principal unknown.

To solve Equation (2) we must accommodate the dependence of the nonlinear functions $K^{n+1} = K(h^{n+1})$, $\theta^{n+1} = \theta(h^{n+1})$ on unknown values h^{n+1} of the pressure head. To do this, we use an iterative method to advance between time levels, solving for iterative increments $\delta h = h^{n+1,m+1} - h^{n+1,m}$ to progress from the known iteration m to the next unknown iteration $m+1$. This scheme allows us to lag the nonlinear coefficients by an iteration in solving for δh:

$$\left[-\frac{1}{\Delta t}\frac{d\theta^{n+1,m}}{dh} + K^{n+1,m}\left(\frac{\partial^2}{\partial x^2} + \frac{\partial^2}{\partial z^2}\right) + \frac{\partial K^{n+1,m}}{\partial x}\frac{\partial}{\partial x} + \frac{\partial K^{n+1,m}}{\partial z}\frac{\partial}{\partial z}\right]\delta h = -R^{n+1,m} \tag{3}$$

where the expression

$$R^{n+1,m} = -\frac{1}{\Delta t}(\theta^{n+1,m} - \theta^n) + K^{n+1,m}\left(\frac{\partial^2 h^{n+1,m}}{\partial x^2} + \frac{\partial^2 h^{n+1,m}}{\partial z^2}\right) + \frac{\partial K^{n+1,m}}{\partial x}\frac{\partial h^{n+1,m}}{\partial x} + \frac{\partial K^{n+1,m}}{\partial z}\left(\frac{\partial h^{n+1,m}}{\partial z} - 1\right)$$

plays a role analogous to that of the residual in standard Newton-Raphson schemes. In executing the iterative method, we begin each time step by setting $h^{n+1,0} = h^n$ and stop the iteration, setting

$h^{n+1,m+1} = h^{n+1}$, when $\|R^{n+1,m}\|_\infty < \epsilon$ for some prescribed tolerance $\epsilon > 0$.

The formulation leading to Equation (3) differs from standard head-based formulations, which typically use the chain rule to expand the accumulation term as $\partial\theta/\partial t = (d\theta/dh)\partial h/\partial t$. Such an expansion calls for the evaluation of the specific moisture capacity $d\theta/dh$ at some time level in the interval $[n\Delta t, (n+1)\Delta t]$ in the temporally discrete approximation. There seems to be no simple (noniterative) way of choosing this time level to guarantee global mass conservation in the sense

$$\oint_{\partial\Omega} (K^{n+1}\nabla h^{n+1} - K^{n+1}\mathbf{e}_z)\cdot\mathbf{n}\,d\mathbf{x} = \frac{1}{\Delta t}\int_\Omega (\theta^{n+1} - \theta^n)\,d\mathbf{x}$$

where Ω represents the spatial domain of the problem and $\mathbf{n}$ is the unit outward normal vector to the boundary $\partial\Omega$. As discussed in (Allen and Murphy, 1985), discretizing the flow equation as in Equation (3) avoids this difficulty, enforcing global mass conservation to within the iterative convergence criterion at each time step.

To discretize Equation (3) in space, we project the spatially varying quantities $h^{n,m}(x,z)$, $\theta^{n,m}(x,z)$, $K^{n,m}(x,z)$ and $d\theta^{n,m}/dh$ onto finite-element subspaces. In particular, we select for the principal unknown $h^{n,m}(x,z)$ trial spaces spanned by tensor products of piecewise cubic Hermite interpolating functions in the x- and z-directions. Thus, for a rectangular region Ω, we adopt a two-dimensional grid $\{x_0 < x_1 < \cdots < x_M\} \times \{z_0 < z_1 < \cdots < z_N\}$ with nodes (denoted $\mathbf{x}_i$) at the points (x_j, z_k) and, for $\mathbf{x} \in \Omega$, set

$$\delta h(\mathbf{x}) \approx \delta\hat{h}(\mathbf{x}) = \sum_{i=1}^{N}\Big[\delta_i\,\varphi_{00i}(\mathbf{x}) + \delta_i^{(x)}\,\varphi_{10i}(\mathbf{x}) + \delta_i^{(z)}\,\varphi_{01i}(\mathbf{x}) + \delta_i^{(xz)}\,\varphi_{11i}(\mathbf{x})\Big] \qquad (4)$$

Here δ_i, $\delta_i^{(x)}$, $\delta_i^{(z)}$, and $\delta_i^{(xz)}$ represent approximate values of δh, $\partial(\delta h)/\partial x$, $\partial(\delta h)/\partial z$, $\partial^2(\delta h)/\partial x\,\partial z$, respectively, at the node $\mathbf{x}_i$. The basis functions φ_{00i}, φ_{10i}, φ_{01i}, and φ_{11i} are tensor products of the one-dimensional Hermite basis functions (Prenter, 1976, Chapter 3): $\varphi_{pqi}(\mathbf{x}) = H_{pi}(x)\,H_{qi}(z)$, where H_{0i} is the one-dimensional basis function associated with the nodal value of the interpolate, and H_{1i} is associated with its nodal slope.

The projection (4) furnishes a continuously differentiable interpolation scheme for the iterative increment $\delta\hat{h}$ in which the nodal parameters are unknown except where given by boundary data. The head h

inherits this interpolation scheme according to the updating rule

$$h^{n+1,m+1}(\mathbf{x}) \approx \hat{h}^{n+1,m+1}(\mathbf{x})$$
$$= \sum_{i=1}^{N} \Big\{ \left[(h_i)^{n+1,m} + \delta_i\right] \varphi_{00i}(\mathbf{x}) + \left[\left(h_i^{(x)}\right)^{n+1,m} + \delta_i^{(x)}\right] \varphi_{10i}(\mathbf{x})$$
$$+ \left[\left(h_i^{(z)}\right)^{n+1,m} + \delta_i^{(z)}\right] \varphi_{01i}(\mathbf{x}) + \left[\left(h_i^{(xz)}\right)^{n+1,m} + \delta_i^{(xz)}\right] \varphi_{11i}(\mathbf{x}) \Big\}$$

Therefore, given initial and boundary data for $\hat{h}$, one can use Equation (3) to solve for $\delta\hat{h}$ at each iteration, updating $\hat{h}$ to step forward in time.

We also let the moisture content θ have a Hermite cubic expansion, using the chain rule to express spatial derivatives of θ in terms of the nodal unknowns $h_i^{(x)}$, $h_i^{(z)}$, and $h_i^{(xz)}$:

$$\hat{\theta}(\mathbf{x}) = \sum_{i=1}^{N} \Big\{ \theta(h_i)\, \varphi_{00i}(\mathbf{x}) + \frac{d\theta}{dh}(h_i)\, h_i^{(x)}\, \varphi_{10i}(\mathbf{x})$$
$$+ \frac{d\theta}{dh}(h_i)\, h_i^{(z)}\, \varphi_{01i}(\mathbf{x}) + \left[\frac{d^2\theta}{dh^2}(h_i)\, h_i^{(x)}\, h_i^{(z)} + \frac{d\theta}{dh}(h_i)\, h_i^{(xz)}\right] \varphi_{11i}(\mathbf{x}) \Big\}$$

This C^1 projection of θ parallels the successful one-dimensional calculations reported in (Allen and Murphy, 1985).

Finally, for the coefficients K and $d\theta/dh$ in Equation (3) we adopt piecewise bilinear approximations:

$$\hat{K}(\mathbf{x}) = \sum_{i=1}^{N} K(h_i)\, L_i(x)\; L_i(z)$$
$$\widehat{\left(\frac{d\theta}{dh}\right)}(\mathbf{x}) = \sum_{i=1}^{N} \frac{d\theta}{dh}(h_i)\, L_i(x)\, L_i(z)$$

where L_i is just the one-dimensional piecewise linear Lagrange (chapeau) basis function associated with node i.

Substituting all of these finite-element projections into Equation (3) yields a temporally discrete scheme with a finite number of unknown nodal degrees of freedom h_i at each time step.

COLLOCATION SOLUTION SCHEME

To determine the nodal values of $\delta\hat{h}$ and therefore advance the head $\hat{h}$ in time, we need a set of algebraic equations at each iterative step. Some of these equations come from boundary conditions; the rest we will

construct using finite-element collocation. Let us begin by reviewing the boundary conditions.

By using the tensor-product basis defined above we have tacitly oriented the computational boundaries parallel to the coordinate axes. For nonrectangular domains, we would isoparametrically transform the (x, y)-plane to a plane endowed with a deformed coordinate system as described in Pinder et al. (1978). In the untransformed system, the unit normal vector $\mathbf{n}$ and unit tangent vector $\boldsymbol{\tau}$ to the boundary will be $\pm\mathbf{e}_x$ or $\pm\mathbf{e}_z$, depending on the position along the boundary. Suppose $\mathbf{x}_i$ is a Dirichlet node. Then $\hat{h}^{n+1}(\mathbf{x}_i) = h_i^{n+1}$ is a fixed, known quantity and therefore $\delta_i = 0$. Moreover, we can differentiate the boundary data tangentially along the Dirichlet boundary $\partial\Omega_D$ to deduce fixed values for $\nabla\hat{h}^{n+1} \cdot \boldsymbol{\tau}$, thus forcing $\delta_i^{(x)} = 0$ if $\boldsymbol{\tau} = \pm\mathbf{e}_x$ and $\delta_i^{(z)} = 0$ if $\boldsymbol{\tau} = \pm\mathbf{e}_z$. Similarly, if $\mathbf{x}_i$ is a Neumann node, then $\nabla\hat{h}^{n+1}(\mathbf{x}_i)$ is a fixed, known quantity, forcing $\delta_i^{(x)} = 0$ if $\mathbf{n} = \pm\mathbf{e}_x$ and $\delta_i^{(z)} = 0$ if $\mathbf{n} = \pm\mathbf{e}_z$. Differentiating the boundary data tangentially in this case will give fixed values for $\nabla(\nabla\hat{h}^{n+1} \cdot \mathbf{n}) \cdot \boldsymbol{\tau}$ along the Neumann boundary $\partial\Omega_N$, forcing $\delta_i^{(xz)} = 0$. Therefore at any boundary node within a boundary line segment the boundary data determine two nodal parameters. At corner nodes the boundary data along the intersecting boundary segments will combine to determine three nodal parameters.

To determine the remaining boundary and interior nodal parameters, we collocate the finite-element approximation to Equation (3) at a set of collocation points $\overline{\mathbf{x}}_k \in \Omega$. This yields a system of linear equations each having the form

$$\left[-\frac{1}{\Delta t}\frac{d\hat{\theta}^{n+1,m}}{dh}(\overline{\mathbf{x}}_k) + \hat{K}^{n+1,m}(\overline{\mathbf{x}}_k)\left(\frac{\partial^2}{\partial x^2} + \frac{\partial^2}{\partial z^2}\right) + \frac{\partial\hat{K}^{n+1,m}}{\partial x}(\overline{\mathbf{x}}_k)\frac{\partial}{\partial x} + \frac{\partial\hat{K}^{n+1,m}}{\partial z}(\overline{\mathbf{x}}_k)\frac{\partial}{\partial z}\right]\delta\hat{h}(\overline{\mathbf{x}}_k) = -\hat{R}^{n+1,m}(\overline{\mathbf{x}}_k)$$

where $\hat{R}$ represents the expression obtained by substituting the appropriate interpolatory projections for the spatially varying quantities in the residual R.

We choose for the collocation points $\overline{\mathbf{x}}_k$ the Gauss points associated with four-point quadrature on each rectangular element $[x_p, x_{p+1}] \times [z_q, z_{q+1}]$ (Pinder et al., 1978). This choice of collocation points furnishes exactly the right number of additional equations for the remaining unknown nodal parameters and gives the best possible accuracy estimates for the linearized problem at each time step (Prenter and Russell, 1976).

SAMPLE PROBLEM

To show the effectiveness of our collocation scheme, we solve a sample problem similar to one solved by van Genuchten (1983) using a Galerkin procedure on Hermite bicubics. This problem describes water infiltrating from a source located 0.15m below the soil surface. The governing differential equation is

$$\nabla \cdot [K(\nabla h - \mathbf{e}_z)] - \frac{\partial \theta}{\partial t} + Q = 0$$

where Q is the water source, measured in s^{-1}. The spatial domain of the problem is $\Omega = (0, 0.61\mathrm{m}) \times (-3.5\mathrm{m}, 0)$. We assume that the left side $\{0\} \times (-3.5\mathrm{m}, 0)$ and right side $\{0.61\mathrm{m}\} \times (-3.5\mathrm{m}, 0)$ are lines of symmetry with no normal flux, that the bottom $(0, 0.61\mathrm{m}) \times \{-3.5\mathrm{m}\}$ is a free-draining boundary, and that the soil surface $(0, 0.61\mathrm{m}) \times \{0\}$ remains at atmospheric pressure. These assumptions lead to the boundary conditions

$$\begin{aligned}
\frac{\partial h}{\partial x}(0, z, t) = \frac{\partial h}{\partial x}(0.61\mathrm{m}, z, t) &= 0, \qquad -3.5\mathrm{m} < z < 0,\ t > 0 \\
\frac{\partial h}{\partial z}(x, -3.5\mathrm{m}, t) &= 0, \qquad 0 < x < 0.61\mathrm{m},\ t > 0 \\
h(x, 0, t) &= -0.14495\mathrm{m}, \qquad 0 < x < 0.61\mathrm{m},\ t > 0
\end{aligned}$$

We impose the initial condition $h(\mathbf{x}, 0) = -0.387\mathrm{m}$, $\mathbf{x} \in \Omega$. For the material properties K and θ we assume the same functional forms as van Genuchten, which in SI units are

$$\begin{aligned}
K(h) &= (1.157 \times 10^{-7})[96.768 \exp(12.58h)]\mathrm{m/s}, \qquad h \le 0 \\
\theta(h) &= 0.10 + 0.40/[1 + 0.0025(100h)^2]^{1/2}, \qquad h \le 0
\end{aligned}$$

We assume a point source of the form $Q(\mathbf{x}) = Q_0 \delta(x - 0)\delta(z + 0.15\mathrm{m})$ with a source strength $Q_0 = 5 \times 10^{-5}\mathrm{s}^{-1}$. In finite-element collocation we must approximate Q by a square-integrable function. We choose a piecewise bilinear approximation of the form $\hat{Q}(\mathbf{x}) = \sum_{i=1}^{N} Q_i L_i(x) L_i(z)$, where the point $\mathbf{x}_i^{\text{source}} = (0, -0.15\mathrm{m})$ is a node, $Q_i = 0$ if $\mathbf{x}_i \neq \mathbf{x}_i^{\text{source}}$, and $\int_\Omega \hat{Q}\, d\mathbf{x} = \int_\Omega Q\, d\mathbf{x}$.

We solve the resulting collocation equations on the five-element-by-eleven-element grid given in (van Genuchten, 1983) using a time step $\Delta t = 3600\mathrm{s}$ (one hour). Figure 1 shows the structure of the matrix that has to be inverted at each iteration in the nonlinear time-stepping procedure. The bandwidth for this matrix is 31. We use a direct solver executing LU factorization with partial pivoting on banded asymmetric matrices.

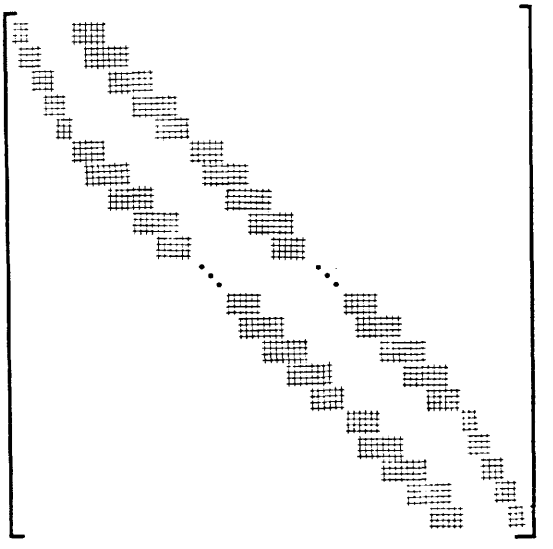

Figure 1. Matrix structure for the sample problem.

Figures 2 through 7 show the spatial variation of $\hat{h}(\mathrm{x}, t)$ at two-hour intervals. At two hours (Figure 2), the source already has a noticeable effect on the pressure head. In the horizontal direction $\hat{h}$ peaks at the source, drops off, and then levels out. In the vertical direction the pressure head gradually increases further down into the column as time progresses. Finally, at $t = 12$ hours (Figure 7) $\hat{h}$ reaches a very close approximation to the steady-state solution in the sense that this solution is virtually identical to solutions at later times.

CONCLUSION

The finite-element collocation method produces good approximations to pressure head distributions in unsaturated flows through porous media. As we have shown, the mass-conserving iterative formulation, demonstrated earlier for one-dimensional flows, extends in a natural way to two space dimensions. One area deserving further investigation is the linear algebra involved at each iterative stage. Since the matrices for the multidimensional problems have an asymmetric block structure without diagonal dominance, better methods for solving the linear iterative systems would be a boon to further applications.

ACKNOWLEDGMENTS

The Wyoming Water Research Center provided partial support for this work. The National Science Foundation also provided support through grants numbered CEE-8404266 and DMS-8504360.

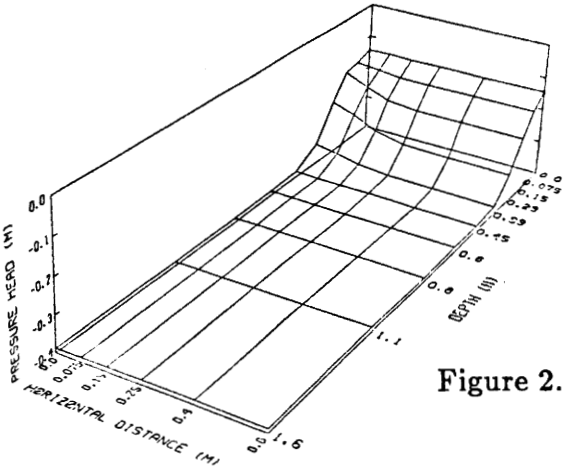

Figure 2. Pressure head solution at 2 hours.

Figure 3. Pressure head solution at 4 hours.

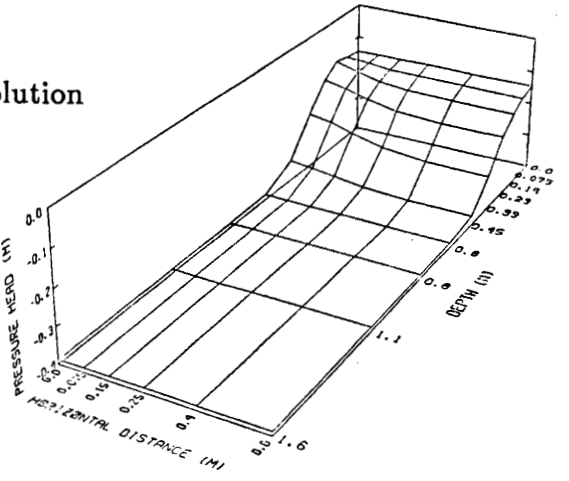

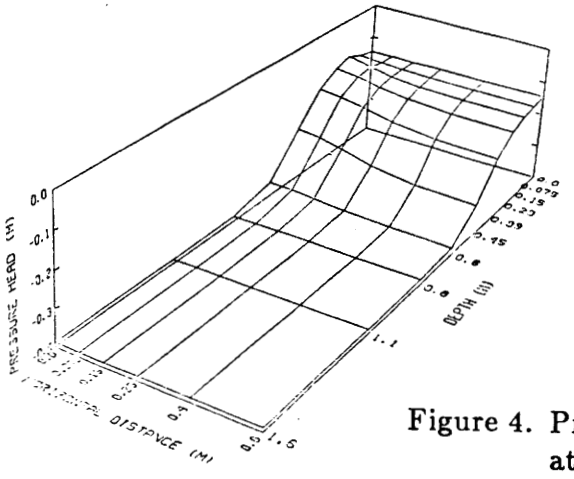

Figure 4. Pressure head solution at 6 hours.

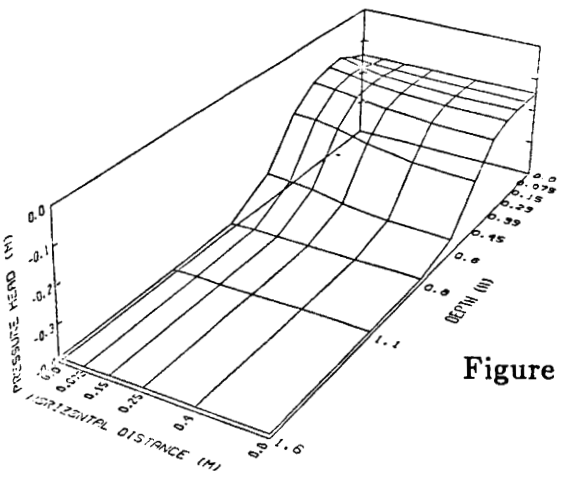

Figure 5. Pressure head solution at 8 hours.

Figure 6. Pressure head solution at 10 hours.

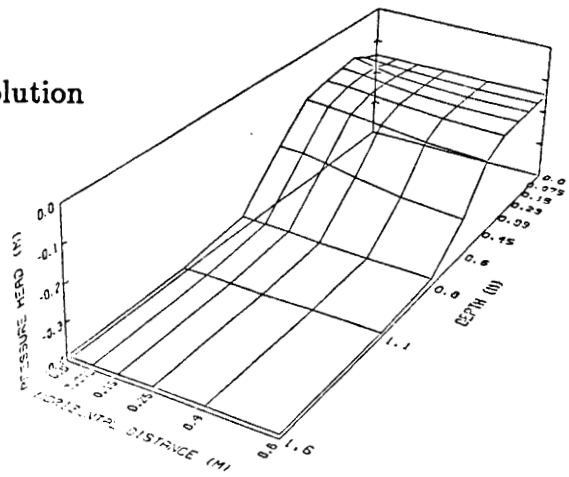

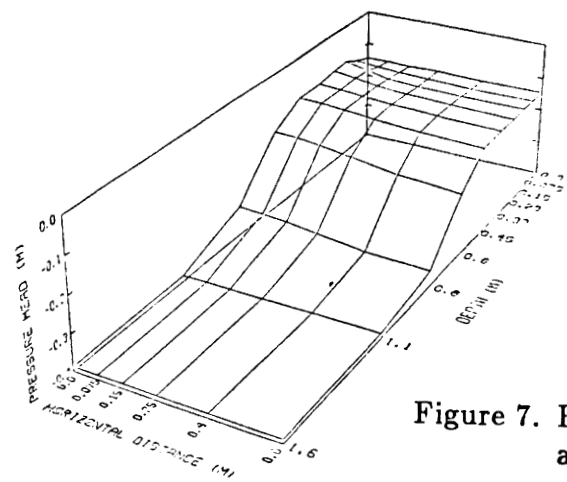

Figure 7. Pressure head solution at 12 hours.

REFERENCES

Allen, M.B. and Murphy, C.L. (1985), A finite-element collocation technique for variably saturated flows in porous media, *Numer. Meth. for PDEs* **3**, 229–239.

Murphy, C.L. (1985), Finite Element Collocation Solution to the Unsaturated Flow Equation, M.S. Thesis, University of Wyoming Department of Mathematics, Laramie, Wyoming, U.S.A.

Pinder, G.F., Frind, E.O. and Celia, M.A. (1978), Groundwater flow simulation using collocation finite elements, in C.A. Brebbia et al., eds., *Proc. Second Intl. Conf. on Finite Elements in Water Resources*, Pentech Press, London, 1.171–1.185.

Prenter, P.M. (1976), *Splines and Variational Methods*, Wiley, New York.

Prenter, P.M. and Russell, R. (1976), Orthogonal collocation for elliptic partial differential equations, *SIAM Jour. Numer. Anal.* **13**, 923–939.

van Genuchten, M.Th. (1983), An Hermitian finite element solution of the two-dimensional saturated-unsaturated flow equation, *Adv. Water Resour.* **6**, 106–111.